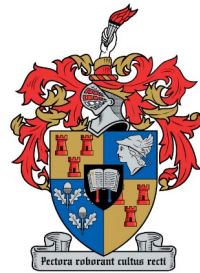


# 36 Chlorine isotope systematics in saline groundwater in the Buffels River Valley

**Jani van Gend**



UNIVERSITEIT  
iYUNIVESITHI  
STELLENBOSCH  
UNIVERSITY

**100**  
1918 · 2018

**Submitted in Full Fulfilment of MSc Earth Science**

**Department of Earth Science**

**University of Stellenbosch**

**March 2018**

**Supervisor: Dr Jodie Miller**

**Co-Supervisor: Dr. Catherine Clarke**

## DECLARATION

I declare that  $^{36}\text{Cl}$  Chlorine isotope systematics in saline groundwater in the Buffels River Valley is my own work, that it has not been submitted for any degree or examination in any other university, and that all the sources I have used or quoted have been indicated and acknowledged by complete references.

By submitting this thesis electronically, I declare that the entirety of the work contained therein is my own, original work, that I am the sole author thereof (save to the extent explicitly otherwise stated), that reproduction and publication thereof by Stellenbosch University will not infringe any third party rights and that I have not previously in its entirety or in part submitted it for obtaining any qualification.

Full name: Jani van Gend

Date: March 2018

Copyright © 2018 Stellenbosch University  
All rights reserved

## ACKNOWLEDGEMENTS

I would like to express my deepest gratitude to the project supervisor, Dr. Jodie Miller, for the opportunity to be a part of this project. I would also like to thank her for all her patients, encouragement and guidance. To my field team, Andrew Watson Jared van Rooyen, Ryan Cloete and Jean Loock, this project would not have been possible without your assistance. Thank you, Jared, for all your help and hours of editing. Thank you to prof. Keith Fifield from the Australian National University for your guidance with the  $^{36}\text{Cl}$  isotope work and to Dr. Laszlo Palcsu from the Hungarian Institute of Nuclear Studies for noble gas analyses. Thank you to Mike Butler from iThemba labs for analysing stable isotopes as well as Petrus Le Roux from the University of Cape Town, for strontium isotope analysis. To Charl Muller, thank you for your endless patients, motivation and endless support during the last two years. Lastly, to my parents and brother, thank you for always putting my best interests first and for the opportunity to pursue my dream. Thank you for your support loads of encouragements and unconditional love.

## ABSTRACT

It is typical for coastal aquifers in arid regions to be affected by salinisation, populations in these areas that rely upon groundwater resources are often directly afflicted by this phenomenon. Large parts of the western coast of South Africa are affected by variably saline groundwater as a result of varying degrees of salinisation, primarily driven by evaporative processes. Initial stable  $\delta^2\text{H}$  and  $\delta^{18}\text{O}$  isotopic investigations suggest rainfall and groundwaters carry evaporative signatures, further investigation has suggested that there are other significant salt contributors in the region, although these sources and pathways are poorly constrained. One such alternate salt source may arise from paleo-termite mounds, called heuweltjies, that are found in areas along the west coast. These structures typically consist of salt- and nutrient-rich sediments and the recorded sediment EC values for these structures are an order of magnitude higher than that of the adjacent interheuweltjies. Furthermore, sediment EC values of heuweltjies increase with depth and the difference between deep and shallow EC values in heuweltjies are between 1000 and 3000  $\mu\text{S}/\text{cm}$ , with the deeper samples having the higher EC value. The possibility of heuweltjie salts entering the groundwater system and contributing to groundwater salinisation in this area has not been investigated as yet. The town of Buffels Rivier in the western region of the Northern Cape has limited surface water resources and is dependent on local groundwater for subsistence. For this reason, it is an ideal site to investigate these atypical salinisation drivers. In order to effectively isolate the additional salt sources, several geochemical, isotopic and geophysical methods were implemented. Highly variable soil and groundwater EC values were observed in the field area. Furthermore,  $^{36}\text{Cl}$  isotope ratios together with noble gas data provides some evidence that aquifer mixing occurs. This is further evidenced by the spatial discontinuity in groundwater  $^{87}\text{Sr}/^{86}\text{Sr}$  ratios. The geology of this area consist of basement granite gneisses and the contribution of rock salt to the groundwater cannot be excluded.  $^{87}\text{Sr}/^{86}\text{Sr}$  ratios in groundwater in the Buffels River Valley are elevated, ranging between 0.73030 and 0.78240, which is typically associated with the water-rock interaction granitic rocks. The extent of the salt contribution from the various systems in the Buffels River Valley is still not fully understood but it is evident that conventional, semi-arid salinisation through evaporation is not the only driver in this regional system.

## TABLE OF CONTENTS

Declaration.....	i
Acknowledgements.....	ii
Abstract.....	iii
List of figures.....	viii
List of tables .....	xii
1. Introduction.....	1
1.1. General Introduction.....	1
1.1.1. Problem statement .....	3
1.1.2. Aims and objectives .....	4
1.2. Salinisation .....	5
1.3. Chlorine-36.....	7
1.3.1. Overview .....	7
1.3.2. <sup>36</sup> Cl fallout and distribution.....	10
1.3.3. Constraining residence time .....	11
1.4. Heuweltjies.....	13
2. Study Area .....	15
2.1. Geological Context .....	16
2.2. Climate .....	19

2.3.	Geomorphology and Vegetation.....	19
2.4.	Buffels River Catchment.....	20
2.4.1.	Aquifer Types .....	20
2.4.2.	River Systems .....	21
3.	Methods and Materials .....	23
3.1.	Selection of sampling sites .....	23
3.1.1.	Groundwater.....	24
3.1.2.	Rainwater .....	24
3.1.3.	Sediments .....	25
3.2.	Sampling Procedures.....	26
3.2.1.	Groundwater sampling .....	26
3.2.2.	Rainwater .....	30
3.2.3.	Sediments .....	30
3.3.	Analytical methods.....	35
3.3.1.	Electrical Conductivity and pH .....	35
3.3.2.	Cations and Anions .....	36
3.3.3.	O and H isotopes.....	37
3.3.4.	Sr isotopes.....	38
3.3.5.	<sup>36</sup> Cl isotopes .....	39

3.3.6.	Noble gases .....	39
3.4.	EM38 .....	41
4.	Results.....	42
4.1.	EC and pH .....	42
4.1.1.	Groundwater.....	42
4.1.2.	Sediments and Soils .....	45
4.2.	Major cations and anions .....	55
4.3.	Isotopes .....	62
4.3.1.	Stable O and H .....	62
4.3.2.	Strontium .....	64
4.3.3.	Chlorine-36.....	66
4.3.4.	Noble gasses .....	68
5.	Discussion .....	69
5.1.	Groundwater and sediment characterisation.....	69
5.2.	Mechanisms of Salinisation.....	71
5.2.1.	Evaporative concentration of salts .....	71
5.2.2.	Heuweltjie salts.....	72
5.2.3.	Groundwater mixing .....	76
5.2.4.	Water-rock interaction .....	78

5.3.	South African water quality standards and management practices .....	80
5.3.1.	Domestic water quality standards .....	81
5.3.2.	Agricultural water quality standards and management.....	81
6.	Conclusion .....	83
7.	References .....	85
8.	Appendix.....	100



## LIST OF FIGURES

Figure 2.1: a) Location of Buffels River Catchment within the Northern Cape and South Africa; b) location of the study area within the Buffels River Catchment. ....	15
Figure 2.2: Geology of the northern section of the West Coast of South Africa (from Macey et al., 2017a).....	18
Figure 2.3: River systems within the Buffels River Catchment.....	22
Figure 2.4: Image of the Buffels River Valley taken in the south, looking towards the north, with the Eselsfontein River joining the Buffels River from the east.....	22
Figure 3.1: Sample locations within the study area. ....	23
Figure 3.2: Map indicating rainfall stations with reference to the Buffels River Valley.....	25
Figure 3.3: a) Bailing for sample BR24; b) solar pump on borehole BR05; c) windmill pumping groundwater at BR09.....	27
Figure 3.4: a) PVC adapter connected to a borehole, copper tubes connect to clear plastic tube on the side of the adapter; b) PVC adapter with its valves open to regulate water pressure into the copper tube which was attached to the clear plastic tube; c) air bubbles being removed from the copper tube which is connected directly to the spring via the clear plastic connection tube.....	29
Figure 3.5: Aerial image of the location of the grid.....	32
Figure 3.6: a) Augering and collection of a grid sample; b) pit with minimum cave in from which a shallow interheuweltjie sample was collected; c) auger head filled sediment sample; d) grid samples after being placed in two sample bags and sealed. ....	33
Figure 3.7: Relationship between sampling location within the grid and relative depths of each sample.....	34

Figure 3.8: Noble gas mass spectrometric system at the Isotope Climatology and Environmental Research Centre of the Institute for Nuclear Research at the Hungarian Academy of Sciences.....40

Figure 3.9: Geonics Limited EM38-MK2 being set up for scanning the marked-out grid. Note the heuweltjie in the background.....41

Figure 4.1: EC for groundwater samples in order from South to North.....43

Figure 4.2: Comparison between EC values for groundwater samples taken both in 2016 and 2017. ....43

Figure 4.3: Groundwater pH in order from South to North. ....44

Figure 4.4: a) Comparison between river sediment EC-values with samples in order from South to North, with RS01 being the southernmost sample; b) Comparison between river sediment EC values in the same order as seen in a), with an adjusted EC scale.....45

Figure 4.5: Relationship between EC values relative to depths and position of the sample; a- b) heuweltjie and interheuweltjie 1; c-d) heuweltjie and interheuweltjie 2; e-f) heuweltjie and interheuweltjie 3; g-h) heuweltjie and interheuweltjie 4; i-j) heuweltjie and interheuweltjie 5; k-l) heuweltjie and interheuweltjie 6; m-n) heuweltjie and interheuweltjie 7. Note that the EC scale is different for each heuweltjie-interheuweltjie set.....49

Figure 4.6: Relationship between heuweltjie and interheuweltjie sediment EC and pH distribution.....50

Figure 4.7: Relationship between sediment EC and sampling location within the grid.....51

Figure 4.8: Relationship between sediment pH and sampling location within the grid.EM-38 .....52

Figure 4.9: Relationship between EC and elevation relative to geographical location within the grid. ....54

Figure 4.10: Sediment EC represented as cross-section through two heuweltjies and interheuweltjies in the grid.....54

Figure 4.11: Comparison between major cation concentrations and sample date relative to groundwater EC; a) Na<sup>+</sup> concentrations relative to groundwater EC; b) K<sup>+</sup> concentrations relative to groundwater EC; c) Ca<sup>2+</sup> concentrations relative to groundwater EC; d) Mg<sup>2+</sup> concentrations relative to groundwater EC.....56

Figure 4.12: Na<sup>+</sup>/Cl<sup>-</sup> ratio for groundwater samples in the Buffels River .....57

Figure 4.13: Comparison between major anion concentrations and sample date relative to groundwater EC; a) Cl<sup>-</sup> concentrations relative to groundwater EC; b) HCO<sub>3</sub><sup>-</sup> concentrations relative to groundwater EC; c) SO<sub>4</sub><sup>2-</sup> concentrations relative to groundwater EC; d) F<sup>-</sup> concentrations relative to groundwater EC.....59

Figure 4.14: Distribution of δ<sup>2</sup>H and δ<sup>18</sup>O ratios for rainwater and groundwater collected during 2013, 2016 and 2017, LMWL and GMWL shown for reference with the local groundwater line (2013 data from Nakwafila, 2015). .....63

Figure 4.15: Comparison between <sup>87</sup>Sr/<sup>86</sup>Sr ratios for groundwater samples collected in the Buffels River catchment in order from South to North. ....65

Figure 4.16: Comparison of <sup>36</sup>Cl/Cl ratios between groundwater samples and a rainwater sample collected from the Buffels River Catchment, ordered from South to North. Groups are separated by stippled lines. ....66

Figure 5.1: Piper diagram of groundwater chemistry for samples collected in 2016 and 2017. ....70

Figure 5.2: Comparison between heuweltjie EC values, interheuweltjie EC values and groundwater EC values. Note that outliers are excluded from the groundwater dataset for this particular comparison.....74

Figure 5.3: Comparison of the spatial distribution of heuweltjies and relative position of groundwater EC, plotted from south to north according to the direction of flow. Note that samples collected in Komaggas are not in the Buffels River Valley, and are plotted at the end.

..... 75

Figure 5.4: Relationship between  $^{36}\text{Cl}/\text{Cl}$  ratios and  $\text{Cl}^-$  concentration in the groundwater and rainwater samples..... 76

Figure 5.5: Relationship between  $^{36}\text{Cl}/\text{Cl}$  ratios and  $^{36}\text{Cl}$  content in groundwater and rainwater.

..... 77

Figure 5.6: Spatial distribution of  $^{87}\text{Sr}/^{86}\text{Sr}$  ratios..... 80

## LIST OF TABLES

Table 3.1: Detection limits and errors for chemical parameters analysed at Bemlab. ....	37
Table 4.1: Major ion chemistry for groundwater in 2016 .....	60
Table 4.2: Major ion chemistry for groundwater in 2017 .....	61
Table 4.3: $^{86}\text{Sr}/^{87}\text{Sr}$ ratios for groundwater .....	64
Table 4.4: $^{36}\text{Cl}$ and $\text{Cl}^-$ data for groundwater samples .....	67
Table 4.5: Noble gas concentrations. ....	68
Table 8.1: Heuweltjie EC and pH data. ....	101
Table 8.2: River sediment EC and pH data.....	102
Table 8.3: EC, pH and depth data for sediment samples taken in the grid .....	103
Table 8.4: Stable isotope data for both groundwater and rainwater samples. Groundwater data is presented on the right while that of rainwater on the left. ....	104

# 1. INTRODUCTION

## 1.1. General Introduction

The world's population is growing rapidly, expecting to hit 8.5 billion by 2030 and 9.7 billion by 2050. Much of this increase will occur in sub-Saharan Africa with an additional 2.4 billion people by 2050 (UN Department of Economic and Social Affairs, 2015). One of the most critical aspects of this increase in population is the demand for fresh or potable water. Although large parts of Sub-Saharan Africa have high rainfall rates, the region has very heterogeneously distributed surface water resources, leaving many areas with very little or no fresh surface water (UN-WWAP, 2015). The high rates of urbanisation, particularly in drought-prone areas, exacerbates this problem and results in an increasing dependence on groundwater to supply domestic, industrial and agricultural water needs (Sheffield et al., 2014; Lapworth et al., 2017). With this dependence, groundwater becomes increasingly vulnerable to factors that directly or indirectly affect the quality and quantity of the groundwater resource.

Salinisation of groundwater, surface water as well as soils and the processes involved have been studied for decades (Scanlon et al., 2006, 2005; Vengosh et al., 1999; Farber et al., 2004; Cook et al., 1989; Jolly et al., 1993; Bouchaou et al., 2008). However, there are still many unknowns regarding region-specific variables that may play a role in the process. Salinisation could be a result of natural or anthropogenic processes or a combination of the two factors (Salama et al., 1993, 1999). Although salinisation occurs in all climatic environments, aquifers in arid to semi-arid regions are more vulnerable to salinisation due to higher evaporation rates together with low rainfall rates (Rengasamy, 2006; Vengosh et al., 1999). Surface salts accumulate as a result of evaporation after which percolation of the salt crust into the groundwater system occur.

The west coast of southern Africa is one such area where no surface water source exists and communities are wholly dependent on groundwater. However, this rapid increase in groundwater use occurred without the complete understanding of the sustainability and quality of local groundwater. A major concern in this semi-arid to arid environment is the

process of groundwater salinisation (Mehta et al., 2000; Vengosh et al., 1999). The deterioration of groundwater quality through the addition of salts is problematic not only for basic human consumption but for agricultural purposes (food security) and biodiversity in this region. The north-west coast of southern Africa is affected by variably saline groundwater, which is typically ascribed to the effects of high evaporation rates and a low rainfall rate (Benito et al., 2010; Adams et al., 2004). However, the larger coastal zone of south-western Africa experience similar climatic conditions but salinisation of groundwater has not occurred to the same extent. Furthermore, there are significant variations in the spatial distribution of salts. This atypical spatial distribution together with the fact that the entire climatic zone does not suffer from saline groundwater suggests that other factors are at play in the development of saline groundwater.

In the Buffels River Valley in the Northern Cape of South Africa, groundwater is variably saline. Several authors (Titus et al., 2009; Adams et al., 2004; Pietersen et al., 2009) have been conducted in this area which indicated that climate is the main controlling factor of salinisation of groundwater in the Buffels River Valley and surrounding areas. However, due to the spatial and chemical variability of salts in the groundwater in such a small area, climatic conditions cannot be the only control on increased salt concentrations. In order to better constrain both the origin and transport mechanisms of salts into and within subsurface systems, further research must be conducted with less conventional methods that account for more than just climatic salinisation drivers. One such factor is heuweltjies, paleo-termite mounds, which are distinct features of the landscape of the west coast region of southern Africa. The soils in these mounds are generally more aerated and nutrient rich with higher levels of micro- and macro than the surrounding material (Picker et al., 2007; Cramer et al., 2012; Francis et al., 2013; Cramer & Midgley, 2015).

This study will aid in better understanding the variable distribution of saline groundwater in the Buffels River Valley and surrounding areas. In doing so, various salt contributors, as well as transport mechanisms, will be investigated. An integrated field and geochemical approach will be used to establish the spatial relationship between saline groundwater and the heuweltjies to understand if heuweltjies could be contributing to groundwater salinisation.

Furthermore, strontium, chlorine-36 and stable oxygen and hydrogen isotopes will be used to evaluate the contribution of salts from other sources. Specific attention will be given to chlorine-36 which will be used to evaluate the role of evaporation or whether additional salts from other sources have been added to the groundwater system.

### **1.1.1. Problem statement**

As the most arid region of South Africa, populations on the west coast are dependent on groundwater as their primary source of fresh water. As regional water budgets are stressed, this dependence drives further deterioration of these subsurface reservoirs. As expected in such a dry, hot environment, the most detrimental effect, besides groundwater depletion, is a result of salinisation. Salinisation has been extensively investigated in this and other arid environments and is typically a result of evaporative processes precipitating salts on the surface, allowing them to be incorporated into the groundwater resource (Vengosh et al., 1999, 2002; Farber et al., 2004; Rengasamy, 2006; Scanlon et al., 2006). Several methods have been developed to identify the salt origins and the degree of salinisation in such environments. These methods include chloride mass and water balance investigations. However, in spatially variable and geologically complex environments conventional methods are less effective.

Previous studies in the Buffels River catchment have suggested that the salinisation issues in the area have typical sources and drivers (Adams et al., 2004; Pietersen et al., 2009). Further investigation has implied that the drivers of salinisation are more intricate. In order to characterise these atypical salinisation patterns, modern isotopic methods must be implemented. A combination of isotopes, namely Cl, Sr, H and O as well as noble gases were used in conjunction with conventional geochemical methods. To better understand the processes by which salts are concentrated on the surface and in groundwater, paleo termite mounds (called heuweltjies) were also investigated through soil chemistry and geophysical methods.

Typically, heuweltjies are nutrient and salt rich sediment zones which have been concentrated by bioactivity, these areas also occur above areas where groundwater has generally elevated salt concentrations. Isotopic investigations could better explain alternative



salt sources and mobilisation pathways and aid in understanding spatial correlations between heuweltjies and saline groundwater. In doing so, the atypical salinisation through rock water interaction, groundwater mixing and concentrated soil salinity may be better interpreted.

### **1.1.2. Aims and objectives**

In order to address the role of heuweltjies in the development and distribution of saline groundwater in the Buffels River Valley, the following objectives and key questions have been defined.

**Objective 1:** To delineate the variation in EC and pH within the sediments in the Buffels River Valley

- How does the sediment EC and pH vary along the course of the river bed and on and off heuweltjies?
- What is the spatial relationship between the sediment and groundwater EC between the river and the heuweltjies?
- Do the patterns of salinisation suggest different salt sources?

**Objective 2:** To characterise the geochemical and isotopic composition of groundwater in the Buffels River Valley

- What is the composition of groundwater in the Buffels River Valley and how does this relate to domestic water quality standards in South Africa?
- How does the groundwater chemistry vary spatially and temporally within the river bed and on and away from the margins of the river?
- What are the  $^{87}\text{Sr}/^{86}\text{Sr}$  and  $^{36}\text{Cl}/\text{Cl}$  ratios in groundwater and how do these relate to the sediments?

**Objective 3:** To evaluate the role of heuweltjie salts to the salinisation of groundwater in the Buffels River Valley

- Can saline groundwater be generated through interaction with the heuweltjies?

- Does groundwater mixing occur and to what extent does mixing contribute to groundwater salinisation?
- Which management structures can be put in place if, in fact, the heuweltjies are contributing to groundwater salinisation?

## 1.2. Salinisation

Salinisation is the long-term process by which water-soluble salts accumulate in soils, regolith as well as groundwater. Salinisation occurs as a result of natural processes but is often enhanced by anthropogenic activities (Salama et al., 1999; Vengosh et al., 1999; Schoups et al., 2005; Rengasamy, 2006; Munns & Tester, 2008). Salinisation of both groundwater and soils not only affect human health and the natural environment but has an impact on global agricultural development and food security.

Natural salinisation processes, also known as primary salinisation, are controlled by various factors including climate and topography (Bennetts et al., 2006; Williams, 2001). Primary salinisation is particularly common in semi-arid to arid environments. Here salts accumulate in soils and groundwater due to the evaporation and evapotranspiration that exceed the mean annual precipitation (MAP). The increase in soluble salts in soils, surface water bodies and groundwater caused by anthropogenic activity is referred to as secondary salinisation. Human activity often results in changes in the hydrological and morphological cycle causing an unnatural accumulation of soluble salts in soils and water bodies (Salama et al., 1999; Peck & Hatton, 2003).

Anthropogenic salinisation could be caused by many different processes, or in some cases, a combination of processes. Agriculture, which is part of the daily activities of rural communities, play a major role in concentrating salts. Dryland salinisation is the hydrogeological response to the majority of crop producing farming activities. The clearing of deep-rooted indigenous vegetation and its replacement with shallow-rooted crops results in a decrease in evapotranspiration and an increase in groundwater recharge (Salama et al., 1999; Rengasamy, 2006; Pannell, 2001). The fluctuations in the water table mobilises salts from deeper soils resulting in more saline environment. Irrigation plays a large role in

recycling of salts in the soil and groundwater system. Irrigation causes a rise in the water table resulting in the dissolution of salts from soils (Schoups et al., 2005). Furthermore, dissolved salts from poor quality irrigation water are added to the system and further contributes to the salinity in the region (Aragüés et al., 2014). Due to seasonality in crop production, this cycle is constantly repeated and could lead to the formation of local hypersaline environments.

Urban salinisation is often overlooked as the soils and groundwater in urban areas are not as intensively used as in rural areas, and therefore, the consequences of urban salinisation are not as easily noticed. The water table in urban environments are continuously disrupted from the start of construction of urban developments, causing mobilisation of subsurface salts. Factors such as clearing of vegetation, sewage processes, over watering of gardens, construction, and landfill sites, contribute to salinisation in urban areas (Spennemann, 2001; Podmore, 2009; Casey et al., 2013). Furthermore, urban environments host many industrial processes that generate waste products in the form of wastewater, gasses as well as solid waste. Due to the chemical processes involved, these waste products often contain various salts. Industries are therefore direct sources of salts which are easily incorporated in the soils and water bodies in and around urban areas.

Apart from primary and secondary salinisation processes, salinity can be classified based on the processes related to the interaction between various components in the critical zone. Groundwater associated salinity occurs when soluble salts are transported and deposited during groundwater discharge. In the case of shallow aquifers where the water table is close to the soil surface, evapotranspiration causes the upward movement of groundwater and salts, effectively concentrating the salts in the zones above the water table, as water is removed from the system (Rengasamy, 2006). During a rain event, salts are flushed into the groundwater system and the process is repeated. In cases where only primary processes are at play, climatic conditions and soil hydraulic properties are the main controls on the amount of salt accumulation within the soil layers in contact with the water table (Rengasamy, 2010). Water table fluctuations as a result of secondary processes or anthropogenic activities, such as pumping of wells and agricultural activities, would enhance the effects of the primary

processes. Non-groundwater associated salinity occur in areas where deep aquifers dominate and drainage is poor. In these cases, salts are introduced to soils and sediments by various processes which include both natural and anthropogenic processes (Rengasamy, 2006, 2010). Although rainwater generally contains little salts, accumulation of these salts over time together with salts from weathering of soil and rock material may lead to saline soil environments. These salts are stored within the deeper solum layers and can be mobilized and transported by pore water. However, in regions where poor hydraulic properties dominate in the shallow solum layers, specifically in arid regions, non-groundwater associated salts accumulate in the shallow solum layers and topsoil (Rengasamy, 2006).

### **1.3. Chlorine-36**

Chloride is one of the most abundant ions in groundwater systems. Due to the mobile but conservative behaviour of chloride ions, processes such as biogeochemical activity and ion exchange reactions within these environmental systems have little impact on the chloride concentrations (Keywood et al., 1998; Scanlon et al., 2006; Carlson et al., 1990). Consequently, chloride can be used to gain valuable information about many processes within a system.

#### **1.3.1. Overview**

Chlorine is part of the halogen series, which in ionic state, are salt-forming elements. It has an atomic number of 17 and a molecular mass of 35.453 $\mu$ . With seven valence electrons in its outermost shell, it is one electron short of a full octet and is, therefore a strong oxidising agent with a high electron affinity and electronegativity. Chlorine is an extremely reactive element which often forms ionic bonds with monovalent cations such as sodium ( $\text{Na}^+$ ). Chlorine then occurs as a monovalent anion. Therefore, in solution, chlorine as a monovalent anion in solution behaves as a conservative ion as its outer electron shell is now a complete octet.

Chlorine has three naturally occurring isotopes with mass numbers  $A = 35, 36$  and  $37$ , of which  $^{35}\text{Cl}$  and  $^{37}\text{Cl}$  are stable chlorine isotopes and  $^{36}\text{Cl}$  the radiogenic chlorine isotope. The relative abundances of  $^{35}\text{Cl}$  and  $^{37}\text{Cl}$  are 0.75779 and 0.24221, respectively (Coplen et al., 2002).

Chlorine 36 ( $^{36}\text{Cl}$ ) is a naturally occurring radioactive isotope with a half-life of  $3.01 \times 10^5$  years (Keywood et al., 1998). It is produced during the following processes:

i) Cosmic-ray-induced spallation of Argon-40 ( $^{40}\text{Ar}$ )

High energy primary cosmic rays, which consist mostly of protons, enter the stratosphere from outer space. Here the primary rays interact with the gases present causing the nuclei to disintegrate (Challan, 2016; Bird et al., 1991; Fifield, 2017). Argon-40 is one such gas that disintegrates during which protons and neutrons are released producing many other products. The nuclei of  $^{40}\text{Ar}$  consist of 18 protons and 22 neutrons. Therefore, in order to produce  $^{36}\text{Cl}$ , three neutrons and one proton must be released from  $^{40}\text{Ar}$ . However, particles require a minimum energy of 38 MeV to bring about the reaction forming  $^{36}\text{Cl}$  (Fifield, 2017). Apart from  $^{36}\text{Cl}$ , many other secondary particles are produced from the disintegration of  $^{40}\text{Ar}$  and other gasses. In cases where secondary particles have sufficient energy, further nuclear reactions are initiated and further particles and energetic neutrons are produced. This series of reactions continue to the point where particle energies are exhausted.

ii) Cosmic ray interactions with  $^{39}\text{K}$  and  $^{40}\text{Ca}$  on and near the Earth's surface

$^{36}\text{Cl}$  can be produced from calcium and potassium isotopes on and near the earth's surface by one of three processes, thermal neutron activation, cosmic ray spallation reactions and muon reactions. During thermal neutron activation,  $^{39}\text{K}$  isotopes at the earth's surface react with neutrons released from spontaneous thorium and uranium decay (Phillips et al., 1986; Evans et al., 1997). This reaction produces  $^{36}\text{Cl}$ , a free neutron and an alpha particle. Cosmic ray spallation occurs at the earth's surface and in the upper few meters of the crust (Stone et al., 1996; Schimmelpfennig et al., 2011).  $^{39}\text{K}$  and  $^{40}\text{Ca}$  isotopes are bombarded with cosmic rays in the form of high energy neutrons. Reactions with  $^{39}\text{K}$  occur in the same way as that of thermal neutron reactions, producing  $^{36}\text{Cl}$ , a free neutron and an alpha particle. On the contrary, reactions with  $^{40}\text{Ca}$ , which contains an additional proton, produce  $^{36}\text{Cl}$ , a free proton and an alpha particle. The third process involves a reaction, within the deeper crust, between  $^{39}\text{K}$  and  $^{40}\text{Ca}$  atoms and muons, which are high energy negatively charged cosmic particles (Stone et al., 1998; Phillips et al., 1986). In this case, the reaction with  $^{39}\text{K}$  produces  $^{36}\text{Cl}$ , a free

proton and two free neutrons whereas reactions with  $^{40}\text{Ca}$  produce  $^{36}\text{Cl}$  and an alpha particle. Weathering of the crustal material mobilises  $^{36}\text{Cl}$ , allowing it to become part of natural earth systems.

iii) Production from  $^{35}\text{Cl}$

Stable  $^{35}\text{Cl}$  present in crustal material is exposed to uranium and thorium decay for long periods of time deep in the subsurface. Neutrons are released into the crustal material as products of the decay reaction. This brings about the production of  $^{36}\text{Cl}$  through thermal neutron capture on the stable  $^{35}\text{Cl}$  nuclide (Phillips et al., 1986; Leavy et al., 1987; Davis et al., 2003). Although very little  $^{36}\text{Cl}$  is produced within the continental crust, it is mobilised during weathering and incorporated in the hydrological system. Similarly, cosmic ray spallation of stable  $^{35}\text{Cl}$  present in the upper atmosphere occurs, during which a neutron is incorporated in the nuclei of the stable  $^{35}\text{Cl}$ , producing a heavier  $^{36}\text{Cl}$  isotope (Andrews et al., 1986; Davis et al., 2003). Furthermore, thermal neutron capture of stable  $^{35}\text{Cl}$  also occurs when chloride containing rocks are exposed to a cosmic neutron flux. Sedimentary rocks such as limestone contain up to 20 000 ppm chloride. If limestone outcrops are exposed to cosmic neutrons in-situ production of  $^{36}\text{Cl}$  will occur due to neutron activation of  $^{35}\text{Cl}$  (Andrews et al., 1986; Bird et al., 1991).

iv) 1950's Nuclear weapons testing

Artificial  $^{36}\text{Cl}$  was produced as a result of nuclear weapons testing during the 1950's. Fusion devices were tested in the western-Pacific during which high fluxes of neutrons were released causing capturing of secondary cosmic ray neutrons by  $^{35}\text{Cl}$  in oceanic  $^{35}\text{Cl}$  (Sturchio et al., 2009; Moran & Rose, 2003). The artificially produced  $^{36}\text{Cl}$  was released into the atmosphere raising  $^{36}\text{Cl}$  values by more than two orders of magnitude (Davis et al., 2003). This increase in the  $^{36}\text{Cl}$  concentration, as well as fall out rate seen between 1952 and 1970's, is known as the bomb-pulse (Andrews et al., 1986). The fallout rate of the artificially produced  $^{36}\text{Cl}$  was not only increased due to the increased production of  $^{36}\text{Cl}$  but because it was produced at low altitudes. Chloride typically remains in the atmosphere for up to 3 years as it moves downwards from the stratosphere. However, due to the low altitude production of  $^{36}\text{Cl}$ ,

fallout occurred much faster (Bird et al., 1991; Purdy et al., 1987; Balderer et al., 2004; Phillips et al., 1986). The  $^{36}\text{Cl}$  fallout rate has returned to the baseline value since the 1970's.

### **1.3.2. $^{36}\text{Cl}$ fallout and distribution**

The bulk (60%) of  $^{36}\text{Cl}$  used for the purposes of constraining ages or as isotopic tracers within environmental systems is produced within the stratosphere as a result of cosmic ray-spallation of  $^{40}\text{Ar}$  at a rate of  $20 \text{ atoms m}^{-2} \text{ s}^{-1}$  (Keywood et al., 1998; Balderer et al., 2004).  $^{36}\text{Cl}$  in the form of gaseous  $\text{H}^{36}\text{Cl}$  or as aerosol-bound particles are transported downwards across the tropopause and into the troposphere over a period of approximately two years (Tosaki et al., 2012; Phillips, 2013; Bird et al., 1991; Purdy et al., 1987). Here production of  $^{36}\text{Cl}$  continue by a combination of cosmic ray-spallation of  $^{40}\text{Ar}$  and capturing of secondary cosmic ray neutrons by  $^{35}\text{Cl}$ . Atmospheric chloride, composed of  $^{35}\text{Cl}$ ,  $^{36}\text{Cl}$  and  $^{37}\text{Cl}$  derived from the ocean and weathering of crustal material, mixes with the  $^{36}\text{Cl}$  produced in the upper atmosphere (Phillips et al., 1986; Leavy et al., 1987). The combined chlorine atoms are dissolved in rain or snow as chloride or incorporated into aerosols in the upper atmosphere (Keywood et al., 1998; Balderer et al., 2004; Nolte et al., 1991). The radiogenic and stable Cl mixture is deposited during rainfall or snow events and is eventually incorporated in groundwater through groundwater recharge.

The global production rate and distribution of  $^{36}\text{Cl}$  are controlled by multiple factors which include latitude, altitude, atmospheric cycling and the presence of aerosols in the upper atmosphere. The shielding effect of the Earth's magnetic field cause deflection of cosmic rays at low latitudes which results in a decrease in cosmic ray-spallation of  $^{40}\text{Ar}$  (Keywood et al., 1998). Consequently, very little  $^{36}\text{Cl}$  is produced around the equator. With increasing latitude towards the poles, cosmic ray deflection decreases and production of  $^{36}\text{Cl}$  increases, causing a latitudinal dependence in the concentration of  $^{36}\text{Cl}$  in the upper atmosphere (Johnston & McDermott, 2008; Beer et al., 2002). Although  $^{36}\text{Cl}$  production occurs mostly in the stratosphere, atmospheric cycling plays a large role in the distribution of  $^{36}\text{Cl}$ . The stratosphere-troposphere mixing cycle is most efficient during spring at latitudes of approximately  $40^\circ$ . Therefore, deposition of  $^{36}\text{Cl}$  during rain and snow events is at a maximum at these latitudes and characteristic increased  $^{36}\text{Cl}$  values are expected. As latitudes increase

or decrease towards the poles or the equator,  $^{36}\text{Cl}$  decrease as continuous deposition removes the  $^{36}\text{Cl}$  during turbulent transport towards the south and north (Phillips, 2013).

High energy cosmic rays bombard  $^{40}\text{Ar}$  in the Earth's outer atmosphere resulting in nuclear interactions and the formation of  $^{36}\text{Cl}$  and other lower energy secondary particles. These interactions resulting in energy losses continue as the particles move downwards and altitude decreases closer to the Earth's surface. Therefore, as the altitude decreases, energy levels of the photons decrease to the point where the energy levels are not sufficient to cause further particle formation. Hence, the  $^{36}\text{Cl}$  production is lower at lower altitudes (Johnston & McDermott, 2008; Masarik & Beer, 1999). The distribution of the  $^{36}\text{Cl}$  is further complicated by the presence of aerosols. It is expected that the concentration of  $^{36}\text{Cl}$  in the troposphere is directly proportional to the deposition thereof on the land surface, but this is not the case. Chloride ions, both stable chloride and  $^{36}\text{Cl}$ , may interact and react directly with atmospheric aerosols or aerosols interact with droplets containing chloride through nucleation or engulfing processes. Depending on the size of the aerosol and the degree of water saturation in the atmosphere, early or delayed deposition of  $^{36}\text{Cl}$  may occur (Phillips, 2013; Fifield, 2017).

### **1.3.3. Constraining residence time**

Due to the long half-life of  $^{36}\text{Cl}$  ( $t_{1/2} = 3.01 \times 10^5$  years), it is a powerful radiogenic dating tool. Most of the  $^{36}\text{Cl}$  present in a system (98.1%) decays to  $^{36}\text{Ar}$  by beta-minus decay, 1.9% by electron capture, while 0.0015% decays to  $^{36}\text{S}$  by beta-plus decay (Challan, 2016). Although decay of  $^{36}\text{Cl}$  start occurring as soon as it has been produced, its residence time in the atmosphere is only two years which is negligible in on the scale of 301 000 years. Dissolved chloride, which contains  $^{36}\text{Cl}$  isotopes, enters the groundwater system through recharge. Due to isolation from the atmospheric production of  $^{36}\text{Cl}$  changes,  $^{36}\text{Cl}$  concentrations in groundwater are controlled mainly by radioactive decay (Phillips, 2013; Howcroft et al., 2017). Therefore, as the groundwater residence time in that particular system increases,  $^{36}\text{Cl}$  decay continues. In the case of an ideal system, where no stable or radiogenic Cl can be added or removed, the  $^{36}\text{Cl}/\text{Cl}$  ratio will decrease as decay occurs and the concentration of  $^{36}\text{Cl}$  decrease. The initial and measured  $^{36}\text{Cl}$  concentrations and  $^{36}\text{Cl}/\text{Cl}$  ratios can be used in the radioactive decay equation to obtain a groundwater ages and residence times. However, natural systems



are very seldom ideal and various sources and sinks of either  $^{36}\text{Cl}$  or stable Cl may exist.  $^{36}\text{Cl}/\text{Cl}$  ratios can be complicated by various processes including evapotranspiration, the addition of both stable Cl as well as radiogenic  $^{36}\text{Cl}$ , subsurface or crustal production of  $^{36}\text{Cl}$ , radioactive decay of  $^{36}\text{Cl}$  as well as mixing of water between various subsurface sources (Phillips, 2013).

A number of equations have been formulated to calculate the residence time of groundwater. The simultaneous interpretation of  $^{36}\text{Cl}$  and stable Cl concentrations, as well as the  $^{36}\text{Cl}/\text{Cl}$  ratio, is considered when these equations are applied (Phillips, 2013).

Subsurface mass balance of  $^{36}\text{Cl}$  can be expressed as follows:

*Equation 1:*

$$\begin{aligned} C_{36} &= R_{meas} C_{meas} \\ &= R_{36,re} C_{re} \exp(-\lambda_{36}t) + R_{36,se1} C_{re} (1 - \exp(-\lambda_{36}t)) \\ &\quad + R_{36,se2} (C_{meas} - C_{re}) \end{aligned}$$

where  $C_{36}$  is the  $^{36}\text{Cl}$  concentration of the groundwater (atoms  $^{36}\text{Cl} \text{ L}^{-1}$ ),  $R_{36,re}$  is the  $^{36}\text{Cl}/\text{Cl}$  ratio in the recharge,  $C_{re}$  is the recharge  $\text{Cl}^-$  concentration in the recharge (atoms  $\text{Cl}^- \text{ L}^{-1}$ ),  $R_{36,se1}$  is the secular equilibrium  $^{36}\text{Cl}/\text{Cl}$  ratio in the aquifer,  $R_{36,se2}$  is the secular equilibrium  $^{36}\text{Cl}/\text{Cl}$  ratio in an external source of  $\text{Cl}^-$  (in the case of possible addition or loss of  $\text{Cl}^-$ ),  $C_{meas}$  is the measured  $\text{Cl}^-$  concentration of the sample (atoms  $\text{L}^{-1}$ ), and  $R_{meas}$  is the measured  $^{36}\text{Cl}/\text{Cl}$  ratio of the sample.  $R_{36,se2}$  may or may not be the same as  $R_{36,se1}$ . In the case where  $R_{36,se2}$  is equal to  $R_{36,se1}$ , Equation 1 is simplified to the following:

*Equation 2:*

$$t = \frac{-1}{\lambda_{36}} \ln \frac{C_{meas} (R_{36,meas} - R_{36,se})}{C_{re} (R_{36,re} - R_{36,se})}$$

Equation 1 can be further manipulated in terms of the various factors that may affect the  $^{36}\text{Cl}/\text{Cl}$  ratio and hence the residence time. If  $\text{Cl}^-$  is added to the system due to the dissolution of bedded halite but no additional  $^{36}\text{Cl}$  is added,  $R_{se}$  equals zero and the equation is as follows:

*Equation 3:*

$$t = \frac{-1}{\lambda_{36}} \ln \frac{C_{meas} R_{36,meas}}{C_{re} R_{36,re}}$$

In areas where evapotranspiration during recharge may vary or in the case of subsurface enrichment, the concentration both  $^{36}\text{Cl}$  and stable  $\text{Cl}^-$  will increase equally, therefore there are no changes in the  $^{36}\text{Cl}/\text{Cl}$  ratio (Phillips, 2013). These variations in the concentration of  $^{36}\text{Cl}$  and stable  $\text{Cl}^-$  along the groundwater flow path result in the following variation of Equation 1:

*Equation 4:*

$$t = \frac{-1}{\lambda_{36}} \ln \frac{R_{36,meas} - R_{36,se}}{R_{36,re} - R_{36,se}}$$

Secular equilibrium of  $^{36}\text{Cl}$  in groundwater sources is controlled by the production and decay rate of  $^{36}\text{Cl}$  in the system. Hence, if secular equilibrium is achieved in a system, the production rate of  $^{36}\text{Cl}$  is equal to its decay rate. In the case where groundwater mixing occurs, the secular equilibrium of all systems involved will be disturbed (Phillips, 2013). The  $^{36}\text{Cl}/\text{Cl}$  ratio will change due to the mixing and the solution will be the following:

*Equation 5:*

$$t = \frac{-1}{\lambda_{36}} \ln \frac{C_{re}(R_{36,se2} - R_{36,se1}) + C_{meas}(R_{36,meas} - R_{36,se2})}{C_{re}(R_{36,re} - R_{36,se1})}$$

#### **1.4. Heuweltjies**

Circular earth mounds are found in many parts of the world and have been a controversial topic amongst researchers for decades (Cramer et al., 2012; Midgley et al., 2012; Francis et al., 2013; Moore & Picker, 1991; Cramer et al., 2017; Picker et al., 2007; Midgley et al., 2002; Washburn, 1988; Reider et al., 1996; Chapman, 1948). Although these features may develop as a result of anthropogenic activity, the majority of studies specifically focus on understanding the mounds originating from non-anthropogenic activity. These natural mounds have been given various names which are unique to the area in which they are found. These include prairie mounds in Canada; pimple mounds or Mima-mounds in the US; Campos de murundus (which translate to mound fields) in Brazil; and the commonly used general term

for circular surface features across the world, fairy circles (Cramer et al., 2012; McAuliffe et al., 2014; Funch, 2015). However, in eastern and southern Africa they are referred to as heuweltjies which is an Afrikaans word for 'small hills' (Midgley et al., 2012; Cramer et al., 2012; Francis et al., 2013). These heuweltjies are common surface features along the west coast of Southern Africa, covering an estimated 14 to 25% of the land surface (Midgley et al., 2012; Francis et al., 2013).

Heuweltjies are dome structures which range between 15 and 20 m in diameter and stand between 1.5 and 2.5 m above the surrounding material (Francis et al., 2013). They are not uniformly distributed and have characteristic vegetation cover that is different from the typical local vegetation (Francis et al., 2013; Midgley et al., 2002). Heuweltjie sediments are distinctly lighter in colour compared to the surrounding sediments (Picker et al., 2007). They are therefore easily identifiable on aerial photography images due to their distinct difference in sediment colour. Both the sediment colour and specific vegetation can be attributed to the sediment composition of the heuweltjies which is more aerated and nutrient-rich with higher levels of micro- and macro elements than the surrounding material (Erens et al., 2015; Cramer et al., 2012). Although the origin of heuweltjies has been a topic of many scientific debates, the majority of researchers have come to the conclusion that heuweltjies were formed as a result of faunal activity most likely being nesting of harvester termites (*Microhodotermes viator*) during the last 2000-4000 years (Moore & Picker, 1991; Midgley et al., 2002, 2012; Picker et al., 2007). Termites build these mounds or heuweltjies by removing the sediments material below the mound and placing it on the surface. During this process, termites replace the removed sediments with nutrient-rich material as well as clays from the surrounding area (Cramer et al., 2012).

## 2. STUDY AREA

The Buffels River Valley is situated approximately 40km west of Springbok in the Northern Cape with the town of Buffelsrivier, on the western banks of the Buffels River in the Buffels River Valley (Figure 2.1). The town has a population of approximately 3000 people and due to the lack of potable water in the area, this community is fully reliant on groundwater as their only source of water. Historically, agricultural and mining related activities have been the main economic drivers in this region. However, in recent years, mining activities in Namaqualand have scaled down or completely stopped resulting in increasing unemployment rates.

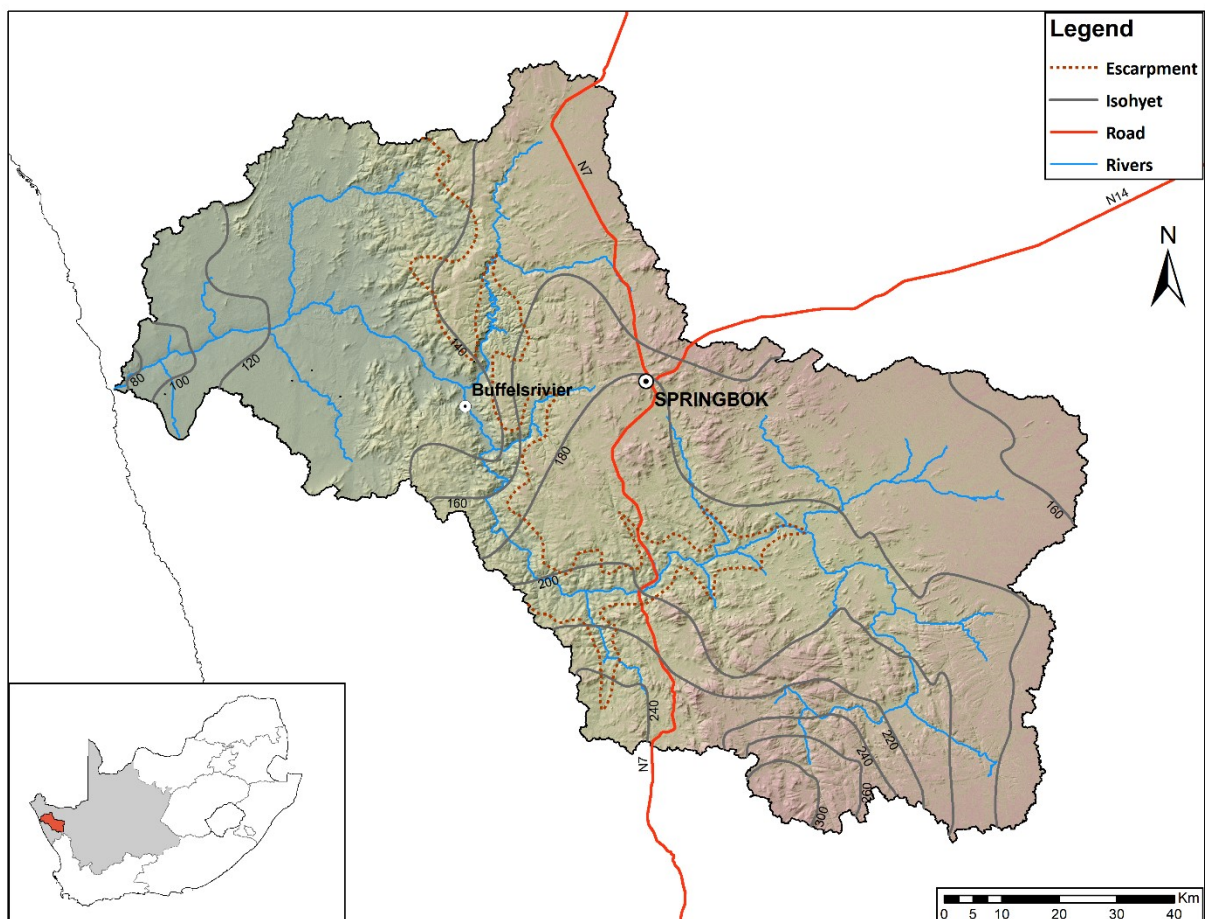


Figure 2.1: a) Location of Buffels River Catchment within the Northern Cape and South Africa; b) location of the study area within the Buffels River Catchment.

## 2.1. Geological Context

The geology of the Buffels River catchment is dominated by the Bushmanland Sub-Province of the Namaqua Sector of the Namaqua-Natal Metamorphic Province. The Mesoproterozoic Namaqua-Natal Metamorphic Province is a continuous arcuate orogenic belt on the SW margin of the Kaapvaal Craton that is composed of two parts, the Namaqua sector located in Northern Cape and the Natal sector of KwaZulu-Natal (Cornell et al., 2006; Eglinton, 2006; Jacobs et al., 2008). The Namaqua Sector has undergone crustal extraction and evolution dating back locally to the Archaean, with major Palaeoproterozoic and minor juvenile Mesoproterozoic crust-forming episodes (Pettersson et al., 2009; Bial et al., 2015). The lithostratigraphy is broadly comprised of polydeformed and polymetamorphosed granitic gneisses and supracrustal rocks that have been so strongly remelted and tectonised during these episodes (Clifford et al., 2004; Eglinton, 2006; Cornell et al., 2006; Thomas et al., 2016; Macey et al., 2017a, 2017b) that the naming and delineation of terranes/subprovinces within the Namaqua sector and their genesis and development is still not consistent across the literature (Blignault et al., 1983; Hartnady et al., 1985; Thomas et al., 1994a; Colliston & Schoch, 1996; Moen & Toogood, 2007; Jacobs et al., 2008; Macey et al., 2017a). However, it is agreed that the Namaqua sector consists of a NW-trending, SW-verging stack of thin vast horizontal sheets bound by thrusts, where sheets are differentiated based on their lithostratigraphy, tectonic and metamorphic histories and are from west to east, the Richtersveld Subprovince, Bushmanland Subprovince, Kakamas, Areachap and Kaaien Terranes (Hartnady et al., 1985; Thomas et al., 1994a; Macey et al., 2015, 2017b)

The central zone of the Namaqua sector consists of the Bushmanland Subprovince which is the largest tectonic domain in the Namaqua Sector (Macey et al., 2017a; Cornell et al., 2006). It is separated from Richtersveld sub-province by the Groothoek Thrust and the Wortel Belt which occurs to the north. The Hartebees River Thrust occurs on the eastern boundary between the Bushmanland sub-province and the Kakamas Terrane. The Bushmanland Subprovince is comprised of a granitic gneiss basement complex ( $\pm 2.0$ - $1.8$  Ga), sedimentary and volcanic supracrustal sequences ( $\pm 1.9$  to  $1.2$  Ga) and syn- to late-tectonic granitic to charnockitic intrusive suites ( $\pm 1.2$  to  $0.95$  Ga)(Cornell et al., 2006; Thomas et al., 1994b).

The Spektakel suite, as seen in Figure 2.2, is a voluminous igneous suite, comprising of late- to post-tectonic granitoids, and forms part of the Bushmanland Subprovince (Macey et al., 2017a). The Spektakel Suite was named after the old Spektakel copper mine which is situated at the northern end of the Buffels River Valley. In the Buffels River Valley, the Spektakel Suite is dominated by the Rietberg-type granitoids. Rietberg-type granitoids generally consist of twinned perthitic alkali feldspar megacrysts in a coarse-grained biotite-rich quartz-feldspar matrix and have been determined to range in age between 1033 and 1098 Ma (Thomas et al., 1994b; Macey et al., 2017a). These granites intruded the granulite facies rocks of the Bushmanland Subprovince forming tabular sheet-like bodies. More specifically, the Rietberg Granites intruded along the foliation planes of the augen gneisses of the Little Namaqualand Suite.

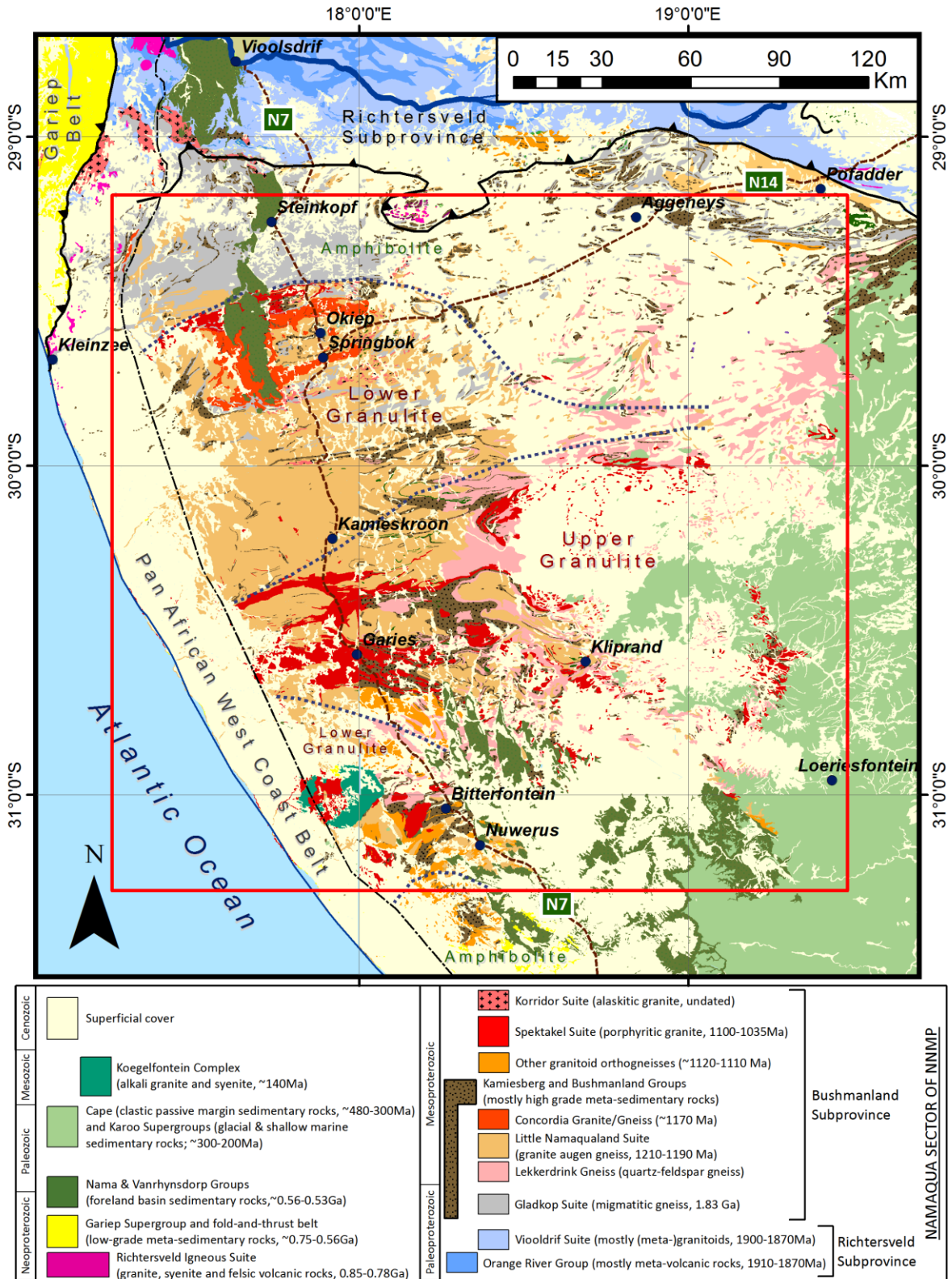


Figure 2.2: Geology of the northern section of the West Coast of South Africa (from Macey et al., 2017a)

## 2.2. Climate

The western region of the Northern Cape of South Africa experiences a semi-arid to arid climatic regime. Average summer temperatures for these regions range between 15 °C at night and a midday temperature of 35°C. Winter temperatures range between below 0°C at night and 17°C during the day. The western regions of the Northern Cape receive winter rainfall associated with frontal systems and gentle rain and drizzle whereas the eastern regions fall within a summer rainfall regime. The mean annual precipitation (MAP) of the coastal region is documented as 44 mm, 215 mm at the Springbok Mountains, while the MAP at the western Bushmanland peneplane and at Komaggas on the coastal plain is 102mm and 110mm respectively. The Kammies Mountains towards the east of the Buffels River catchment, which are the headwaters of the Buffels River, fall within the summer rainfall region. Here the MAP is 450-480 mm (Titus et al., 2009; Benito et al., 2010). Inland mountainous areas typically have a higher MAP than the low lying coastal areas due to orographic effects (Titus et al., 2009; Benito et al., 2011; Pietersen et al., 2009). High evaporation rates are typical in arid to semi-arid environments such as Namaqualand. Evaporation rates typically exceed the precipitation rates which results in a concentration of salts within and on top of the sediments. It has been found that evaporation can occur from depths of around 90 cm in the alluvial material (Adams et al., 2004).

## 2.3. Geomorphology and Vegetation

The Namaqualand region has been subdivided into three geomorphological zones based on several geomorphological cycles which include changes in climatic conditions, fluvial erosion and tectonic events (Adams et al., 2004; Titus et al., 2009). The Western Plateau slopes or the Western Coastal Lowland is characterised by crystalline basement rocks overlain by modern sands. The Great Escarpment zone occurs inland from the Western Coastal Lowland and has a combination of highland and lowland regions. Plains and hills, exposed domes, thick layers of weathered material, fractured rocks and alluvial paleochannels are typical of this zone (Adams et al., 2004). The vegetation on Namaqualand is dominated by the Nama Karoo biome and the succulent Karoo biome towards the west. Grasses and low shrubs are the prominent



plant types of the Nama Karoo biome while succulent shrubs occur towards the west in the succulent Karoo biome (Adams et al., 2004; Mucina & Rutherford, 2006). The flora in Namaqualand is known to be drought resistant with deep root systems (Mucina & Rutherford, 2006). The alluvial plains of the Buffels River are dominated by Acacia Karoo shrubs and trees as well as thicket species. Due to their dependence on groundwater, these riparian plant species are good indicators of groundwater availability.

## **2.4. Buffels River Catchment**

The catchment is situated towards the west of Springbok. It covers an area of approximately 9250 km<sup>2</sup> and drains into the Buffels River which is the largest ephemeral river in Namaqualand (Marais et al., 2001a; Benito et al., 2010, 2011). The headwaters are located in the Kamiesberg Mountains on the Bushmanland Plateau and the river subsequently cuts down through the escarpment before emerging onto the Tertiary coastal plain and enters the Atlantic Ocean at Kleinsee. The aquifer system in the Buffels River catchment consists of two alluvial aquifers. The Spektakel aquifer is located approximately 80 km inland of the river mouth and the Kleinsee aquifer is situated towards the coast, just before the Buffels River mouth.

### **2.4.1. Aquifer Types**

Groundwater in the larger Namaqualand area is hosted by three different aquifer systems which are closely interlinked. These are fractured bedrock aquifers, weathered zone or regolith aquifers and sandy or alluvial aquifers. Fractured bedrock aquifers and weathered zone aquifers can be grouped as basement aquifers (Pietersen et al., 2009). These aquifers typically develop in crystalline intrusive and metamorphic rocks of Precambrian age (Wright, 1992). Basement bedrocks of Precambrian age have generally been exposed to various phases of stress and deformation resulting in ductile folding and brittle fracturing. These fault controlled aquifers are known to have high transmissivity values and low storage capacity. These aquifers are generally deeper aquifers. The weathered zone above the fractured basement rocks provide pathways for subsurface intergranular flow and are therefore connected to the basement aquifers (Titus et al., 2009). Alluvial aquifers, which are the only

characterised aquifers in the Buffels River catchment are generally shallow primary aquifers overlying the basement geology. They are associated with the river systems and palaeochannels and are composed of unconsolidated alluvial material such as gravels and finer alluvial sands (Pietersen et al., 2009).

There are currently only two significant aquifer systems that have been characterised in the Buffels River catchment. The Spektakel aquifer and the Kleinsee aquifer are both alluvial aquifers situated in the lower Buffels River (Benito et al., 2010, 2011; Marais et al., 2001a; Pietersen et al., 2009). The Kleinsee aquifer is situated in the west, towards the mouth of the Buffels River. The Spektakel aquifer is situated where the river flows downwards from the escarpment onto the inland flats at the edge of the coastal plain (Marais et al., 2001a; Benito et al., 2010). This alluvial aquifer is 4-20 m deep and forms part of an approximately ~15 km long sand-filled basin which lies above the granitic gneiss basement (Marais et al., 2001b). Although the Kleinsee and Spektakel aquifers are the only aquifers that have been characterised, some researchers have noted a deeper groundwater source where borehole of up to ~80m deep are pumped for local water use (Adams et al., 2004; Titus et al., 2009).

#### **2.4.2. River Systems**

The Buffels River is approximately 250km in length, making it the largest ephemeral river in Namaqualand (Benito et al., 2011, 2010). The Buffels River is classified as a fourth order river system which implies that it has many smaller tributaries (Figure 2.3). Many first and second order tributaries join the Buffels River at 90° angles throughout the course of the river (Benito et al., 2011, 2010). The significant second-order tributaries in the upper catchment are the Gasab, Drodap and Wolwepoort Rivers. The lower catchment has two-second order tributaries, the Skaap River and the Stry River. The largest and only third-order tributary, the Brak River, joins the Buffels River in the upper part of the catchment. The only significant first-order tributary is the Eselsfontein River which joins the Buffels River as it flows downwards from the escarpment onto the inland flats, see Figure 2.4. These flats form the southern end of the Buffels River Valley and the Spektakel Aquifer. The Skaap River, which is a second-order tributary, joins the Buffels River at the northern end of the Buffels River Valley, which is the central zone of the Spektakel Aquifer.

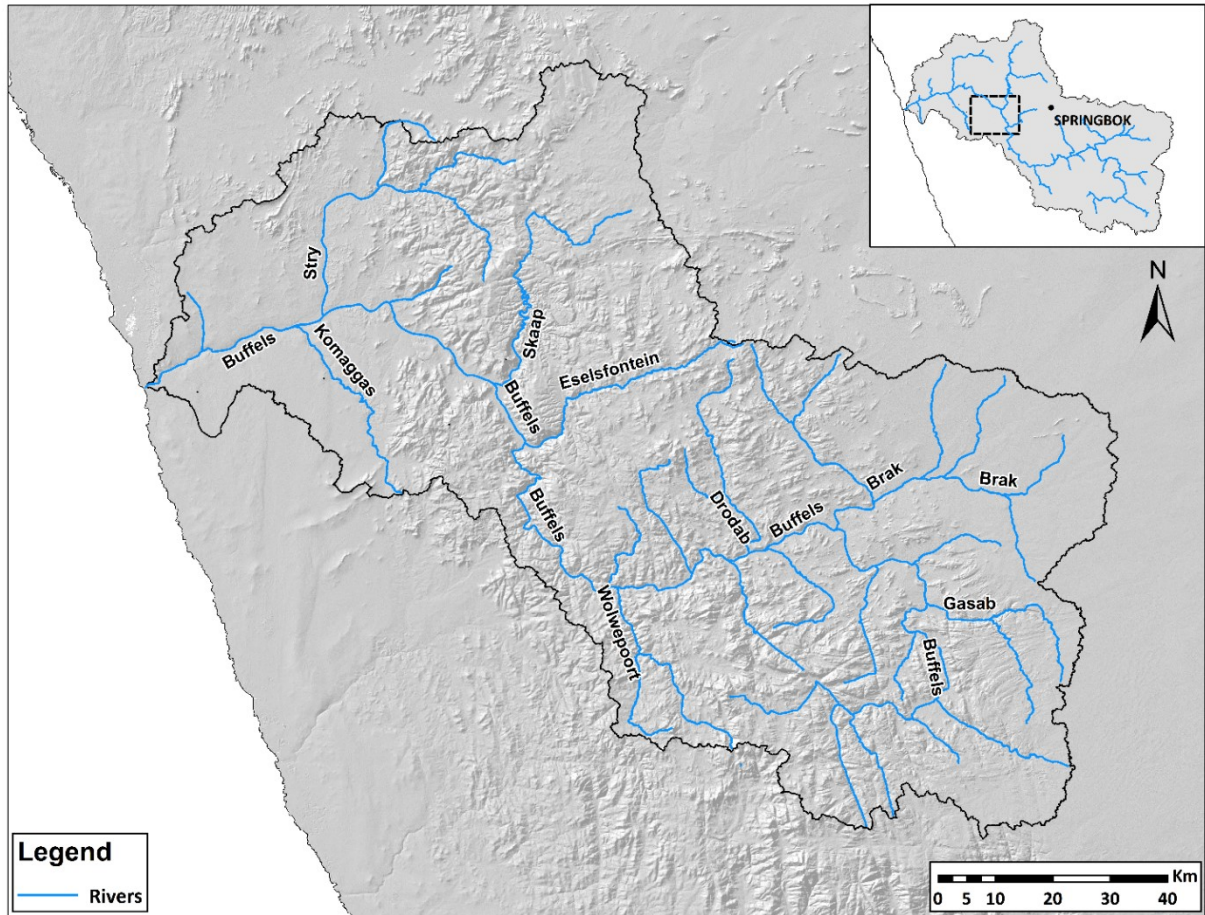


*Figure 2.3: River systems within the Buffels River Catchment.*



*Figure 2.4: Image of the Buffels River Valley taken in the south, looking towards the north, with the Eselsfontein River joining the Buffels River from the east.*

### 3. METHODS AND MATERIALS

Various methods and materials were followed and used in order to conduct this study. Groundwater, rainwater and sediment samples were collected and processed between November 2016 and July 2017

#### 3.1. Selection of sampling sites

Desktop studies were conducted before fieldwork could occur to ensure that the fieldwork and sampling were done efficiently. Due to limited research in the Buffels River area, very few boreholes and sampling sites have been identified previously. Despite the limited information, existing data was compiled to create a database of various sampling sites.

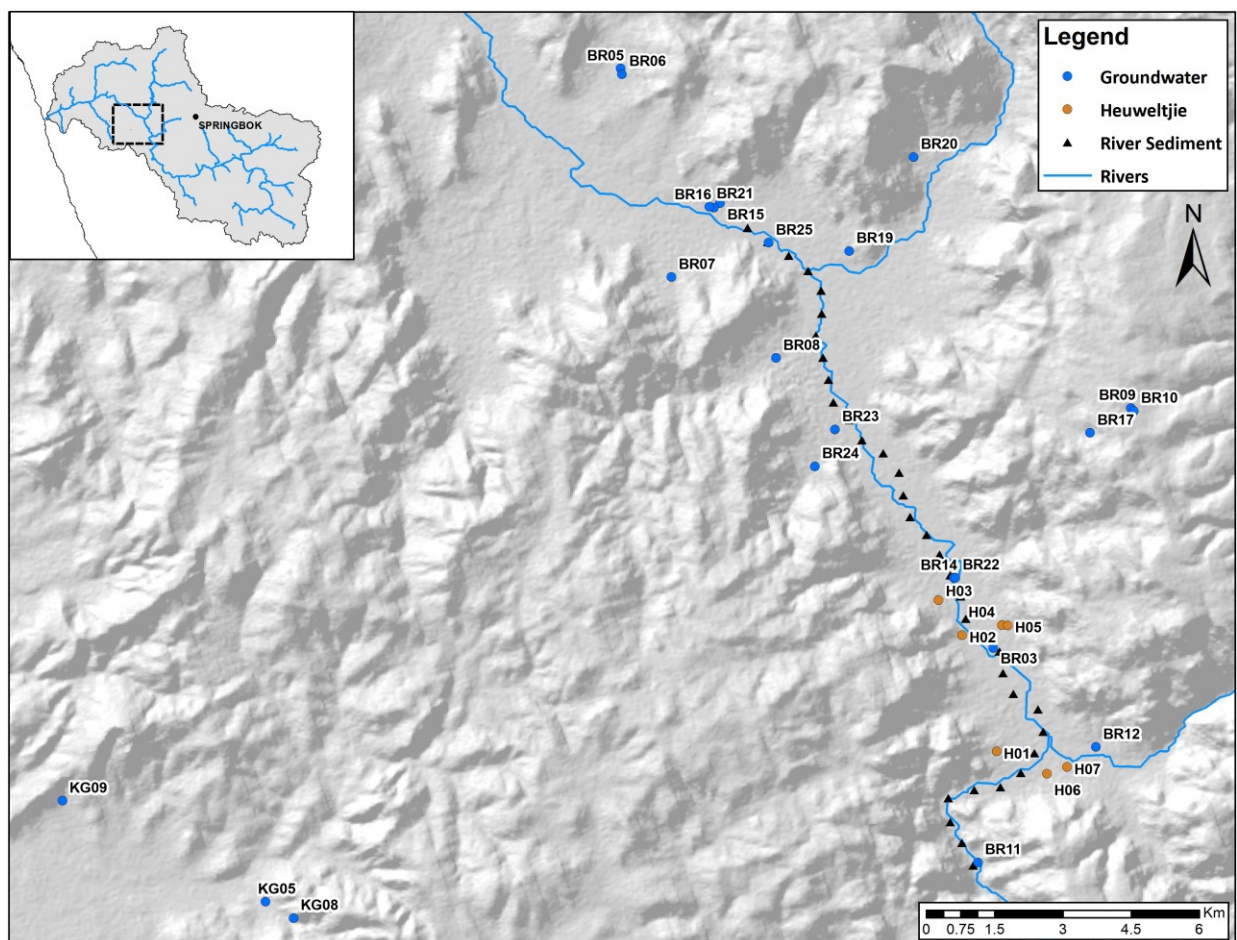


Figure 3.1: Sample locations within the study area.

### **3.1.1. Groundwater**

During a desktop hydrocensus prior to field sampling, boreholes were identified that could be targeted for groundwater sampling in the Buffels River Valley. The National Groundwater Archives were used in combination with a database from previous field trips and approximately 20 boreholes were identified for sampling. During a subsequent field hydrocensus, the target boreholes were assessed in terms of infrastructure and pumping rates. In the end, a total of 23 sampling sites were identified and sampled (Figure 4). These included springs, boreholes and wells.

### **3.1.2. Rainwater**

Rainfall collectors have been set up at two locations in Buffels River, one location in Komaggas and one location in Kleinzee (see Figure 3.2). Local community members assisted in managing the sample collection and therefore the sites were identified based on the proximity to towns or settlements. Rainwater sampling started in 2015 and continued after this study was completed.

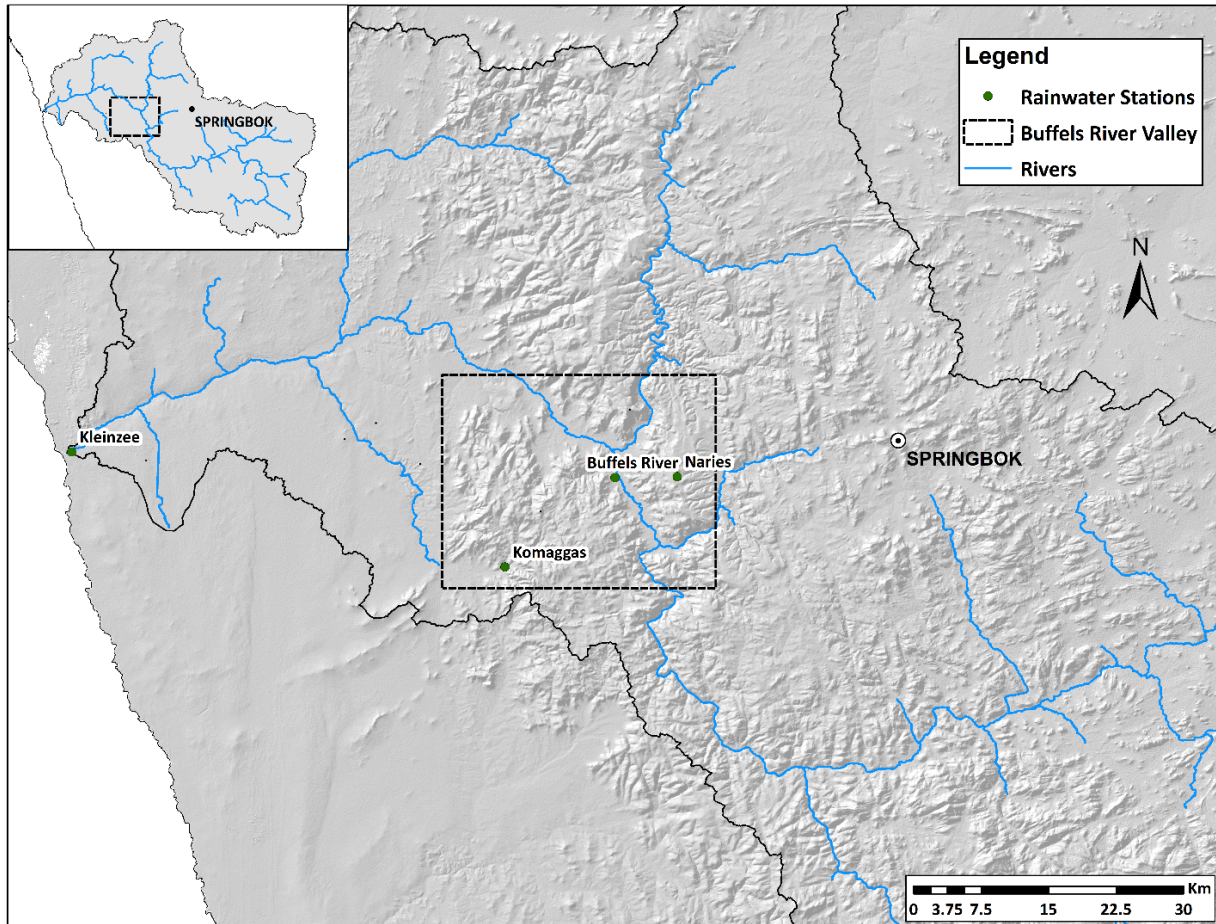


Figure 3.2: Map indicating rainfall stations with reference to the Buffels River Valley.

### 3.1.3. Sediments

A series of sediment sampling sites were identified (Figure 3.1) and collected between March and May 2017. River sediment samples were collected from the centre of the river bed. Samples were collected every 500m from the southern end of the valley towards the northern end where the valley widens. The second set of samples were collected from heuweltjies and their interheuweltjies across the valley. Seven heuweltjies and their respective interheuweltjies in three different locations, with minimum human activity, were chosen. The last set of samples were collected on a grid. An area where heuweltjies are abundant was chosen and a grid was set up across three heuweltjies and their respective interheuweltjie zones.

## **3.2. Sampling Procedures**

Groundwater, rainwater and sediments were sampled for various parameters. Samples were taken according to laboratory specifications. These procedures are outlined in the following section.

### **3.2.1. Groundwater sampling**

There are 25 known boreholes and one spring were identified in the in the Buffels River Valley. The town of Komaggas has eight boreholes and one spring. These sampling locations have varying infrastructure. Before any sampling took place, a dipmeter was used to determine the static water level and possible borehole depth of each borehole. Furthermore, downhole EC profiling was performed by means of a Solinst Level Logger. Eight of the boreholes in the Buffels River Valley and five of the boreholes in Komaggas have pumps which are either operated by generator or by solar panels and was sampled via pumping, see Figure 3.3 b. Two of the boreholes in Buffels River Valley are connected to windmills while the remaining six do not contain any infrastructure and required bailing (Figure 3.3 a & c). Two of the boreholes in Komaggas required bailing. Both of the springs, one in Buffelsriver and one in Komaggas, flow continuously and are connected to a piping system. The boreholes were purged according to Weaver, Cavé and Talma, (2007) before sampling. Before the sample was collected from the well in the river bed, a garden shovel was used to deepen the trench and remove sediments from the sidewall of the trench for the inflow of fresh seepage water. The sample was collected by placing the sampling vessel against the fresh trench wall, allowing seeping water to flow into the vessel. Groundwater sampling took place in November 2016 and March 2017.

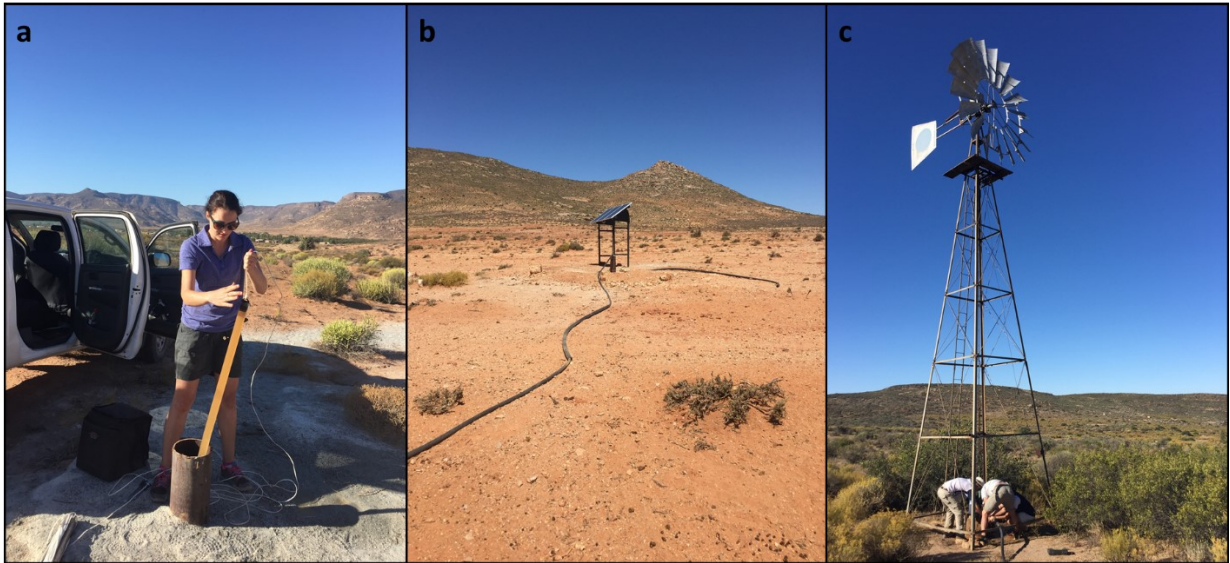


Figure 3.3: a) Bailing for sample BR24; b) solar pump on borehole BR05; c) windmill pumping groundwater at BR09.

#### ***Sampling procedure for major cations, anions and isotopes***

Groundwater samples were collected in sterilized Nalgene bottles. As part of the sample collection process, in-field EC (electrical conductivity), pH, temperature and Eh (oxidation-reduction potential) were measured using ExTech EC500 and ORP probes. The probes were calibrated every morning before sampling took place. Calibration was done by means of pH and EC standard solutions. Samples were then filtered through sterilized 0.45 $\mu$ m cellulose acetate filters, connected to a syringe, into sterilized Polypropylene conical tubes and labelled according to the sampling site and analyses to be performed. Sampling vessels were filled completely to ensure that no air remained. Samples for cation analyses were collected in 15ml tubes and acidified to a pH of 2 with ultra-pure HNO<sub>3</sub>.  $\delta^{18}\text{O}$  and  $\delta^2\text{H}$  samples were also collected in 15ml tubes. 50ml conical tubes were used to collect samples for anion, alkalinity, EC and pH,  $^{87}\text{Sr}$  and  $^{36}\text{Cl}$  isotope analyses. All samples were kept refrigerated at 4°C until analyses took place.

#### ***Sampling procedure for noble gas analyses***

Samples for noble gas and tritium analyses were collected in November 2016. Sampling sites were identified based on the accessibility and flow rate. Seven sampling sites were identified



and samples were taken in duplicate (total of 14 samples). Samples were collected in copper tubes with a length of 50cm and a diameter of 10mm, by means of a PVC adapter. The PVC adapter was attached directly to the groundwater outlet and sealed to ensure that the connection was airtight, see Figure 3.4 a & b. Groundwater flow pressure was controlled by two tap outlet systems, fixed to the PVC adapter. The copper tube was attached to the third outlet and the groundwater was left to run through the system. Air bubbles were removed from the copper tube by tapping a metal rod against the tube. A metal clamp used to close down the far end of the copper tube, allowing water to still flow into the tube, but not out as seen in Figure 3.4 c. A second metal clamp was used to close off the end attached to the PVC adapter, trapping the sample within the copper tube. Tritium samples were collected in 1 litre Nalgene bottles. The bottles were rinsed three times before the sample was taken. The groundwater sample was taken directly from the outlet system and all bottles were filled completely to ensure that no air bubbles have been trapped inside the sampling vessel.



*Figure 3.4: a) PVC adapter connected to a borehole, copper tubes connect to clear plastic tube on the side of the adapter; b) PVC adapter with its valves open to regulate water pressure into the copper tube which was attached to the clear plastic tube; c) air bubbles being removed from the copper tube which is connected directly to the spring via the clear plastic connection tube.*

### **3.2.2. Rainwater**

Rainfall collectors have been set up at two locations in Buffels River, one location in Komaggas and one location in Kleinzee. Rainwater was collected by various nominated community members. After each rainfall event, the date, time and volume were documented and a sample was taken in a sterilized conical tube. These samples are stored at 4°C in a refrigerator by the nominated community member. Samples were collected from the community members during fieldwork campaigns. These rainwater samples were filtered through sterilized 0.2µm cellulose acetate filters into the appropriate containers depending on the analyses as described in the groundwater sampling section. Samples were prepared for analysis in the same manner as the borehole and spring samples.

### **3.2.3. Sediments**

Four sets of sediment samples were collected from the study area. At each site, a sample of approximately 1kg was collected in a large clear plastic bag and a second sample of approximately 50g was collected in smaller clear plastic bags. Sediments were collected by using a garden spade and a hand auger. GPS coordinates were recorded at each sampling site.

#### ***River sediments***

Samples were collected from a 17 km section of the river bed of the Buffels River. Starting at the southern end of the Buffels River Valley, a sample was collected every 500 m until the northern end of the Buffels River Valley was reached. A total of 32 samples were taken. A garden shovel was used to dig sampling pits to depths of between 30 cm and 50 cm depending on the amount of cave in. Samples were taken and GPS coordinates were recorded.

#### ***Heuweltjies and interheuweltjies***

Sediment samples were collected from heuweltjies and their respective interheuweltjie areas. To ensure that the data is representative of the entire Buffels River Valley, seven heuweltjies in three different locations within the valley were identified and sampled. Samples were taken at various depths from the centre and 10m away from to the north and south on the

heuweltjies. Interheuweltjie zones were sampled in 4 areas around the heuweltjies. Samples were taken in a northern, eastern, southern and western direction with respect to the centre of the heuweltjie. The four sampling points around each heuweltjie were the same distance from the centre of the heuweltjie. This distance depended on the size and slope of the heuweltjie as the sample had to be taken off the heuweltjie and in the low-lying area around the heuweltjies. Samples were collected using a hand auger and garden shovel as seen in Figure 3.6 a, b & c. A surface sample was collected at each sampling point on the heuweltjies together with a sample at 30 cm to 50 cm deep and at 1 m deep where possible. The depths at which samples were taken from was dependant on sediment hardness as well as cave in. Samples were placed in plastic sampling bags, labelled and taped. Each sample was placed in a second plastic bag to avoid contamination (Figure 3.6 d).

A grid was set up using Google Earth and ESRI Arc Map to target sampling locations for the third set of sediment samples (Figure 3.5). An area where three heuweltjies are closely spaced was identified and sampling locations were spaced 8.5m apart. A total of 100 samples were taken in an area of 76.5m x76.5m. The hand auger and garden shovel were used to sample the sediment material at each location (Figure 3.6 a, b & c). The initial idea was to sample at a depth of 50cm, but due to the hardness of the sediment layers, samples were taken at various depths (Figure 3.7). A total of 17 samples were taken at a depth of 50cm, seven samples at depths between 40 and 49cm, 11 samples at depths between 30 and 39cm, 28 samples at depths between 20 and 29cm, 26 samples at depths between 10 and 19cm and 11 samples at a depth of 5cm.

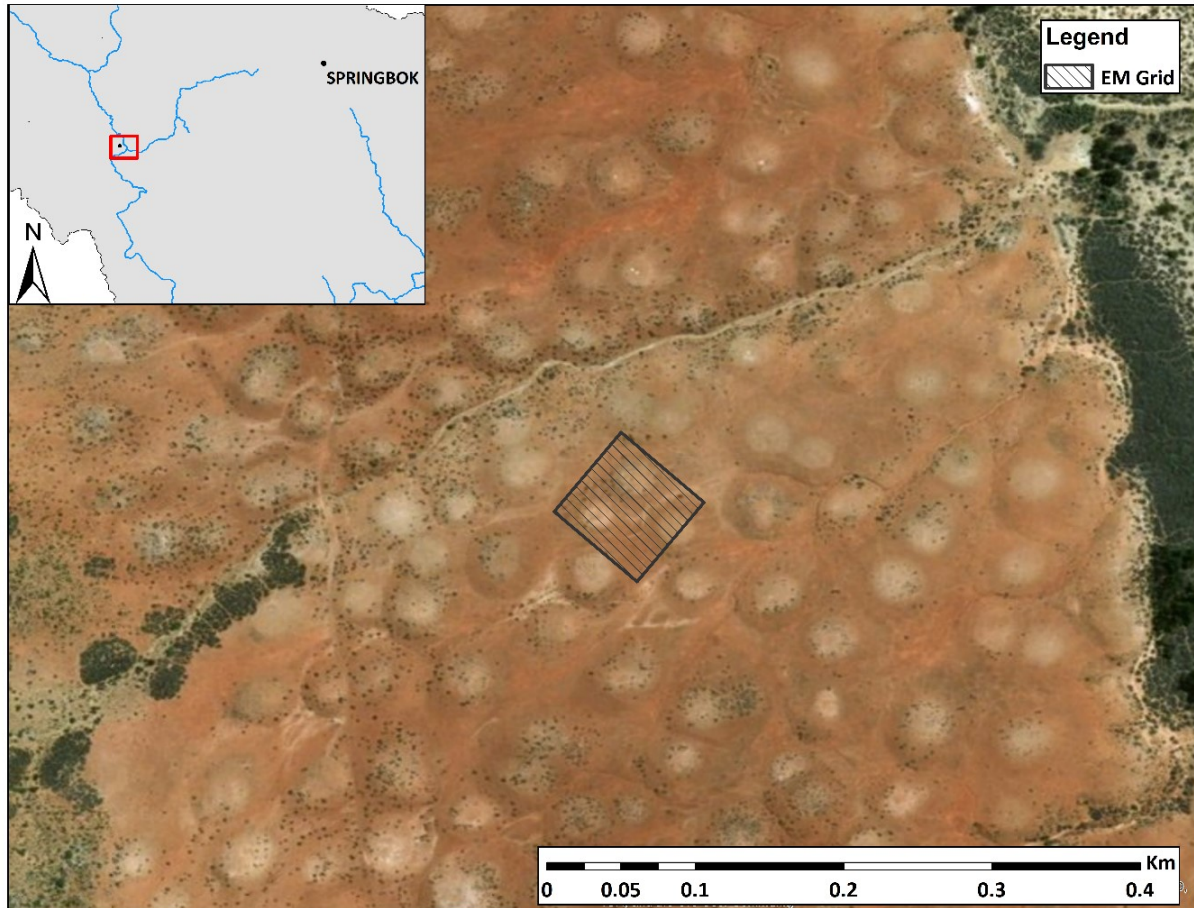


*Figure 3.5: Aerial image of the location of the grid.*

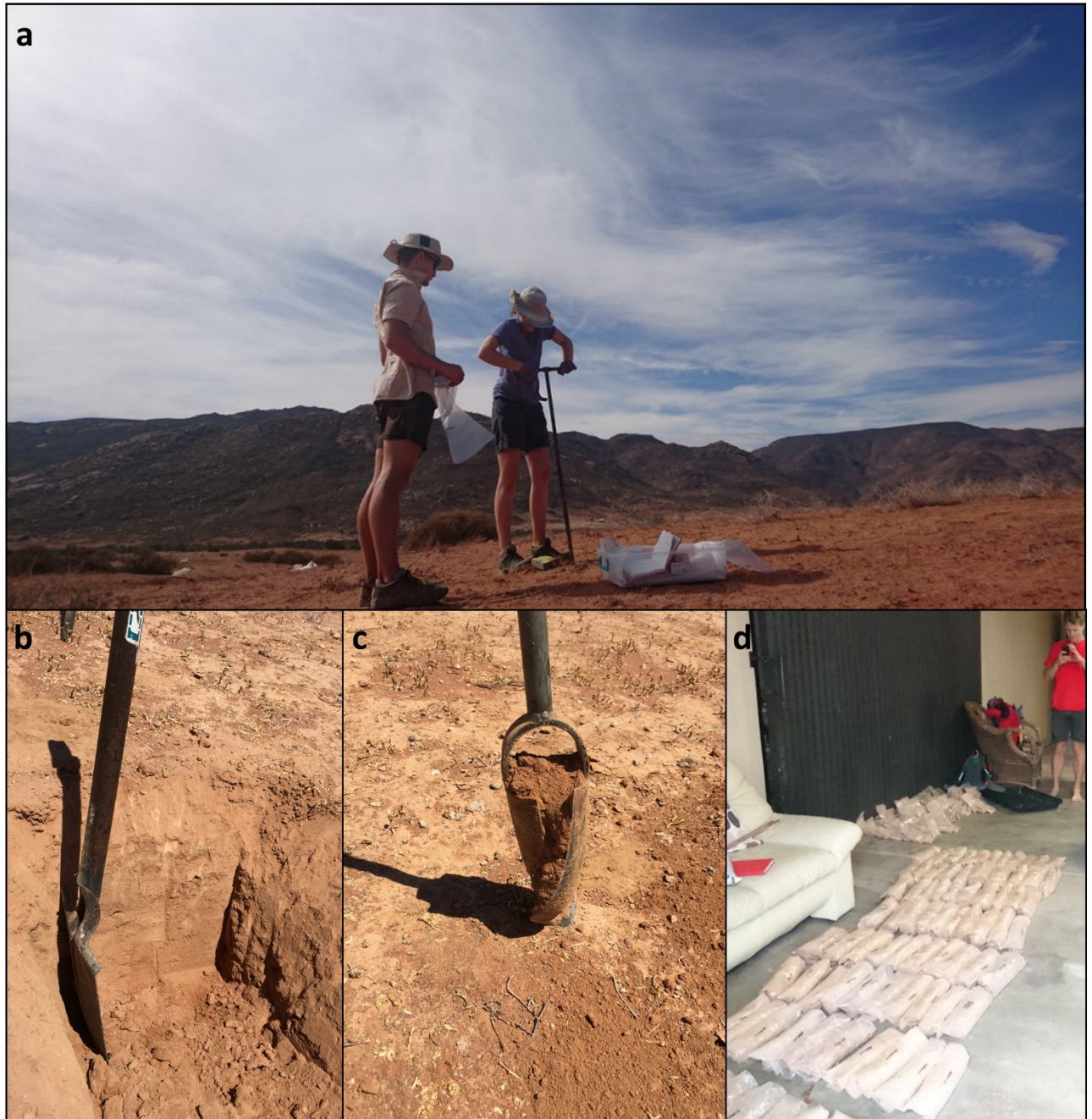


*Figure 3.6: a) Augering and collection of a grid sample; b) pit with minimum cave in from which a shallow interheuweltjie sample was collected; c) auger head filled sediment sample; d) grid samples after being placed in two sample bags and sealed.*

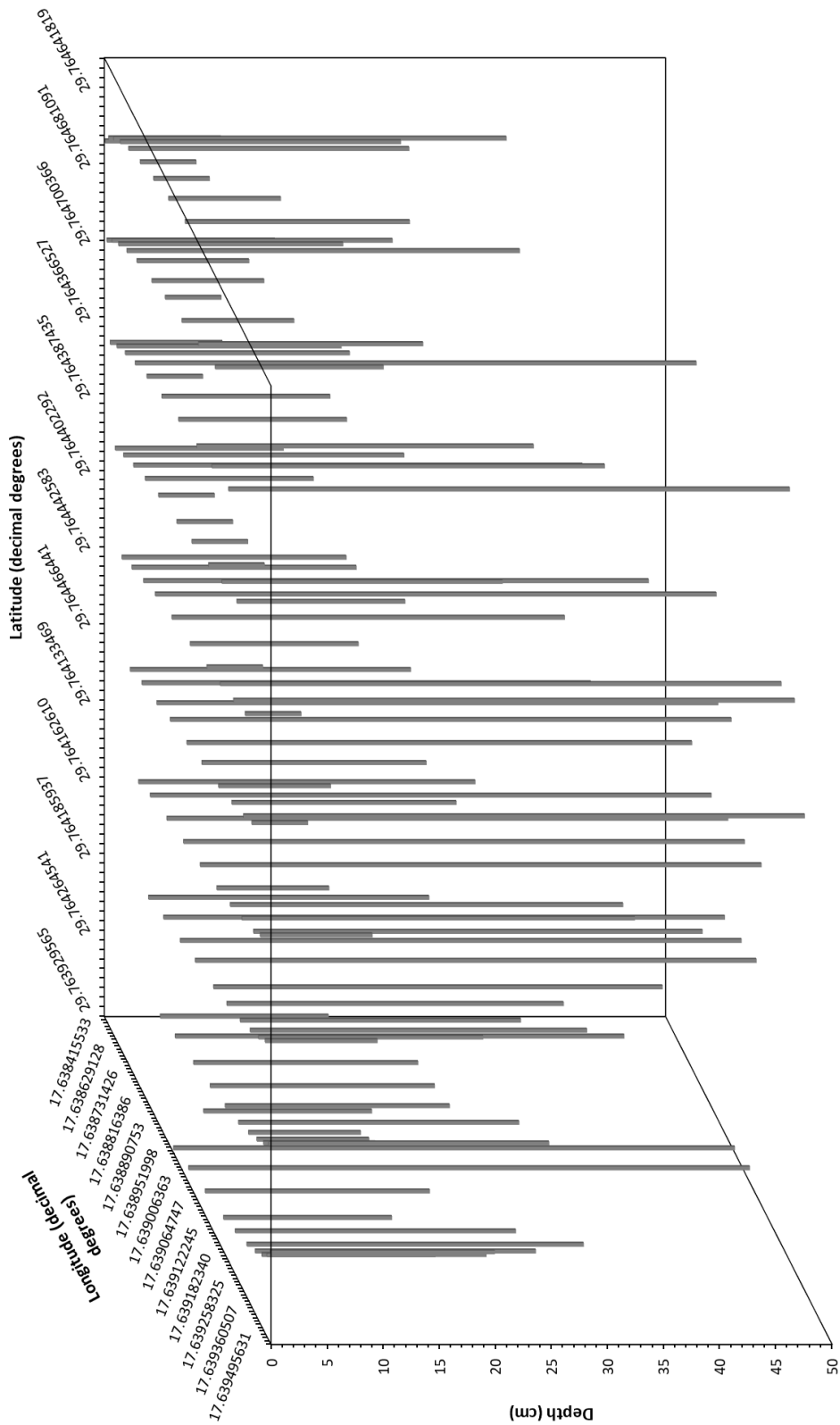


Figure 3.7: Relationship between sampling location within the grid and relative depths of each sample.

### 3.3. Analytical methods

#### 3.3.1. *Electrical Conductivity and pH*

Groundwater and sediment EC and pH were measured at various stages during sampling and processing.

##### **Groundwater**

Although EC and pH were measured in the field, accurate laboratory measurements were done after field trips. Alkalinity, pH and EC were measured in the laboratories of the Department of Soil Science at the University of Stellenbosch using of a 702 SM Titrino auto-titrator and a Jenway 4510 conductivity probe. All the instruments were calibrated appropriately before analyses took place. The temperature of each sample was measured during EC measurements in order to convert and report EC at 25°C. The following conversion was used to report EC at a temperature of 25°C:

*Equation 6:*

$$K_{25} = \frac{K_T}{1 + (\alpha/100)(T - T_{25})}$$

Where  $\alpha$  is the temperature correction coefficient, T is the measured temperature,  $K_T$  the EC at temperature T,  $K_{25}$  the EC at 25°C and  $T_{25}$  the reference temperature of 25°C.

As a control, these parameters were also measured by Bemlab in Somerset West. Alkalinity and pH were measured by a titration method using an electrically operated titrator, while EC was measured by a conductivity probe. Results for EC was reported at 25°C.

##### ***Soils and sediments***

Sediment samples were dried in a temperature and humidity controlled drying room in the Department of Soil Science at the University of Stellenbosch. A fraction of each sample was sieved through a 2mm sediment sieve for further analyses. EC and pH measurements were performed on the same samples. 10g of the sieved fraction and 25 ml of MQ water was placed



in a clean vile and placed in the shaker for the first 30 minutes shaking cycle. Sediment pH was measured first via a Metrohm 827 pH lab. After the addition of a second aliquot of 25ml of MQ water and the second 30 minute cycle of shaking, the sediment EC was measured using a Jenway 4510 EC probe. Temperature corrections for sediment EC were done by the same equations used for water samples.

### **3.3.2. Cations and Anions**

The pre-acidified 15ml cation samples, as well as the 50ml anion samples, were sent to Bemlab in Somerset West for analyses. Cation analyses and sulphate analyses were performed by means of inductively coupled plasma optical emission spectrometry (ICP-OES) Chloride analyses were done according to the silver nitrate titration with chromate indicator method. The sample was acidified with  $\text{HNO}_3$ , a chromate indicator was added and silver chloride was added in known aliquots by titration. Chloride in the sample reacted with the silver ions to form a precipitate of silver chloride. The reaction was complete when the excess silver ions started to react with the chromate indicator to form a red-brown silver chromate precipitate. The chloride concentration was then calculated based on the known amount of silver added and the 1:1 stoichiometric relationship between silver and chloride. Nitrate and ammonia were analysed by continuous flow analysis in combination with flow injection analysis and spectrometric detection. **Error! Reference source not found.** provides the detection limits and errors for each parameter.

Table 3.1: Detection limits and errors for chemical parameters analysed at Bemlab.

Parameter	Detection limit	Uncertainty
EC (mS/m)	0.759	0.02
Na (mg/L)	0.52	0.036
K (mg/L)	0.467	0.028
Ca (mg/L)	0.047	0.06
Mg (mg/L)	0.062	0.032
Fe (mg/L)	0.037	0.145
B (mg/L)	0.083	0.415
Cu (mg/L)	0.026	1.194
Zn (mg/L)	0.0256	0.379
Cl <sup>-</sup> (mg/L)	0.33	12.98
HCO <sub>3</sub> <sup>-</sup> (mg/L)	4.02	0.691
SO <sub>4</sub> <sup>2-</sup> (mg/L)	1.429	0.21
P (mg/L)	0.0111	0.592
F (mg/L)	Not reported	Not reported
NO <sub>3</sub> -N (mg/L)	0.357	0.028
NH <sub>4</sub> -N (mg/L)	0.278	0.013

### 3.3.3. O and H isotopes

Samples were analysed for  $\delta^{18}\text{O}$  and  $\delta^2\text{H}$  isotopes using a Los Gatos Research (LGR) Liquid Water Isotope Analyser by the Environmental Isotope Group (EIG) at iThemba LABS in Johannesburg. Laboratory standards which have been calibrated against the VSMOW2 ( $\delta^2\text{H}$  0.0,  $\delta^{18}\text{O}$  0.0) international reference materials were analysed with each batch of samples. The analytical precision for stable oxygen isotopes is 0.5‰, while that of hydrogen isotopes is 1.5‰. Results were reported as  $\delta^{18}\text{O}$  and  $\delta^2\text{H}$  where:

$$\delta (\text{‰}) = \left[ \frac{R_{\text{sample}}}{R_{\text{standard}}} - 1 \right] \times 1000$$

Delta values were reported as per mil deviation relative to the standard mean ocean water (SMOW). Due to time constraints, samples taken in March 2017 were sent to the Department of Geological Sciences at the University of Cape Town (UCT). During the analytical procedure at UCT, samples were placed in glass tubes and analysed by wavelength-scanned cavity ring-down spectroscopy using a Picarro L2120-i. Six injections were made for each sample, with the first three being discarded to avoid memory effects. The standards ACTMP ( $\delta^2\text{H} = -0.2 \text{ ‰}$ ,  $\delta^{18}\text{O} = -0.78 \text{ ‰}$ ) and RMW were used to convert raw data to the SMOW scale and to correct for drift, and scale compression. Evian Water was analysed as blanks every 10 analyses and  $\delta\text{D}$  and  $\delta^{18}\text{O}$  values of  $-71.6 \text{ ‰}$  ( $1\sigma = 1.36$ ,  $n = 12$ ) and  $-10.33 \text{ ‰}$  ( $1\sigma = 0.33$ ,  $n = 12$ ), respectively were within the accepted values for Evian Water ( $\delta\text{D} = -73.1 \text{ ‰}$  and  $\delta^{18}\text{O} = -10.2 \text{ ‰}$ ). The results obtained from analyses at UCT were reported in the same manner as that of iThemba Labs. All  $\delta\text{D}$  and  $\delta^{18}\text{O}$  values are reported relative to SMOW.

#### **3.3.4. Sr isotopes**

Strontium isotope sample preparation and analyses were performed at analytical facilities at UCT. In preparation for the analysis, the sample was dried down as 6ml aliquots.  $\text{HNO}_3$  was added to the solid phase remaining from each aliquot, followed by a second drying cycle. 1.5ml of 2M  $\text{HNO}_3$  was again added to each Teflon vial and the sample was decanted into a standard cation exchange column in which Sr ions were extracted. The extracted Sr ions were washed from the cation exchange column, dried down and sent for analysis. In preparation for the analysis, each sample was dissolved in 0.2%  $\text{HNO}_3$  and diluted to Sr concentration of 200ppb.  $^{87}\text{Sr}/^{86}\text{Sr}$  ratios were analysed for using a NuPlasma HR multi-collector-ICP-MS and a NIST SRM 987 solution, with a  $^{87}\text{Sr}/^{86}\text{Sr}$  reference value of 0.710255. The data were corrected for isobaric interferences and mass fractionation of  $^{85}\text{Rb}$  according to the exponential law.

### **3.3.5. <sup>36</sup>Cl isotopes**

Chlorine-36 samples were prepared for analyses in the Department of Soil Science laboratories at the University of Stellenbosch. Samples were decanted into acid washed glass beakers and acidified with 2ml of ultrapure HNO<sub>3</sub>. Thereafter, samples were moved to a dark room where the sample preparation was completed since AgCl is light sensitive. 1ml of a 50g/l AgNO<sub>3</sub> solution was then added to the sample to produce a white AgCl precipitate. After a settling period of 30 minutes, the supernatant was discarded and the wet precipitate was decanted into sterilized PP tubes, followed by a cycle in the centrifuge. Again, the remaining supernatant was decanted and the precipitate was dried down at 60°C. The tubes containing the resultant precipitate were wrapped in aluminium foil to prevent any light from entering the tubes. Samples were sent to the Australian National University in Canberra, Australia where the concentration of the <sup>36</sup>Cl isotope was measured via AMS.

### **3.3.6. Noble gases**

The copper tubes containing water samples for noble-gas analysis and the 1-litre bottles containing the tritium samples were sent to the Isotope Climatology and Environmental Research Centre of the Institute for Nuclear Research at the Hungarian Academy of Sciences in Debrecen, Hungary. Samples were transferred into stainless steel vessels and stored during degassing for 20-80 days. Degassing of <sup>3</sup>He, the product of radioactive decay of <sup>3</sup>H is required to remove all the initial <sup>3</sup>He, so that new tritiogenic <sup>3</sup>He can accumulate for analyses (Palcsu et al., 2010). Helium concentrations and isotope ratios were determined using a noble gas mass spectrometric system (Figure 3.8) which includes a cryogenic preparation line and a VG5400 noble gas mass spectrometer. The cryogenic cold system allows gasses to be adsorbed onto various traps as the temperature is increased or decreased. Argon and other chemically active gasses were trapped first at a temperature of 25K. Then, at a temperature of 10K, neon and helium were adsorbed onto a charcoal trap. The temperature was then increased and helium and neon were trapped at 42K and 90K respectively. At 150K, a fraction of the remaining gas that was trapped in a stainless-steel trap was injected into a getter trap. Each trapped fraction was then analysed by the noble gas mass spectrometer. Known air aliquots were used to calibrate all the procedures. Relative analytical uncertainties were 1%

for He and Ar concentrations, 2% for Ne, Kr and Xe concentrations, and 2.5% for  $^3\text{He}/^4\text{He}$  ratios.



*Figure 3.8: Noble gas mass spectrometric system at the Isotope Climatology and Environmental Research Centre of the Institute for Nuclear Research at the Hungarian Academy of Sciences.*

### 3.4. EM38

An electromagnetic survey was conducted using a Geonics Limited EM38-MK2 (Figure 3.9). The same 76.5x 76.5m area that was sampled as a grid was used for this survey (Figure 3.5). A set of markers were placed on the surface to guide the survey. Survey lines were spaced every two meters to ensure full coverage. The instrument was held approximately 10cm above the surface as the operator walked across the marked-out area. The EM38-MK2 is fitted with a transmitter on the one end and a receiver on the other. The transmitter produces an electromagnetic pulse which penetrates the surface to a depth of 1.5m. The pulse interacts with the material and a return pulse is produced which is sent back to the receiver. The electrical conductivity and magnetic susceptibility of the sediments, were measured during the survey. The data was downloaded and interpreted to produce an EC profile.



*Figure 3.9: Geonics Limited EM38-MK2 being set up for scanning the marked-out grid. Note the heuweltjie in the background.*

## 4. RESULTS

### 4.1. EC and pH

EC and pH were measured in the groundwater and the sediments. For the sediments, EC was measured in three different contexts: (i) river sediment EC; (ii) heuweltjie and interheuweltjie sediments; and (iii) using an EM38 electromagnetic scanner to make a detailed map of the sediment EC variation across three heuweltjies and the interheuweltjie spaces between them. These results are presented below.

#### 4.1.1. *Groundwater*

Groundwater EC values range between 804  $\mu\text{S}/\text{cm}$  and 19 580  $\mu\text{S}/\text{cm}$  for samples taken in 2016 and between 868  $\mu\text{S}/\text{cm}$  and 21 300  $\mu\text{S}/\text{cm}$  for samples taken in 2017. Sample BR15 had the highest EC measured in 2016 (19 580  $\mu\text{S}/\text{cm}$ ), while sample BR21 has the highest EC of measured in 2017 (21 300  $\mu\text{S}/\text{cm}$ ). Sample BR25, which is a sample collected from a well in the river bed, had an EC value of 12 090  $\mu\text{S}/\text{cm}$ . In 2016, the two spring samples, BR17, which is in close proximity to the town of Buffels River and KG08, which is in Komaggas, had EC values of 1114 and 853  $\mu\text{S}/\text{cm}$ , respectively. In 2017, the EC value for BR17 decreased to 868  $\mu\text{S}/\text{cm}$  while that of KG08 increased to 887  $\mu\text{S}/\text{cm}$  in 2017. Data from 2016 data and 2017 data follow similar trends (Figure 4.1). Four out of the 20 samples collected in 2017 have EC values higher than 4000  $\mu\text{S}/\text{cm}$ , while two of 17 samples collected in 2016 have EC values above 4000  $\mu\text{S}/\text{cm}$ . Although a similar overall trend can be observed in 2016 and 2017, seven of the 14 samples that were sampled in both years, have higher EC values in 2017 than 2016, as seen in Figure 4.2.

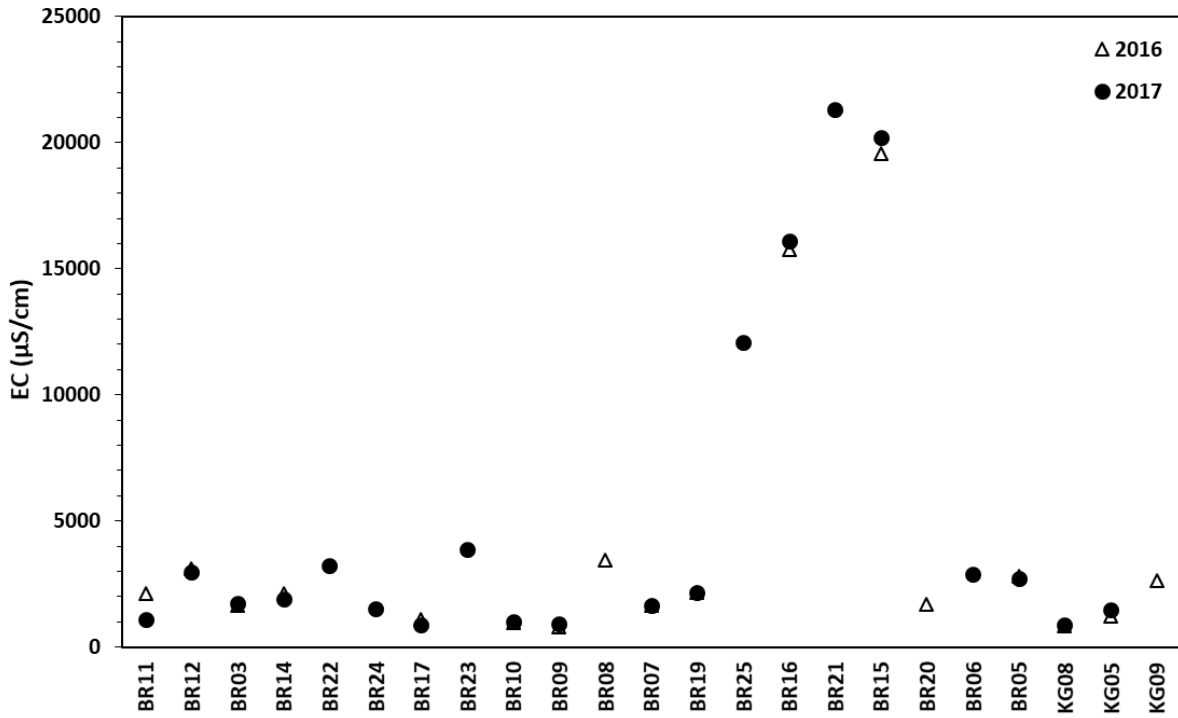


Figure 4.1: EC for groundwater samples in order from South to North.

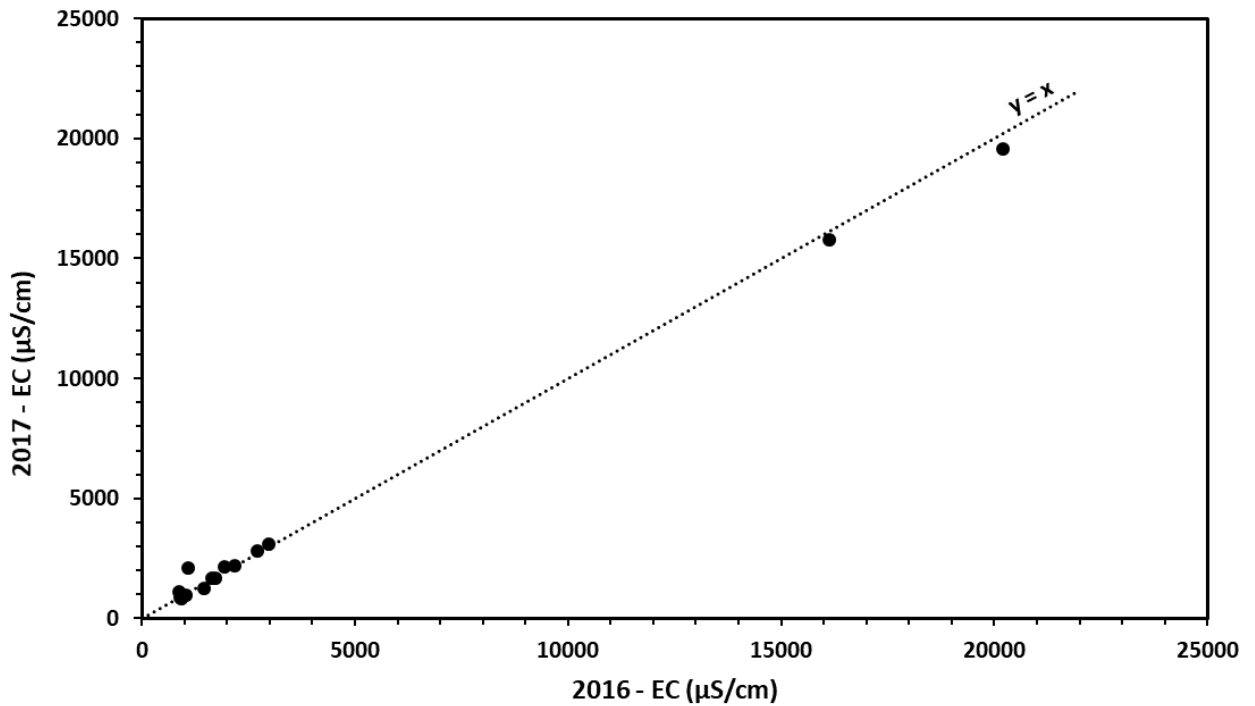


Figure 4.2: Comparison between EC values for groundwater samples taken both in 2016 and 2017.



Groundwater pH values, with the exception of a single sample, measured in 2016 ranged between 6.7 and 7.6. Sample BR15 has the lowest pH values measured with a pH of 3.10 in 2016 and 3.3 in 2017. Sample BR 14 has the highest pH value of 7.6 for the 2016 sample set. Most of the pH values for samples taken in 2017 ranged between 5.6 and 8.1. Sample BR16 has the highest pH value, 8.1 for samples measured in 2017. As with EC, samples measured in 2016 and 2017 follow the same trend (Figure 4.3). Of the 14 samples that were taken in both 2016 and 2017, samples BR03, BR05 and BR12 have the same pH recorded in 2016 and 2017. Samples BR07, BR10, BR19, KG05 and KG08 have lower pH values measured in 2017 than in 2016. The pH values for samples BR09, BR11, BR14, BR15, BR16 and BR17 measured in 2017 were higher than those measured in 2016.

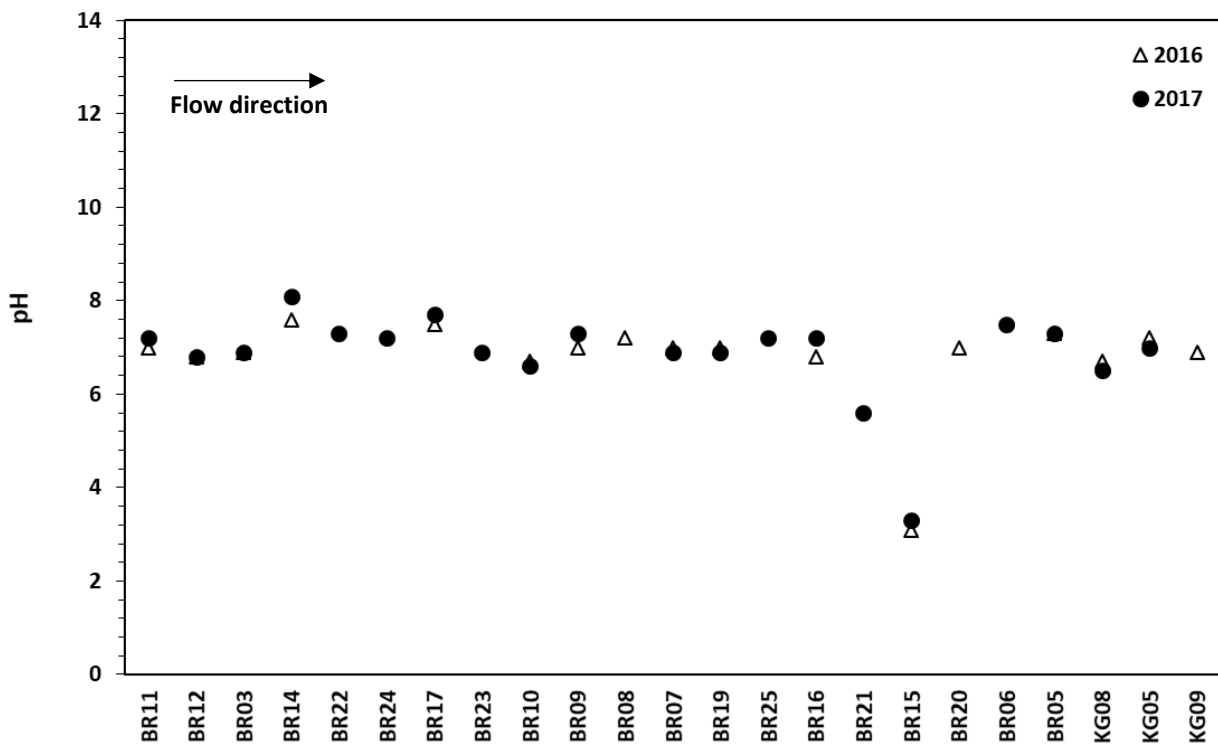


Figure 4.3: Groundwater pH in order from South to North.

#### 4.1.2. Sediments and Soils

##### River Sediments

The river sediment EC, with the exception of two samples, ranged between 7.99  $\mu\text{S}/\text{cm}$  and 92.57  $\mu\text{S}/\text{cm}$  as seen in Figure 4.4. Of the 35 samples, 28 samples had EC's below 20  $\mu\text{S}/\text{cm}$ , while five samples had EC values between 20 and 100  $\mu\text{S}/\text{cm}$ . The sediment EC of two outlier samples, RS11 and RS12, are 289.13  $\mu\text{S}/\text{cm}$  and 2156.33  $\mu\text{S}/\text{cm}$ , respectively. The measured pH values range between 7.13 and 9.02. Of the 35 samples analysed, six samples had pH values between 7.13 and 7.50, 15 samples had pH ranging between 7.50 and 8.00, 11 samples with pH ranging between 8.00 and 8.50 while only 3 samples had a pH above 8.50.

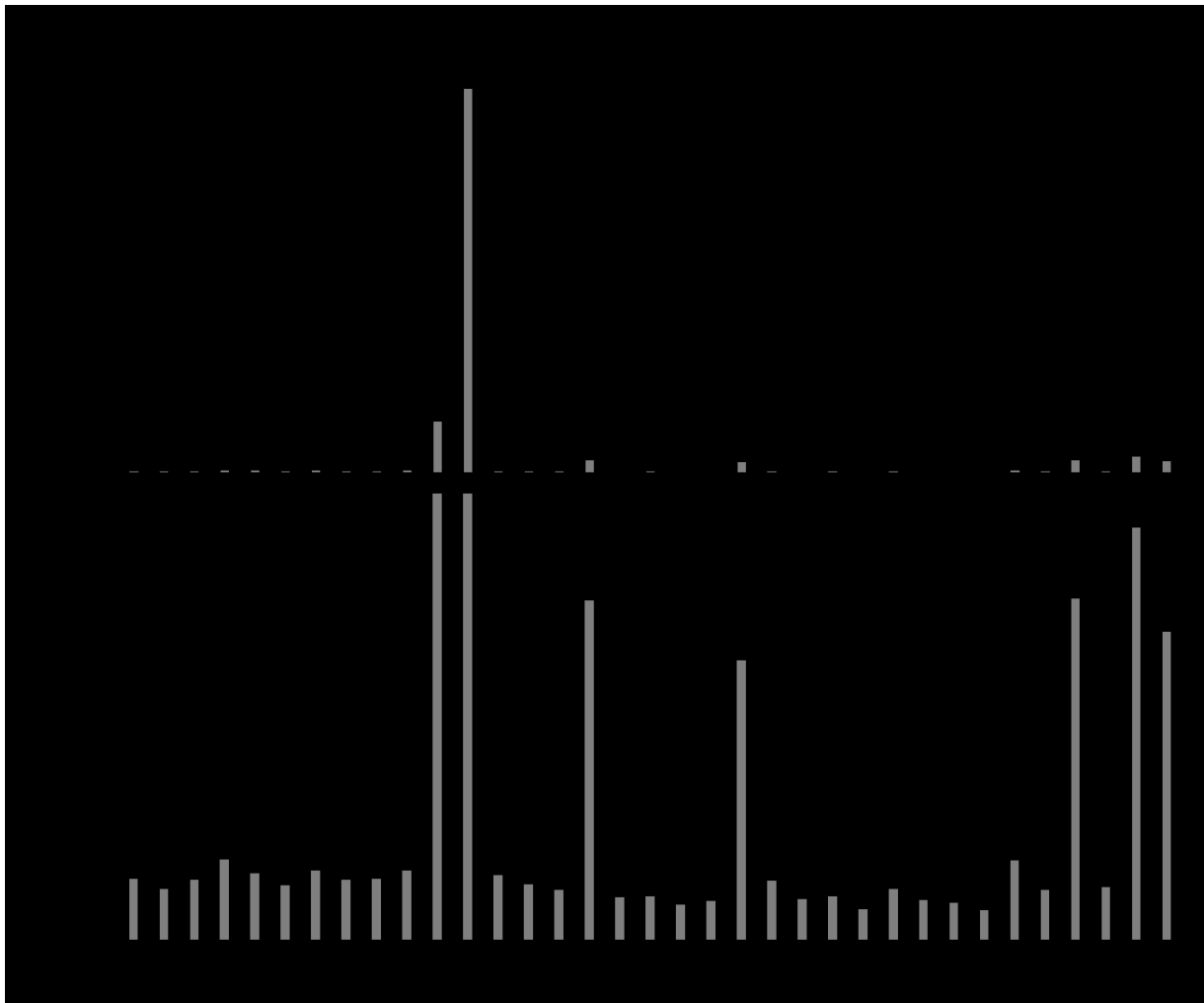


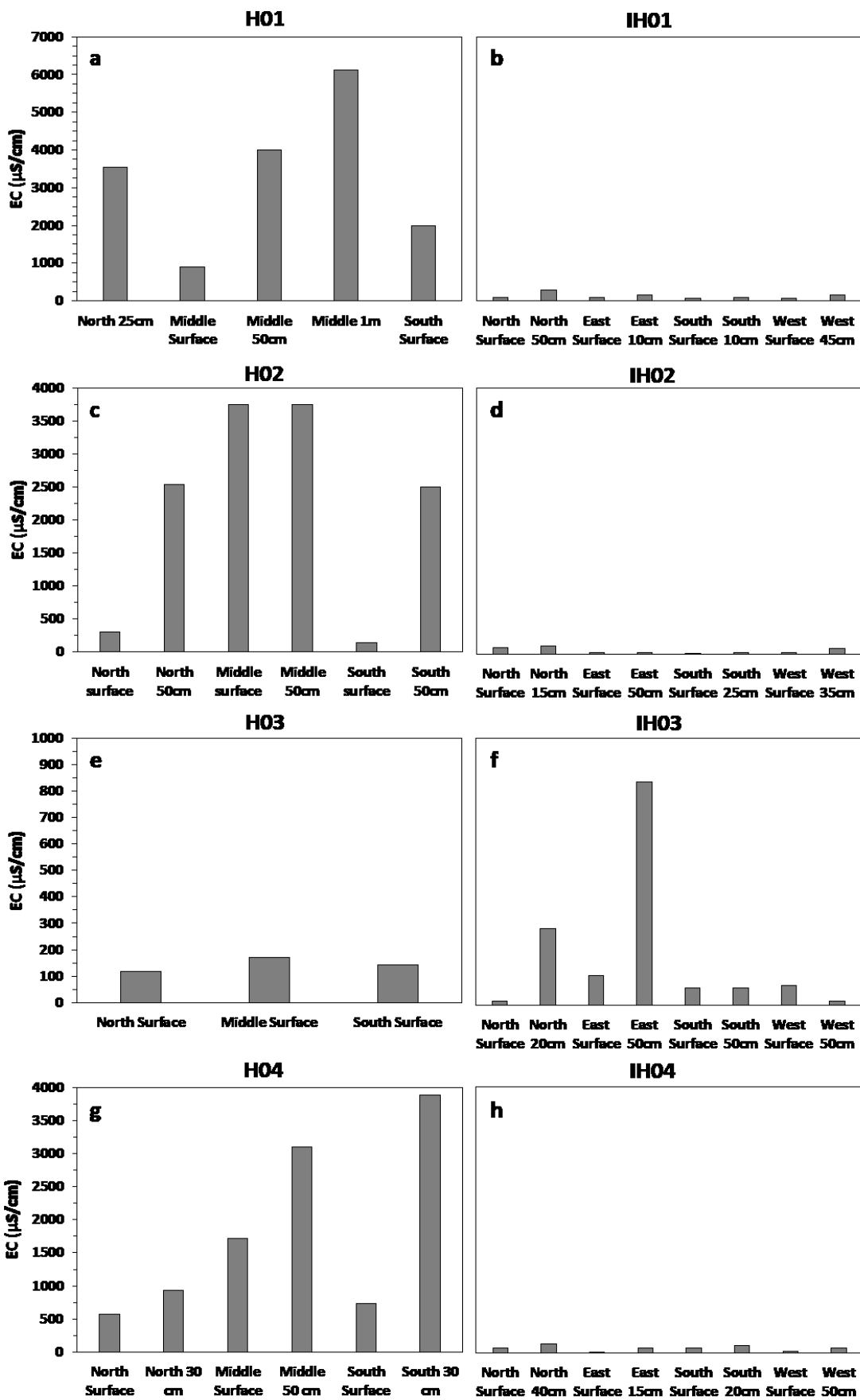
Figure 4.4: a) Comparison between river sediment EC-values with samples in order from South to North, with RS01 being the southernmost sample; b) Comparison between river sediment EC values in the same order as seen in a), with an adjusted EC scale.

### ***Heuweltjies and interheuweltjies***

The sediment EC values for heuweltjies are generally higher than that of the interheuweltjies. Furthermore, EC values of samples taken from the centre of the heuweltjies are higher than EC values of samples taken 10m away from the centre as seen in Figure 4.5 a-m and Figure 4.6. However, there are some exceptions. H03 and IH03 is the only set of samples where the EC values of the interheuweltjies are higher than that of the heuweltjies (Figure 4.5 e & f). The maximum and minimum EC values for H03 were 171.88  $\mu\text{S}/\text{cm}$  (H03 Middle Surface) and 118.53  $\mu\text{S}/\text{cm}$  (H03 North Surface) (Figure 4.5 e). Interheuweltjie sample IH03 East Surface had an EC value of 838.53  $\mu\text{S}/\text{cm}$ , while IH03 West 50cm had the lowest EC value of 14.61  $\mu\text{S}/\text{cm}$  for this particular heuweltjie and interheuweltjie set (Figure 4.5 f). Interheuweltjie IH03 showed the largest variation in EC values of all the interheuweltjies. H04 also deviates from the general trend (Figure 4.5 g & h). The EC value for sample H04 South 30cm, which is 10 m south of the centre of the heuweltjie, has the highest EC value of the H04 and IH04 sample set. The maximum EC value for H04 is 3876.75  $\mu\text{S}/\text{cm}$  for sample H04 South 30cm while sample H04 South Surface had the lowest EC value of 738.72  $\mu\text{S}/\text{cm}$ . Sample IH04 North 40cm has the highest EC value (134.63  $\mu\text{S}/\text{cm}$ ) of IH04, with sample IH04 East 30cm having the lowest EC value of 13.62  $\mu\text{S}/\text{cm}$ .

The average sediment EC for heuweltjie samples, with the exception of H03, is 2801.44  $\mu\text{S}/\text{cm}$ . In contrast to heuweltjie samples, average sediment EC for interheuweltjie samples is 121.55  $\mu\text{S}/\text{cm}$ . Another general trend among most of the heuweltjie and interheuweltjie samples is that deeper samples have higher sediment EC values than shallow samples collected at the same point. The difference between deep and shallow EC values in heuweltjie samples are between 1000 and 3000  $\mu\text{S}/\text{cm}$ , with the deeper samples having the higher EC value. Deep and shallow interheuweltjie samples have a smaller difference in EC values with deep sample EC values being between 50 and 200  $\mu\text{S}/\text{cm}$  higher than that of the shallow samples. Heuweltjies H05 and H06 are exceptions. The surface sample H05 Middle Surface has a higher EC value than sample H05 Middle 10cm (Figure 4.5 i). Similarly, in sample set H06, sample H06 Middle 1m has a lower EC value than sample H06 Middle 50cm. However, the surface sample H06 Middle Surface still has the lowest EC value of the H06 sample set, see Figure 4.5

k. Therefore, in the case of sample set H06, the general trend of an increase in EC values with depth holds true for the surface sample and the sample collected at 50cm, whereas the sample taken at a depth of 1m deviates from the trend. The pH values of heuweltjies and interheuweltjies show very little variation. The average pH value for heuweltjie samples is 8.69 with a standard deviation of 0.38 while that of the interheuweltjie samples is 8.89 with a standard deviation of 0.41, see Figure 4.6. The maximum pH value among the heuweltjies is 9.39 and the minimum value is 8.08. Similarly, respective the maximum and minimum pH values for the interheuweltjie samples are 9.83 and 7.92.



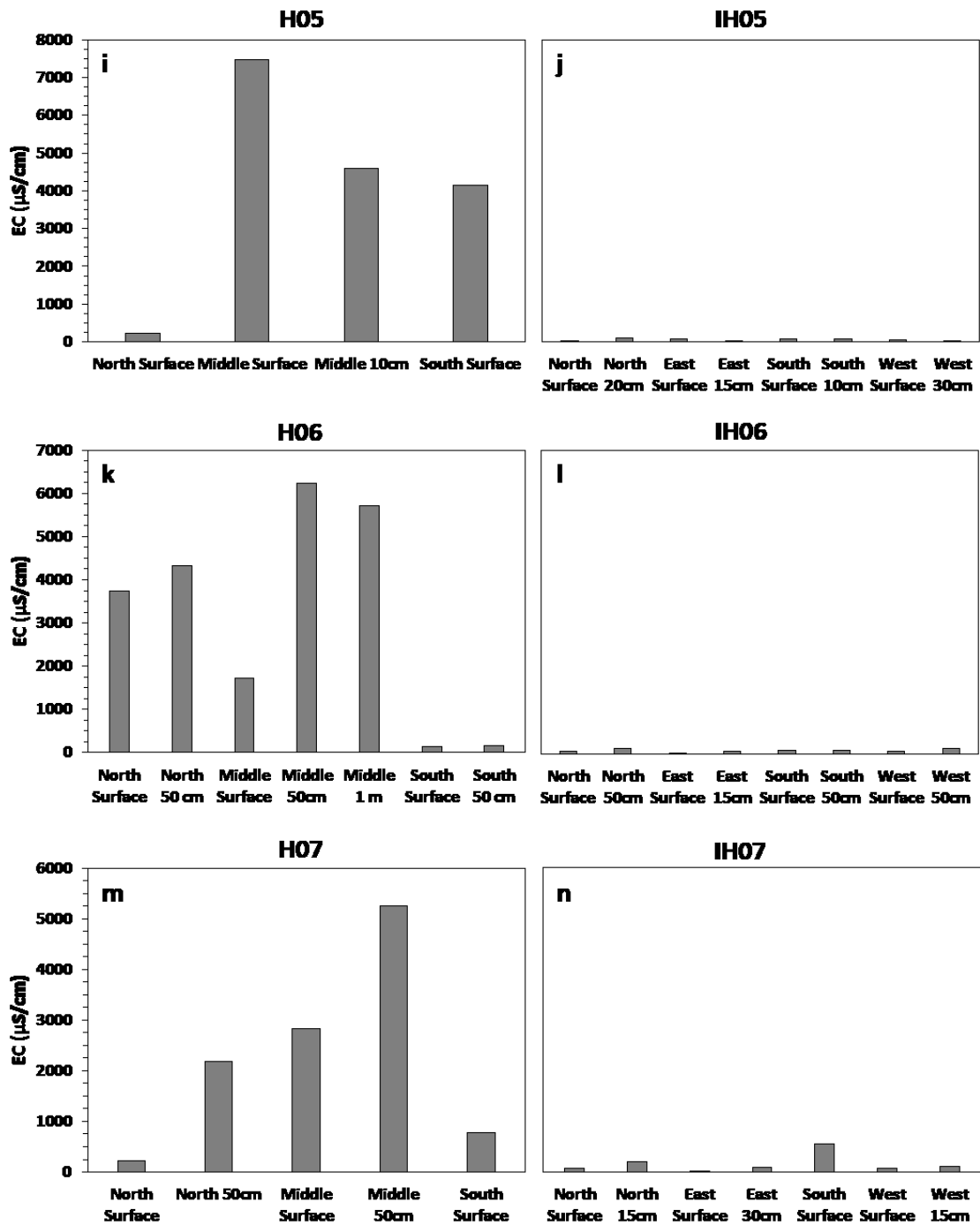


Figure 4.5: Relationship between EC values relative to depths and position of the sample; a-b) heuweltjie and interheuweltjie 1; c-d) heuweltjie and interheuweltjie 2; e-f) heuweltjie and interheuweltjie 3; g-h) heuweltjie and interheuweltjie 4; i-j) heuweltjie and interheuweltjie 5; k-l) heuweltjie and interheuweltjie 6; m-n) heuweltjie and interheuweltjie 7. Note that the EC scale is different for each heuweltjie-interheuweltjie set.

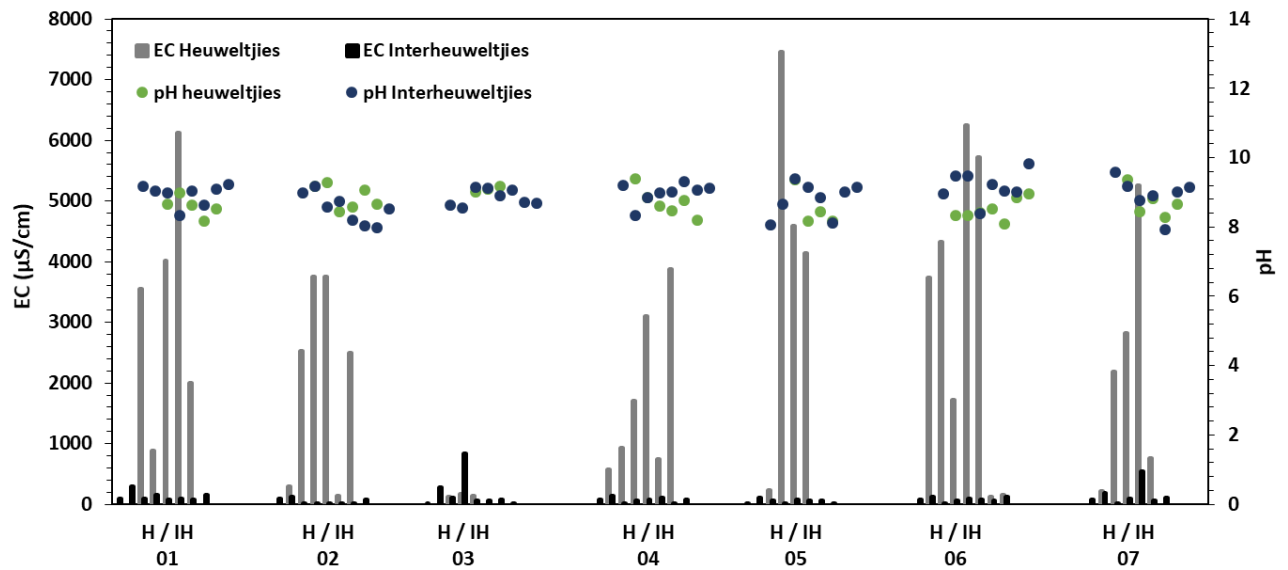


Figure 4.6: Relationship between heuweltjie and interheuweltjie sediment EC and pH distribution.

### Grid

There are large variations in the EC values of the 100 samples collected in the grid. Sample GR74 has the highest recorded EC value of 4790.96  $\mu\text{S}/\text{cm}$ , while sample GR77 has the lowest EC value of 17.54  $\mu\text{S}/\text{cm}$ . Of the 100 samples, 73 samples had an EC below 500  $\mu\text{S}/\text{cm}$  of which 33 samples have EC values between 100  $\mu\text{S}/\text{cm}$  and 200  $\mu\text{S}/\text{cm}$  and 26 samples have EC values between 200  $\mu\text{S}/\text{cm}$  and 500  $\mu\text{S}/\text{cm}$  and 13 samples have EC values higher than 2000  $\mu\text{S}/\text{cm}$ . The mean EC value is 708  $\mu\text{S}/\text{cm}$ . High EC values are clustered together with the highest EC values in the centre of the cluster. When compared to the landscape features, higher EC values are found on heuweltjies. The low EC values are found between a cluster of higher EC values in both Figure 4.7 and Figure 4.9. This can be directly compared to the positions of the heuweltjies and their relative interheuweltjies as seen on the aerial imagery (Figure 3.5). The sediment pH values ranged between 7.39 and 9.83 with a mean pH of 8.58 and standard deviation of 0.42, see Figure 4.8. Sample GR81 has the lowest pH value while sample GR05 has the highest pH.

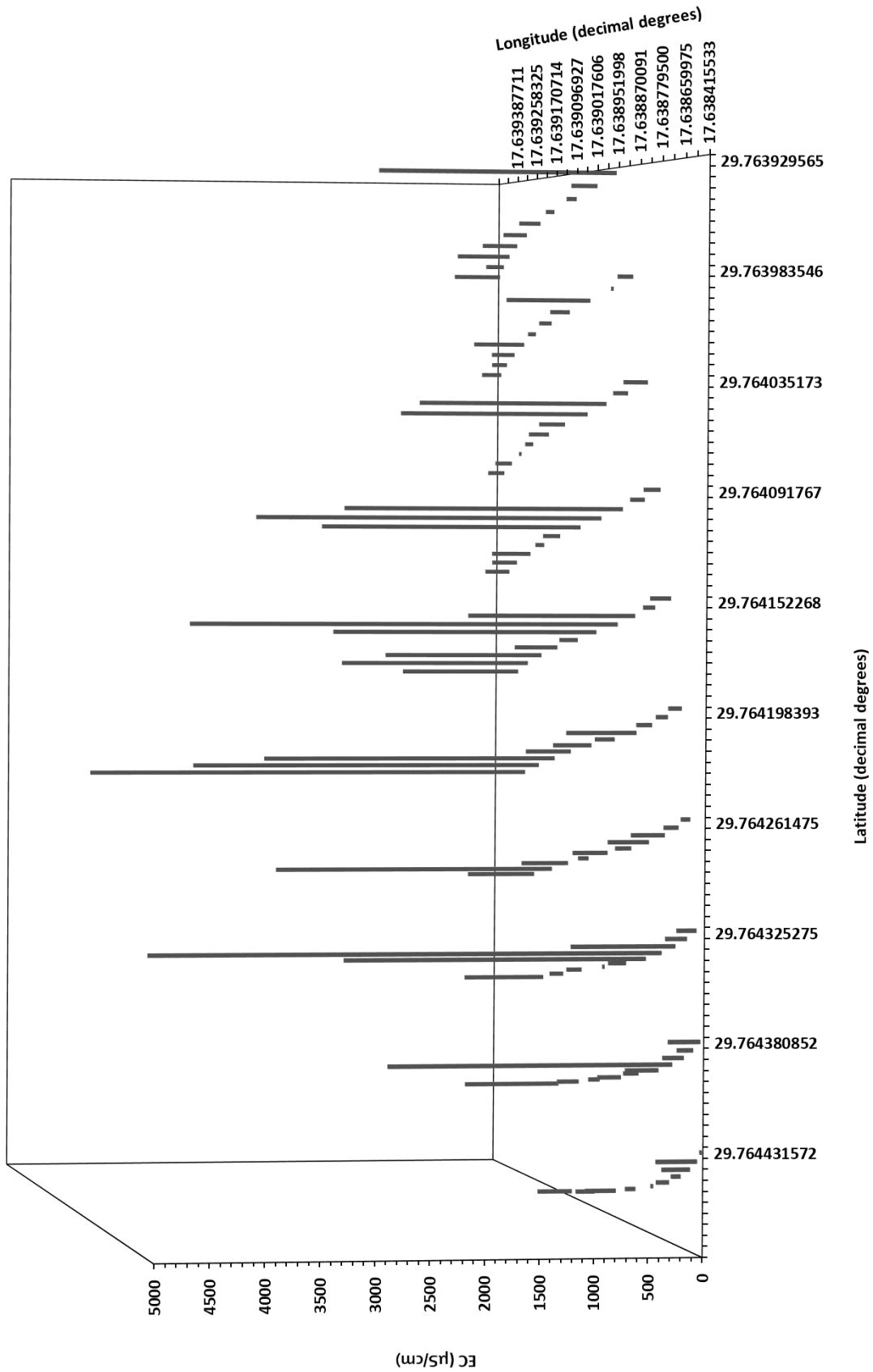


Figure 4.7: Relationship between sediment EC and sampling location within the grid.



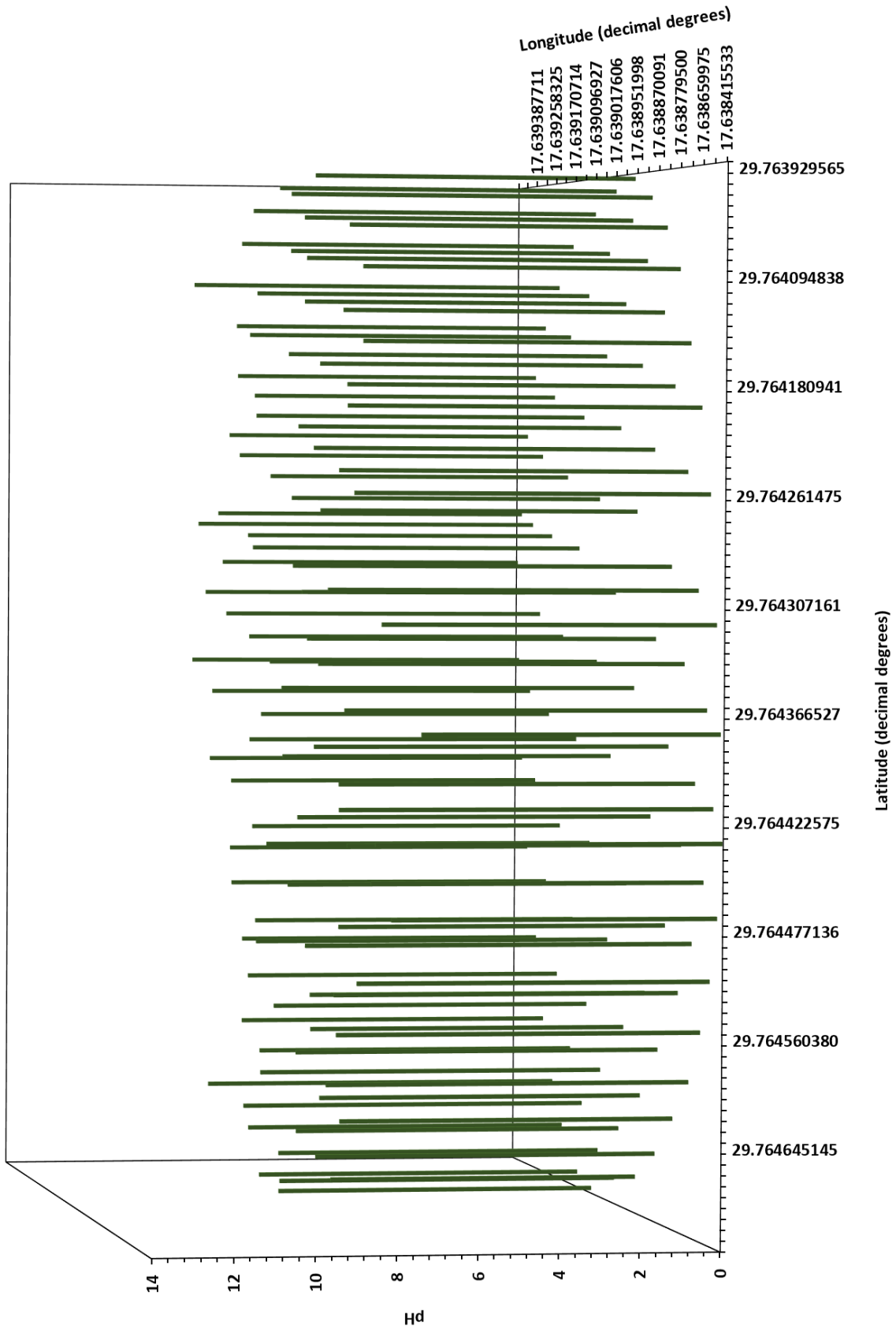


Figure 4.8: Relationship between sediment pH and sampling location within the grid EM-38

**EM-38**

Great variation in sediment EC values is evident in the data obtained from the EM38 scans (Figure 4.9 Figure 4.10). Furthermore, the spatial distribution of EC variations is represented. High EC values are clustered with the EC decreasing gradually from the centre of the clusters and EC values are higher at higher elevations (Figure 4.9). EC values range between 59.38  $\mu\text{S}/\text{cm}$  and 1101.95  $\mu\text{S}/\text{cm}$ . When compared to aerial imagery, the elevated zones with high EC values are spatially related to the heuweltjies (Figure 4.9 and Figure 3.5). The low EC values fall on interheuweltjie areas. Although the EM-38 results follow similar trends to the sediment EC measured in the laboratory, the overall EC measured by the EM-38 is much lower. The maximum EC value of grid sediments that was measured in the laboratory is 4790.96  $\mu\text{S}/\text{cm}$  compared to the maximum EC of 1101.95  $\mu\text{S}/\text{cm}$  measured by the EM-38. When comparing the spatial distribution of EC values from EM-38 data to EC values obtained from grid sediments, high EC values occur in the same spatial areas. The highest EC value is found in the centre of the cluster in both sets of data. The EC values gradually decrease from the highest value in the centre outwards.

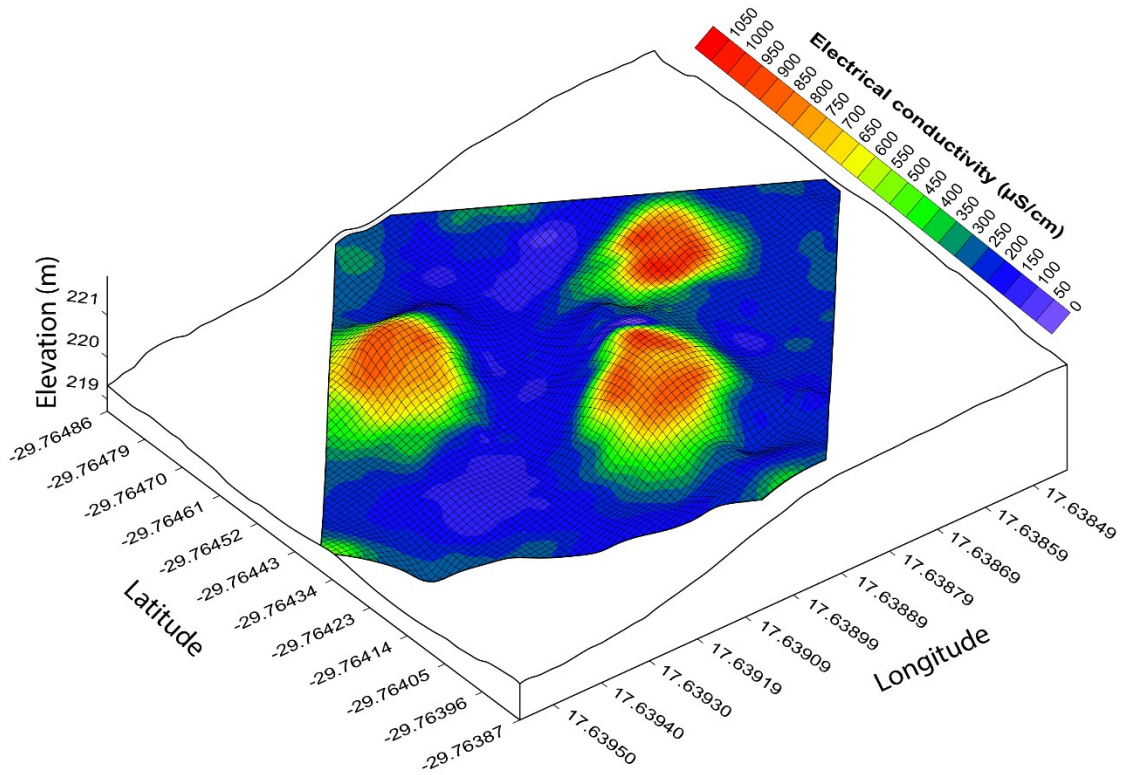


Figure 4.9: Relationship between EC and elevation relative to geographical location within the grid.

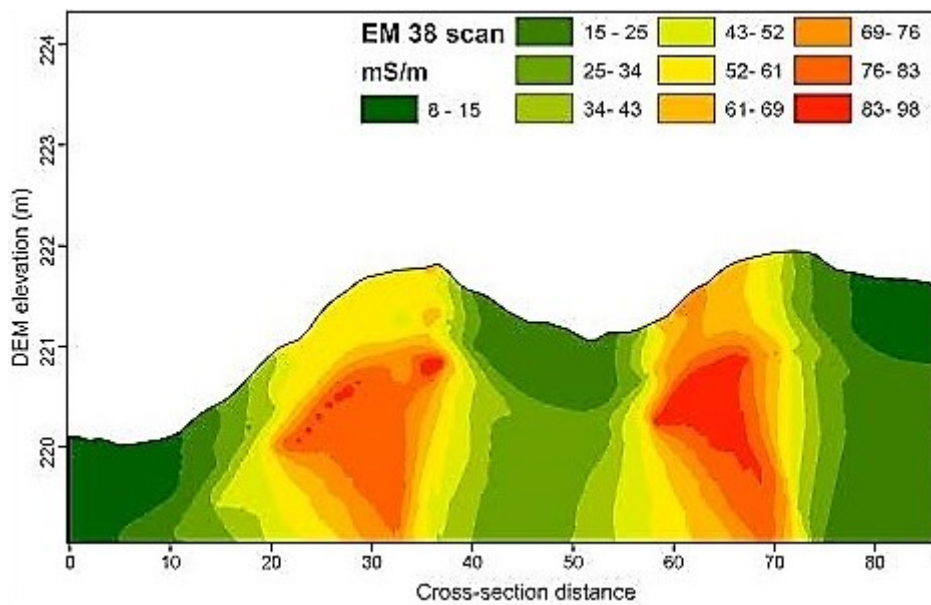


Figure 4.10: Sediment EC represented as cross-section through two heuweltjies and interheuweltjies in the grid

## 4.2. Major cations and anions

Sodium concentrations for groundwater samples collected in 2016, with the exception of two outliers, ranged between 72.9 mg/L and 443.3 mg/L (Figure 4.11 a). The sodium concentrations for the two outliers, BR15 and BR16, are 1932.1 mg/L and 2496.3 mg/L, respectively in 2016 and 2106.0 mg/L and 2904.9 mg/L, respectively respectively in 2017 (see Table 4.1 and Table 4.2). If sodium is calculated as a percentage of all cations in milli-equivalents, it becomes clear that it is the predominant cation in all groundwater samples collected ranging between 73 and 92% in 2016. Samples collected during 2017 have similar sodium concentrations. BR21 and BR25 were only sampled in 2017. Both of these samples are outliers among the 2017 sample set. Sample BR25 has a sodium concentration of 2154.5 mg/L. Sample BR21 has the highest sodium concentration of 3940.8 mg/L. Besides these outliers, the sodium concentrations of the remaining 16 samples ranged between 72.4 mg/L and 359.4 mg/L. Sodium remained the dominant cation in groundwater with milli-equivalent percentages of between 39 and 78%.

Calcium, magnesium and potassium concentrations were lower than that of sodium. Calcium and magnesium concentrations were however more variable than potassium concentrations (Figure 4.11 b & c). Calcium concentrations for samples collected in 2016 generally ranged between 8.8 mg/L and 169.50 mg/L, with the exception of two outliers, BR15 and BR16 with calcium concentrations of 462.0 mg/L and 295.8 mg/L, as seen in Figure 4.11 c. Calcium concentrations in samples collected during 2017 are slightly elevated and more variable compared to 2016 ranging between 12.8 mg/L and 267.0 mg/L. In 2017, samples BR15, BR21, and BR25 are outliers with calcium concentrations ranging between 398.9 mg/L and 513.7 mg/L. Magnesium concentrations followed a similar trend as calcium, see Figure 4.11 c & d. Magnesium concentrations are generally slightly lower in 2016, ranging between 10.7 and 74.7 mg/L while concentrations in 2017 ranged between 17.7 and 105.5 mg/L (Table 4.1 and Table 4.2). Samples BR15 and BR16 are again outliers in both cases. The concentrations of these samples for 2016 were 192.5 and 258.3 mg/L. However, the 2017 sample set have additional outliers, which were not sampled during 2016, with concentrations ranging between 105.5 mg/L and 263.5 mg/L. Potassium concentrations in samples collected during

2016 generally ranged between 0.6 mg/L and 21.3 mg/L (Figure 4.11 b). Samples BR15 and BR16 are outliers with potassium concentrations of 61.9 mg/L and 49.3 mg/L. The samples collected in 2017 generally contain less potassium than samples collected in 2016. Potassium concentrations for 2017 samples ranged between 1.8 mg/L and 11.4 mg/L, with the exception of the outliers. Samples BR21, BR22, and BR25 which have not been sampled in 2016 have similar potassium concentrations than that of the outliers of 2016. Furthermore, the potassium concentrations of samples BR15 and BR16 which have been sampled in 2016 remain elevated in 2017. There are therefore five samples from the 2017 sample set with much higher potassium concentrations. Samples BR15, BR16, BR21, BR22, and BR25 with potassium concentrations of between 50.2 mg/L and 66.7 mg/L.

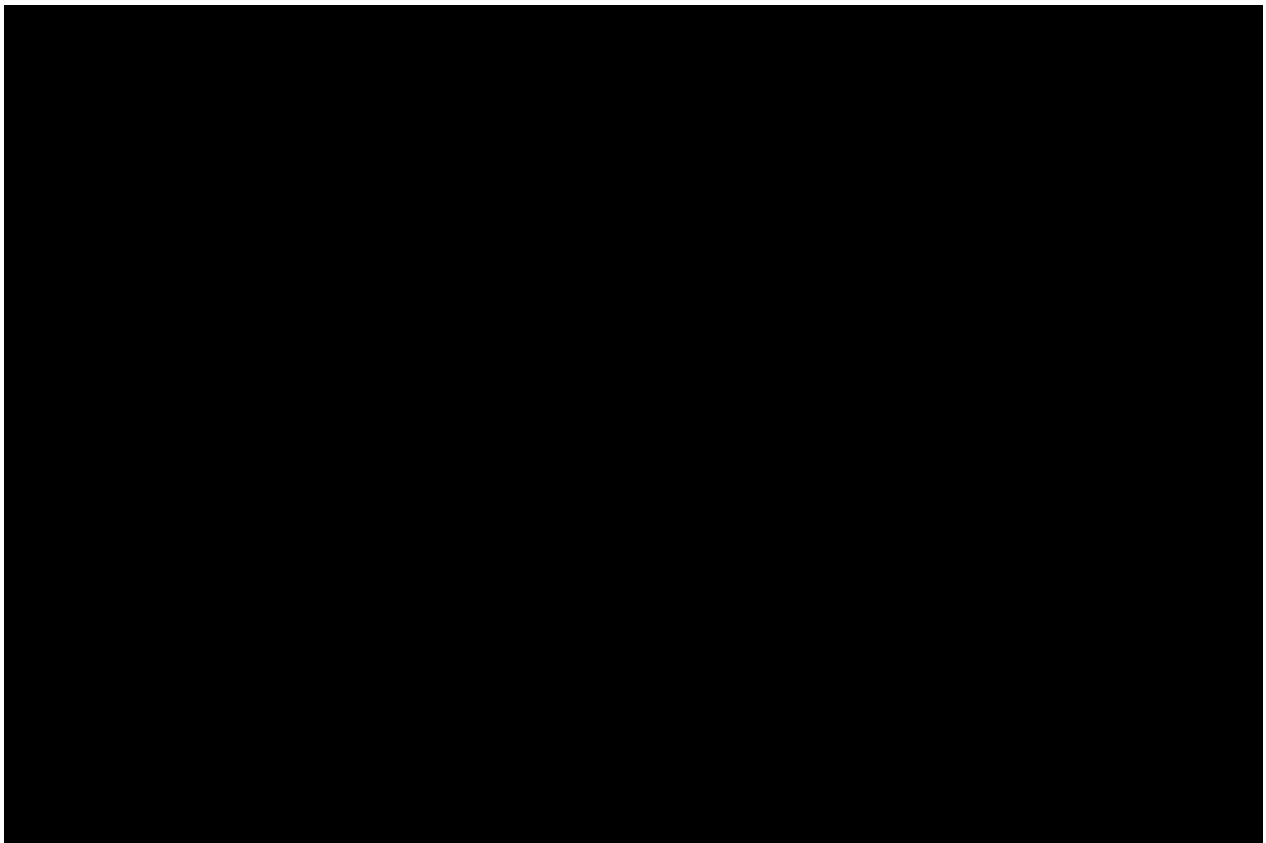


*Figure 4.11: Comparison between major cation concentrations and sample date relative to groundwater EC; a)  $\text{Na}^+$  concentrations relative to groundwater EC; b)  $\text{K}^+$  concentrations relative to groundwater EC; c)  $\text{Ca}^{2+}$  concentrations relative to groundwater EC; d)  $\text{Mg}^{2+}$  concentrations relative to groundwater EC.*

Chloride is the dominant anion found in all samples of 2016 and 2017, which can be seen in Table 4.1 and Table 4.2. Chloride percentage milli-equivalents for 2016 range between 62 and 92%. Similarly, the percentages for samples collected in 2017 range between 56 and 88%. Chloride concentrations for 2016 generally range between 146.1 and 877.5 mg/L as seen in Figure 4.13 a. There are two outliers, BR15 and BR16, with concentrations of 4801.3 and 5362.8 mg/L, respectively. Samples collected in 2017 have chloride concentrations, generally ranging between 155.5 and 999.9 mg/L. However, there are four outliers, of which only two were sampled in 2016 as well, with concentrations ranging between 3707.2 and 7716.7 mg/L. Chloride concentrations in these samples are however more elevated than that of sodium for these two samples are elevated both in 2016 and 2017 (Figure 4.11 a and Figure 4.13 a). The average  $\text{Na}^+/\text{Cl}^-$  (in terms of concentration) for 2016 is 0.47 and 0.46 for 2017 (see Figure 4.12).

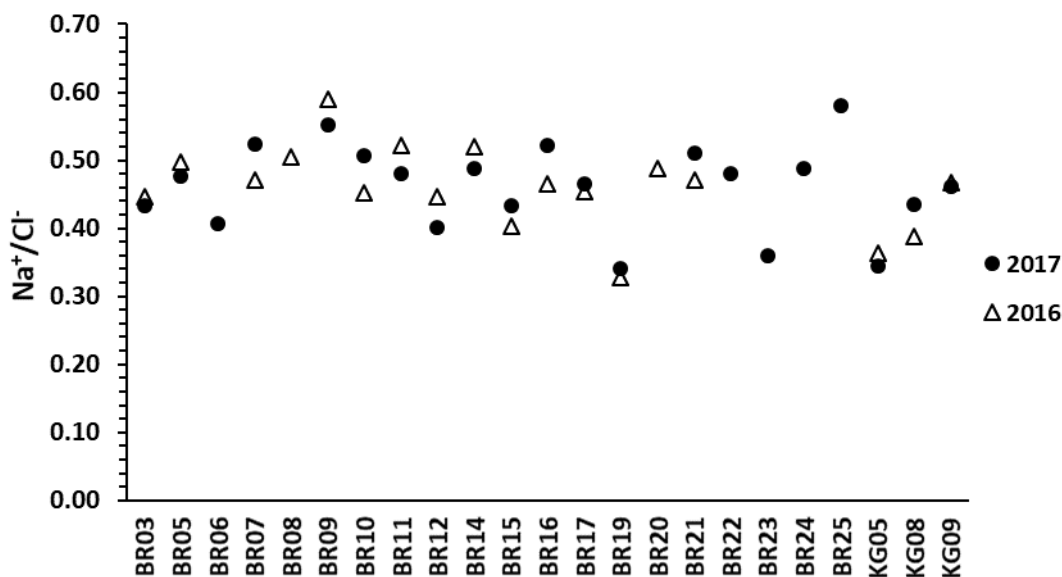


Figure 4.12:  $\text{Na}^+/\text{Cl}^-$  ratio for groundwater samples in the Buffels River

Bicarbonate concentrations for samples collected in 2016 range between 71.3 and 165.4 mg/L with the exception of three outliers (Figure 4.13 b). Samples KG05 and KG08, which were collected from Komaggas, have bicarbonate concentrations of 38.5 and 34.1 mg/L, respectively. Sample BR15 has the lowest bicarbonate concentration of 4.0 mg/L. Bicarbonate concentrations in the samples collected in 2017 are more variable with 6 outliers in the 2017 sample set. Concentrations of 14 samples range between 82.6 and 162.0 mg/L. Sample BR15 has a bicarbonate concentration of 4.02 which is the lowest recorded value among the 2017

samples. Bicarbonate concentrations in samples KG05 and KG08 are 33.9 and 30.2 mg/L, respectively. Sample BR21, which was only collected in 2017 has a bicarbonate concentration of 25.6 mg/L. The highest recorded bicarbonate concentration was that of sample BR25 with a concentration of 425.1 mg/L.

The distribution of sulfate concentrations in groundwater collected in 2016 is highly variable as seen in Figure 4.13 c. Four samples have sulfate concentrations between 30 and 65 mg/L of which sample KG08 has the lowest concentration. Seven samples have sulfate concentrations ranging between 79 and 139 mg/L while the sulfate concentrations of three samples range between 232 and 287 mg/L with sample BR05 having the highest sulfate concentration. Samples BR15 and BR16 are outliers with sulfate concentrations of 6190 and 1392 mg/L, respectively. Similar trends are seen in the samples collected in 2017. Four samples have sulfate concentrations between 10 and 61 mg/L. Sample BR22 has the lowest sulfate concentration. Seven samples have sulfate concentrations between 63 and 119 mg/L, while four samples have sulfate concentrations ranging between 215 and 286 mg/L. The four outliers in this sample set are BR16, BR21, and BR25 with concentrations between 1068 and 1421 mg/L and sample BR15 with a sulfate concentration of 5799 mg/L.

Fluoride and nitrate concentrations are much lower than the anions mentioned previously. Fluoride concentrations for samples collected in 2016 range between 0 and 1.5 mg/L (Figure 4.13 d). The average fluoride concentration for this sample set is 0.82 mg/L. The concentrations of fluoride in the groundwater collected in 2017 is very similar to that of 2016, ranging between 0.1 and 1.5 mg/L. The average fluoride concentration is 0.89 mg/L. Nitrate concentrations in samples collected in 2016 are more variable. Ten of the 17 samples have nitrate concentrations between 0.2 and 3.5 mg/L. The remaining seven samples have nitrate concentrations ranging between 6.0 and 10.5 mg/L.

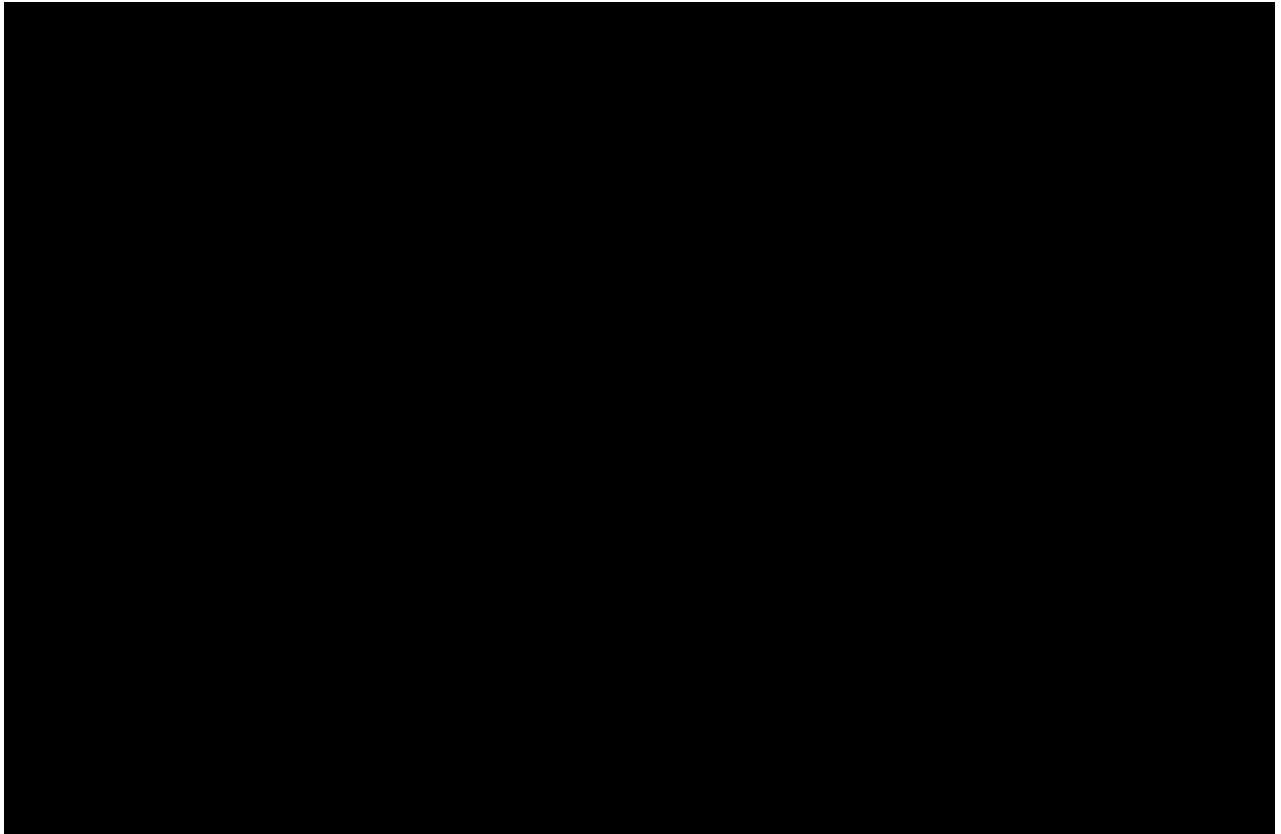


*Figure 4.13: Comparison between major anion concentrations and sample date relative to groundwater EC; a)  $Cl^-$  concentrations relative to groundwater EC; b)  $HCO_3^-$  concentrations relative to groundwater EC; c)  $SO_4^{2-}$  concentrations relative to groundwater EC; d)  $F^-$  concentrations relative to groundwater EC.*



Table 4.1: Major ion chemistry for

Sample ID	EC µS/cm	pH	Alkalinity mg/l	TDS mg/l	Na mg/l	K mg/l	Ca mg/l	Mg mg/l	Fe mg/l	B mg/l	Mn mg/l	Cu mg/l	Zn mg/l	Cl mg/l	HCO3- mg/l	SO4 mg/l	P mg/l	F mg/l	NO3-N mg/l	NH4-N mg/l
BR03	1674.00	6.90	138.90	1002.00	171.40	9.30	62.40	31.40	0.70	0.15	0.05	0.02	<0.03	384.00	138.90	103.00	0.08	0.70	0.20	0.28
BR05	2820.00	7.30	114.30	1692.00	336.00	10.00	169.50	25.80	0.10	0.25	<0.03	0.02	0.07	675.20	114.30	287.00	0.08	0.10	2.80	0.28
BR07	1668.00	7.00	137.00	999.00	181.60	1.90	67.20	31.20	0.10	0.24	<0.03	<0.02	0.08	385.50	137.00	99.00	0.06	1.50	7.00	0.28
BR08	3440.00	7.20	128.80	2040.00	443.30	6.00	126.90	74.70	0.20	0.51	<0.03	0.02	0.07	877.50	128.80	271.00	0.07	1.30	10.90	0.28
BR09	804.00	7.00	58.10	483.00	86.10	0.60	25.40	10.70	0.10	0.09	<0.03	0.02	<0.03	146.10	58.10	47.00	0.06	0.80	9.90	0.28
BR10	972.00	6.70	82.70	583.00	107.40	1.60	41.60	16.90	0.10	0.08	<0.03	0.02	<0.03	237.90	82.70	65.00	0.09	0.10	9.40	0.28
BR11	2120.00	7.00	165.40	1274.00	265.50	14.00	74.60	33.80	3.10	0.19	0.04	0.03	0.23	509.60	165.40	122.00	0.02	1.40	0.81	0.29
BR12	3090.00	6.80	110.50	1855.00	340.00	4.40	132.90	67.30	0.20	0.21	<0.03	<0.02	<0.03	760.90	110.50	232.00	0.07	1.00	10.50	0.28
BR14	2140.00	7.60	116.20	1283.00	264.90	7.50	95.50	19.60	0.10	0.17	0.03	<0.02	0.13	509.30	116.20	125.00	0.06	1.40	0.20	1.14
BR15	19580.00	3.10	4.00	11780.00	1932.10	61.90	462.00	258.30	166.10	1.74	74.72	91.93	6.54	4801.30	4.00	6190.00	2.40	0.00	0.20	73.19
BR16	15780.00	6.80	71.30	9480.00	2496.30	49.30	295.80	192.50	1.60	0.75	0.61	0.30	0.03	5362.80	71.30	1392.00	0.05	1.50	0.20	6.95
BR17	1114.00	7.50	148.40	673.00	72.90	3.70	59.50	17.30	0.70	<0.08	0.34	0.12	0.04	160.90	148.40	54.00	0.06	1.30	0.20	3.64
BR19	2180.00	7.00	106.10	1309.00	165.60	4.60	109.80	38.60	0.30	0.15	<0.03	0.04	<0.03	505.00	106.10	111.00	0.04	1.10	6.00	0.64
BR20	1682.00	7.00	96.00	1008.00	181.70	5.60	117.10	46.00	0.20	0.19	<0.03	0.03	<0.03	371.80	96.00	110.00	0.04	1.40	7.50	0.75
KG05	1234.00	7.20	38.50	739.00	109.60	10.10	22.80	37.80	0.10	0.09	<0.03	0.02	0.03	300.90	38.50	79.00	0.07	0.00	3.50	0.28
KG08	853.00	6.70	34.10	512.00	88.40	6.50	8.80	19.80	0.10	0.09	<0.03	0.02	0.03	228.20	34.10	30.00	0.06	0.00	1.70	0.28
KG09	2650.00	6.90	102.90	1591.00	341.10	21.30	64.60	59.60	0.10	0.50	<0.03	<0.02	<0.03	729.90	102.90	139.00	0.06	0.40	2.70	0.28

Table 4.2: Major ion chemistry for ground

Sample ID	EC $\mu\text{S/cm}$	pH	Alkalinity	TDS	Na	K	Ca	Mg	Fe	B	Mn	Cu	Zn	Cl	HCO <sub>3</sub> <sup>-</sup>	SO <sub>4</sub>	P	F	NO <sub>3</sub> -N	NH <sub>4</sub> -N
			mg/l	mg/l	mg/l	mg/l	mg/l	mg/l	mg/l	mg/l	mg/l	mg/l	mg/l	mg/l	mg/l	mg/l	mg/l	mg/l	mg/l	mg/l
BR03	1728.00	6.90	126.90	1036.00	182.90	11.40	73.40	43.50	<0.04	0.13	<0.03	<0.02	0.09	422.20	126.90	117.00	0.07	0.60	1652.85	0.28
BR05	2720.00	7.30	117.10	1622.00	324.80	11.40	191.10	33.90	<0.04	0.25	<0.03	<0.02	0.05	681.00	117.10	286.00	0.02	0.70	1290.74	0.28
BR06	2900.00	7.50	118.30	1738.00	326.60	12.40	180.90	41.90	<0.04	0.26	<0.03	<0.02	<0.03	801.20	118.30	281.00	0.03	0.70	1304.53	0.28
BR07	1651.00	6.90	136.80	989.00	179.90	2.60	70.70	39.70	<0.04	0.22	<0.03	<0.02	0.14	344.10	136.80	103.00	0.02	1.20	1525.56	0.28
BR09	914.00	7.30	88.70	549.00	101.10	2.00	35.90	17.70	<0.04	<0.08	<0.03	<0.02	0.04	183.20	88.70	51.00	0.02	0.60	1696.87	0.28
BR10	1031.00	6.60	84.40	617.00	115.70	1.80	52.00	24.20	0.10	<0.08	<0.03	<0.02	0.05	228.20	84.40	73.00	<0.01	0.20	1711.48	0.28
BR11	1083.00	7.20	82.60	648.00	141.80	7.50	39.30	24.20	<0.04	0.09	<0.03	<0.02	<0.03	295.10	82.60	73.00	0.02	0.80	1683.08	0.28
BR12	2980.00	6.80	103.50	1790.00	312.90	5.40	139.50	82.80	<0.04	0.20	<0.03	<0.02	<0.03	780.30	103.50	245.00	0.02	0.90	1632.81	0.28
BR14	1929.00	8.10	119.50	1158.00	242.80	11.40	62.70	23.20	<0.04	0.13	<0.03	<0.02	<0.03	497.40	119.50	47.00	0.02	1.20	1606.34	0.28
BR15	20200.00	3.30	4.00	12070.00	2106.00	66.00	472.20	263.50	251.20	1.82	91.00	119.11	6.69	4858.90	4.02	5799.00	0.37	0.10	1518.02	7.95
BR16	16120.00	7.20	98.00	9650.00	2904.90	51.00	267.00	240.20	1.00	0.77	1.06	0.26	<0.03	5557.10	98.00	1105.00	0.04	1.10	1593.84	0.28
BR17	868.00	7.70	134.90	529.00	72.40	3.10	62.50	21.00	0.30	<0.08	0.32	0.05	<0.03	155.50	134.90	51.00	<0.01	1.50	1625.37	0.28
BR19	2180.00	6.90	95.50	1305.00	201.60	7.60	132.00	66.60	0.10	0.23	0.05	0.03	<0.03	592.10	95.50	119.00	0.02	0.90	3260.18	0.28
BR21	21300.00	5.60	26.50	12780.00	3940.80	66.70	513.70	250.80	8.00	1.28	6.36	0.05	<0.03	7716.70	26.50	1421.00	<0.01	1.30	1580.15	1.42
BR22	3240.00	7.30	277.20	1944.00	302.20	50.20	107.10	35.70	0.10	0.21	0.43	<0.02	4.41	629.10	277.20	10.00	0.12	1.40	1672.24	0.38
BR23	3860.00	6.90	130.00	2320.00	359.40	9.50	218.20	105.50	<0.04	0.44	<0.03	<0.02	0.57	999.90	130.00	215.00	0.02	1.40	1635.11	0.28
BR24	1530.00	7.20	162.00	920.00	143.70	4.30	89.10	27.50	<0.04	0.16	<0.03	<0.02	0.10	294.10	162.00	63.00	0.01	1.40	1519.86	0.28
BR25	12090.00	7.20	425.10	7260.00	2154.50	64.10	398.90	184.00	<0.04	0.94	1.73	0.02	0.06	3707.20	425.10	1068.00	0.05	1.30	1598.07	0.50
KG05	1470.00	7.00	33.90	886.00	120.40	9.70	28.20	48.90	<0.04	0.10	<0.03	<0.02	0.07	349.10	33.90	80.00	<0.01	0.20	1513.52	0.28
KG08	887.00	6.50	30.20	531.00	100.70	6.30	12.80	26.90	<0.04	<0.08	<0.03	<0.02	0.05	231.40	30.20	33.00	<0.01	0.20	1485.76	0.28

## 4.3. Isotopes

### 4.3.1. *Stable O and H*

$\delta^{18}\text{O}$  values for groundwater generally ranged between -4.28 and -1.8‰, with the exception of outliers, as seen in Figure 4.14. However, there are two samples that are more depleted in the heavy isotope with  $\delta^{18}\text{O}$  ratios of -4.5 and -4.71‰ and five samples that are more enriched in the heavy isotope with  $\delta^{18}\text{O}$  ratios ranging between -0.71 and 1.0‰. Groundwater  $\delta^2\text{H}$  values range between -25 and -0.9‰ with the exception of one outlier with  $\delta^2\text{H}$  ratios of 2.2 ‰. Deuterium excess values for groundwater samples ranged between 5.9 and 17.8 with two outliers having deuterium excess values of less than 1.1. The other outlier is a sample that was collected in 2016 and 2017 with deuterium excess values of 1.1 and -0.3, respectively. The  $\delta^{18}\text{O}$  isotope ratios for rainwater collected in the Buffels River catchment ranged between -6.75 and -0.20‰, with the exception of one sample that is more depleted in the heavy oxygen isotope with  $\delta^{18}\text{O}$  ratios of -7.32‰ and 6 samples enriched in the heavy isotope. The  $\delta^{18}\text{O}$  ratios of these samples range between 0.69 and 2.64‰. However, most of the rainwater samples have  $\delta^{18}\text{O}$  ratios between -3.52 and 1.12. The  $\delta^2\text{H}$  ratios of rainwater samples also show great variation between -45.39 and 13.42‰. There are two samples which are enriched in deuterium with  $\delta^2\text{H}$  ratios of 23.71 and 34.17. Deuterium excess values for rainwater is more variable than that of groundwater ranging between 8.2 and 29.6. However, there are four outliers among the samples collected in 2016. Two samples collected in the Town of Buffels River have deuterium excess values of -19.3 and -1.7, respectively. The remaining two outliers are samples collected in Komaggas and Kleinsee with deuterium excess values of 3.2 and -11.5, respectively.

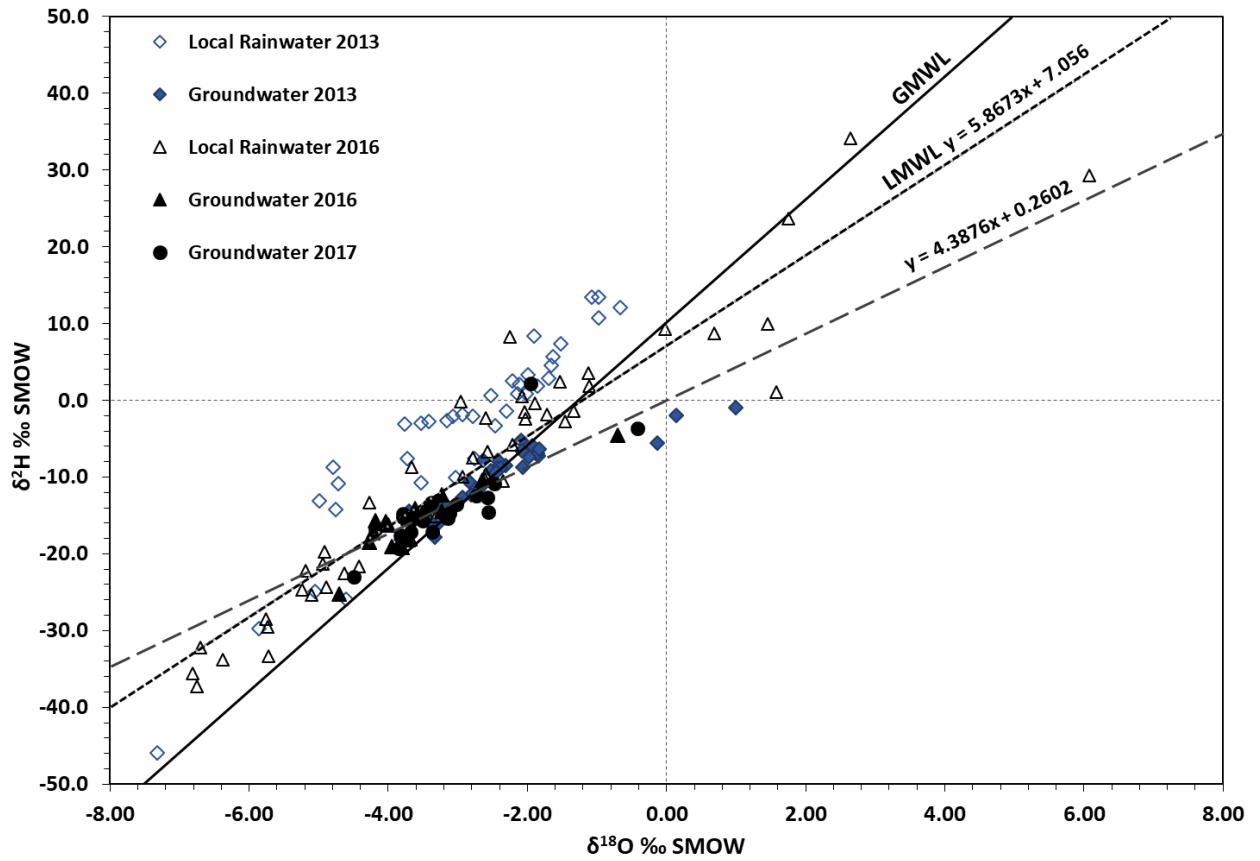


Figure 4.14: Distribution of  $\delta^2\text{H}$  and  $\delta^{18}\text{O}$  ratios for rainwater and groundwater collected during 2013, 2016 and 2017, LMWL and GMWL shown for reference with the local groundwater line (2013 data from Nakwafila, 2015).

### 4.3.2. Strontium

$^{87}\text{Sr}/^{86}\text{Sr}$  ratios ranged between 0.73030 and 0.78240 (Table 4.3). Figure 4.15 shows the distribution of  $^{87}\text{Sr}/^{86}\text{Sr}$  ratios with BR11 being the southernmost sampling site and BR05 the northernmost in the Buffels River Valley. Samples KG05 and KG09 were collected in Komaggas and is situated on the same latitude as BR11 but to the west of BR11. Sample BR20 had the highest  $^{87}\text{Sr}/^{86}\text{Sr}$  ratio while sample KG09, which was collected in Komaggas had the lowest  $^{87}\text{Sr}/^{86}\text{Sr}$  ratio. However, the  $^{87}\text{Sr}/^{86}\text{Sr}$  ratio of 10 of the 17 samples collected ranged between 0.74101 and 0.75784 while only four samples had  $^{87}\text{Sr}/^{86}\text{Sr}$  ratios between 0.73030 and 0.73970. The remaining three sample have  $^{87}\text{Sr}/^{86}\text{Sr}$  ratios between 0.76582 and 0.78241. The mean  $^{87}\text{Sr}/^{86}\text{Sr}$  ratio, excluding the three elevated ratios, is  $0.74480 \pm 0.00752$  (2s, n=14).

Table 4.3:  $^{86}\text{Sr}/^{87}\text{Sr}$  ratios for groundwater

Sample	$^{87}\text{Sr}/^{86}\text{Sr}$
BR03	0.74101
BR05	0.73624
BR07	0.74643
BR08	0.74656
BR09	0.76581
BR10	0.75358
BR11	0.74917
BR12	0.75410
BR14	0.77814
BR15	0.73490
BR16	0.73970
BR17	0.75784
BR19	0.74643
BR20	0.78240
KG05	0.74762
KG08	0.74331
KG09	0.73030

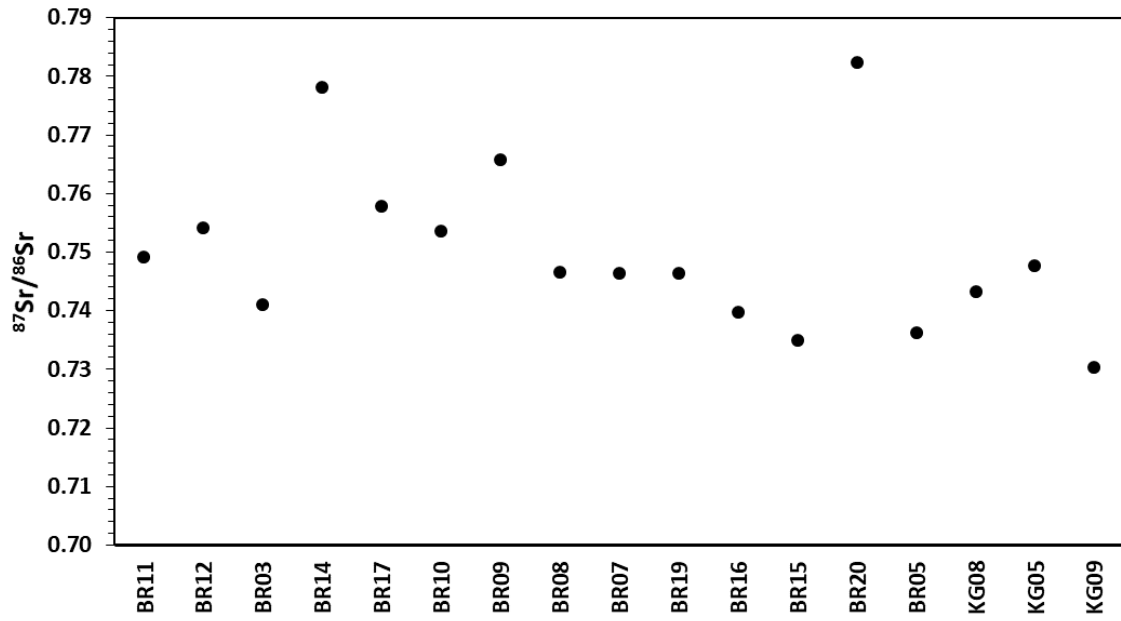


Figure 4.15: Comparison between  $^{87}\text{Sr}/^{86}\text{Sr}$  ratios for groundwater samples collected in the Buffels River catchment in order from South to North.

### 4.3.3. Chlorine-36

$^{36}\text{Cl}/\text{Cl}$  ratios the groundwater samples collected in the Buffels River catchment varies between  $21.70 \times 10^{-15}$  and  $156.19 \times 10^{-15}$  that can be further divided into four groups (Figure 4.16). The first group, samples BR03 and BR11, have very high  $^{36}\text{Cl}/\text{Cl}$  ratio of  $156.19 \times 10^{-15}$  and  $152.80 \times 10^{-15}$  respectively. The second group consists of five samples with  $^{36}\text{Cl}/\text{Cl}$  ratios ranging between  $104.25 \times 10^{-15}$  and  $112.71 \times 10^{-15}$ . The third group contains four samples. This group has a maximum  $^{36}\text{Cl}/\text{Cl}$  ratio of  $67.73 \times 10^{-15}$  and a minimum of  $56.77 \times 10^{-15}$ . The last group consisted of five samples. These ratios vary between  $21.70 \times 10^{-15}$  and  $30.64 \times 10^{-15}$ . The  $^{36}\text{Cl}/\text{Cl}$  ratios of rainwater collected in Kleinzee, which is a coastal town, is  $4.21 \times 10^{-15}$ . This is much lower compared to that of the groundwater as seen in Figure 4.16.

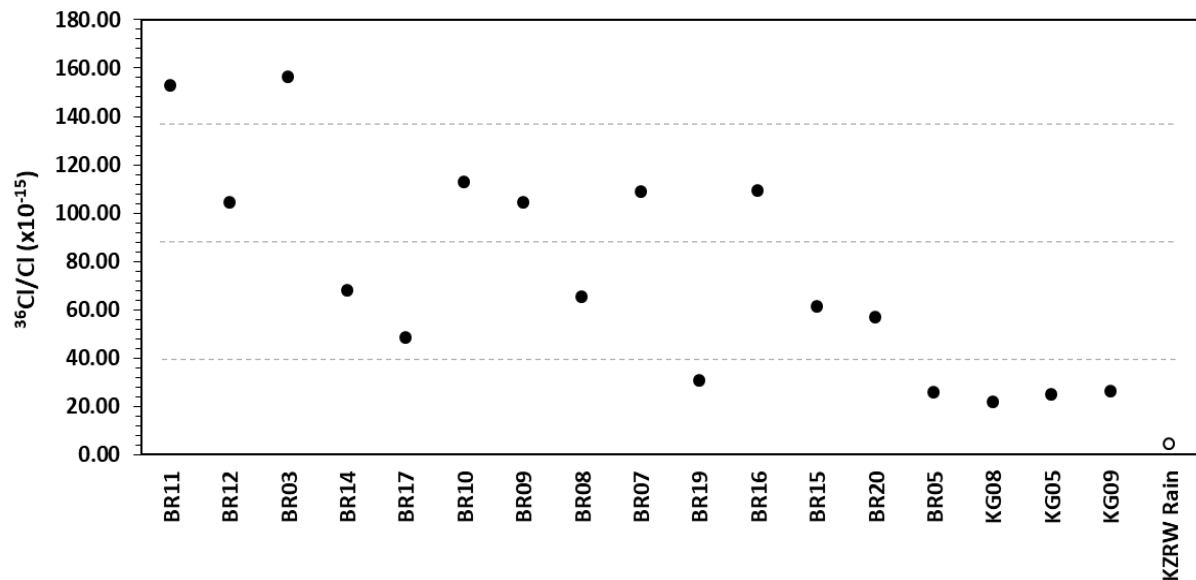


Figure 4.16: Comparison of  $^{36}\text{Cl}/\text{Cl}$  ratios between groundwater samples and a rainwater sample collected from the Buffels River Catchment, ordered from South to North. Groups are separated by stippled lines.

Table 4.4:  $^{36}\text{Cl}$  and  $\text{Cl}^-$  data for groundwater samples

Sample ID	$\text{Cl}^-$ mg/l	$^{36}\text{Cl}/\text{Cl}$ $\times 10^{-15}$	$^{36}\text{Cl}$ atoms/L	$^{36}\text{Cl}$ mg/L
BR11	509.6	152.80	$1.32 \times 10^9$	$7.76 \times 10^{-14}$
BR12	760.9	104.25	$1.34 \times 10^9$	$7.91 \times 10^{-14}$
BR03	384	156.19	$1.01 \times 10^9$	$5.98 \times 10^{-14}$
BR14	509.3	67.73	$5.83 \times 10^8$	$3.44 \times 10^{-14}$
BR17	160.9	48.37	$1.32 \times 10^8$	$7.76 \times 10^{-14}$
BR10	237.9	112.71	$4.53 \times 10^8$	$2.67 \times 10^{-14}$
BR09	146.1	104.29	$2.58 \times 10^8$	$1.52 \times 10^{-14}$
BR08	877.5	65.38	$9.70 \times 10^8$	$5.72 \times 10^{-14}$
BR07	385.5	108.92	$7.10 \times 10^8$	$4.18 \times 10^{-14}$
BR19	505	30.64	$2.61 \times 10^8$	$1.54 \times 10^{-14}$
BR16	5362.8	109.17	$9.90 \times 10^9$	$5.84 \times 10^{-13}$
BR15	4801.3	61.26	$4.97 \times 10^9$	$2.93 \times 10^{-13}$
BR20	371.8	56.77	$3.57 \times 10^8$	$2.10 \times 10^{-14}$
BR05	675.2	25.49	$2.91 \times 10^8$	$1.72 \times 10^{-14}$
KG08	228.2	21.70	$8.37\text{E}+07$	$4.94 \times 10^{-15}$
KG05	300.9	24.97	$1.27 \times 10^8$	$7.49 \times 10^{-15}$
KG09	729.9	26.07	$3.22 \times 10^8$	$1.90 \times 10^{-14}$
KZRW Rain	58.16	4.21	$4.14 \times 10^6$	$2.44 \times 10^{-16}$



#### 4.3.4. Noble gasses

The Helium, neon, argon, krypton and xenon concentrations of seven samples were measured with results shown in Table 4.5. The helium content was highly variable ranging between  $7.871 \times 10^{-8}$  and  $1.087 \times 10^{-4}$   $\text{cm}^3$  STP/g. The neon, argon and krypton concentrations among the samples were more consistent. Neon and argon concentrations range between  $3.537 \times 10^{-7}$  and  $2.115 \times 10^{-7}$   $\text{cm}^3$  STP/g and  $3.192 \times 10^{-4}$  and  $4.694 \times 10^{-4}$   $\text{cm}^3$  STP/g, respectively. Krypton concentrations are much lower than that of argon, with an average concentration of  $7.335 \times 10^{-8}$ . Xenon concentrations were slightly more variable than that of neon, argon and krypton with concentrations ranging between  $8.644 \times 10^{-9}$  and  $1.103 \times 10^{-8}$   $\text{cm}^3$  STP/g.  $R/R_a$  values for five of the samples are below 0.1. The remaining two samples have  $R/R_a$  values of 0.5209 and 0.9882.

Table 4.5: Noble gas concentrations.

Sample	He $\text{cm}^3$ STP/g	Ne $\text{cm}^3$ STP/g	Ar $\text{cm}^3$ STP/g	Kr $\text{cm}^3$ STP/g	Xe $\text{cm}^3$ STP/g	R/R <sub>a</sub>
<b>BR03</b>	$7.871 \times 10^{-8}$	$3.531 \times 10^{-7}$	$4.694 \times 10^{-4}$	$9.038 \times 10^{-8}$	$1.103 \times 10^{-8}$	0.9882
<b>BR05</b>	$1.087 \times 10^{-4}$	$2.285 \times 10^{-7}$	$3.461 \times 10^{-4}$	$7.026 \times 10^{-8}$	$9.162 \times 10^{-9}$	0.0101
<b>BR10</b>	$9.355 \times 10^{-8}$	$2.115 \times 10^{-7}$	$3.192 \times 10^{-4}$	$6.919 \times 10^{-8}$	$9.238 \times 10^{-9}$	0.5209
<b>BR12</b>	$9.741 \times 10^{-7}$	$2.442 \times 10^{-7}$	$3.327 \times 10^{-4}$	$7.011 \times 10^{-8}$	$9.147 \times 10^{-9}$	0.0693
<b>BR17</b>	$3.592 \times 10^{-6}$	$3.537 \times 10^{-7}$	$4.017 \times 10^{-4}$	$7.914 \times 10^{-8}$	$9.980 \times 10^{-9}$	0.0290
<b>BR19</b>	$7.932 \times 10^{-6}$	$2.626 \times 10^{-7}$	$3.325 \times 10^{-4}$	$6.692 \times 10^{-8}$	$8.644 \times 10^{-9}$	0.0130
<b>BR20</b>	$2.409 \times 10^{-5}$	$2.376 \times 10^{-7}$	$3.241 \times 10^{-4}$	$6.747 \times 10^{-8}$	$8.835 \times 10^{-9}$	0.0117

## 5. DISCUSSION

In this section, the results presented previously will be used to evaluate salt contributors and salinisation mechanisms in the Buffels River Valley. This will be done based on the major ion chemistry and isotope data of the groundwater and rainwater together with the EC and pH values of the river sediments and heuweltjies. An overview of groundwater and sediment characteristics as well as spatial relationships between groundwater and soil EC will be discussed. Furthermore, the role of the heuweltjie salts in salinisation of groundwater in the Buffels River Valley will be considered. In addition to this, the groundwater quality will be evaluated in terms of human consumption and agricultural purposes.

### 5.1. Groundwater and sediment characterisation

Groundwater quality in the Buffels River catchment is highly variable. EC values which are one of the proxies for water quality, range between 804 and 19 580  $\mu\text{S}/\text{cm}$  in 2016 and between 868 and 21 300  $\mu\text{S}/\text{cm}$  in 2017. Elevated sodium, calcium, chloride and sulfate concentrations were found in the majority of groundwater samples. However, sodium is the dominant cation while chloride is the dominant anion in all groundwater samples. The piper diagram, shown in Figure 5.1, was constructed for samples from 2016 and 2017. These indicate that groundwater in the Buffels River catchment can be classified as Na-Cl-type water. Overall the groundwater had higher EC in 2016 compared to 2017 but that pH was slightly more variable in 2017 than 2016

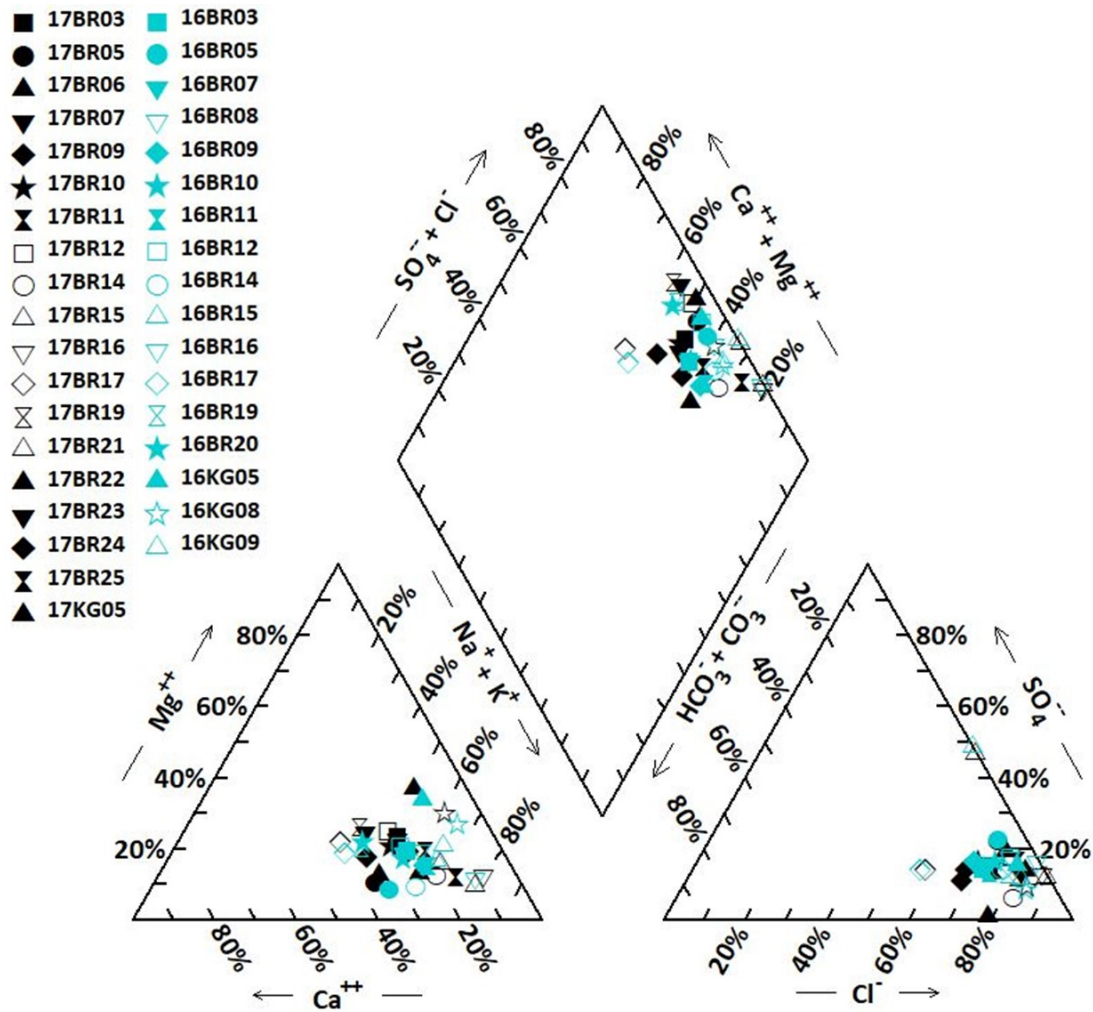


Figure 5.1: Piper diagram of groundwater chemistry for samples collected in 2016 and 2017.

River sediment EC values were generally very low, below 20  $\mu\text{S}/\text{cm}$ . However, there are two extremely high outliers from sediments collected towards the southern end of the Buffels River Valley after the confluence of the Eselsfontein and Buffels rivers. Heuweltjie sediments were found to have elevated EC values compared to that of the interheuweltjies. The EC values are generally the highest in the centre of heuweltjies with EC values decreasing towards the outer zones of the heuweltjies. Furthermore, in most cases, EC values of deeper samples collected from both heuweltjies and interheuweltjies were higher than that of shallower samples. The EM-38 scans confirmed that EC values of the upper 1.5m of heuweltjies are elevated in comparison to interheuweltjies. The scans also indicated that EC values increase with elevation, therefore, increasing from the low lying interheuweltjies to the highest zone which is the centre of the heuweltjies.

## 5.2. Mechanisms of Salinisation

As discussed above, groundwater in the Buffels River Valley can be characterised as Na-Cl type waters. In this section, the possible sources of salt in the groundwater will be evaluated. Three possible salt sources will be considered including: (i) evaporative concentration of salts; (ii) water-rock interaction; and (iii) heuweltjie salts. Thereafter, the mobilisation of salts will be considered and the role of groundwater mixing in controlling the salt concentrations will be assessed.

### 5.2.1. *Evaporative concentration of salts*

Evaporative concentration of salts typically occur in semi-arid to arid conditions (Vengosh et al., 1999; Schoups et al., 2005; van Weert et al., 2009; Wu et al., 2014). During rainfall events in these climatic conditions, rainwater accumulates in low lying areas where infiltration of rainwater deeper into soils occur slowly and is often exceeded by evaporation (Salama et al., 1999; Farber et al., 2004; Hogan et al., 2007). Although rainwater contains low concentrations of salts, several wetting and drying cycles result in the accumulation of salts, specifically in low-lying areas (Peck & Hatton, 2003; Rengasamy, 2006). The intensity and volume of rain in semi-arid to arid conditions are often not sufficient to leach salts that have accumulated on the surface into the deeper soil zones (Rengasamy, 2006; van Weert et al., 2009). In cases where infiltration has taken place and shallow pore waters are present, salts are concentrated in shallow soils (Salama et al., 1999; Munns & Tester, 2008). Dissolution of these salts may occur in shallow aquifers with highly fluctuating groundwater levels, subsequently increasing the salt content of the groundwater.

The semi-arid to arid climatic conditions in the Buffels River Valley have been thought to be the main cause of the salinisation of groundwater and soils by evaporative concentration of salts (Adams et al., 2004; Pietersen et al., 2009; Titus et al., 2009). An evaporation signature is visible on the stable hydrogen and oxygen plot for both rainwater and groundwater in Figure 4.14. Rainwater is generally enriched in the heavy isotope with a local meteoric water line  $\delta^2\text{H}/\delta^{18}\text{O}$  slope of 5.867. The  $\delta^2\text{H}/\delta^{18}\text{O}$  slope of a meteoric waterline of evaporative waters typically have slopes ranging between 4 and 6 (Gat, 1996; Gibson & Edwards, 2002;

Sharp, 2017). Groundwater samples are more depleted in the heavy isotopes than the rainwater and the plot indicates that groundwater data has a  $\delta^2\text{H}/\delta^{18}\text{O}$  slope of 4.387. This suggests that evaporative concentration does occur. However, due to the evaporation signature seen in the rainwater, the role of evaporative concentration in salinisation may not be as large as expected.

River sediment and interheuweltjie sediment samples were collected at depths of up to 50cm and at these depths, evaporation of moisture can still occur causing salts to accumulate within the surface layer of sediments. However, both river and interheuweltjie sediment samples generally have low EC values, which provides some uncertainty whether evaporative concentration of salts is the only contributor to salinisation in the Buffels River Valley. A shallow groundwater sample or seepage sample, sample BR25, was collected from a trench of approximately 60cm deep the river bed. An EC value of 12 090  $\mu\text{S}/\text{cm}$  was measured for sample BR25 (water sample), which is much higher than that of the majority of the other groundwater samples. Interestingly, a river sediment sample collected in the river bed, at the same depth as sample BR25, but 30m towards the north of sample BR25, had an EC value of 92.57  $\mu\text{S}/\text{cm}$ . Both samples were collected at a depth of approximately 60 cm, which is well in the range at which moisture can be removed from sediments by evaporation. Given the semi-arid to arid climatic conditions in the Buffels River Valley, evaporative concentration of salts should contribute to the salinisation of soils and groundwater to some extent. However due to the variability in the groundwater and sediment EC, differential evaporative concentration cannot be the only salt contributing factor.

### **5.2.2. Heuweltjie salts**

The average heuweltjie sediment EC is 2801.44  $\mu\text{S}/\text{cm}$ , which is much higher than that of the interheuweltjies with an average of 121.55  $\mu\text{S}/\text{cm}$ . However, the EC values of heuweltjies are comparable to groundwater EC values which has an average value of 1916.52  $\mu\text{S}/\text{cm}$ , if outliers are excluded. Furthermore, as seen in Figure 5.2, the maximum EC value of the heuweltjies (7463.69  $\mu\text{S}/\text{cm}$ ) is higher than the maximum groundwater EC value of 3860.00  $\mu\text{S}/\text{cm}$  (outliers excluded) implying that heuweltjie sediments contain large amounts of salts. This is in agreement with many previous studies (Moore & Picker, 1991; Midgley et al., 2012;

Cramer et al., 2012; Francis et al., 2013) which concluded that heuweltjies consist of nutrient rich sediments containing increased concentrations of salt forming ions.

It is important to note that four outliers among the groundwater sample set are not considered for this particular comparison. Sample BR25 is a seepage water sample collected from a trench in the river bed and EC value of 12 090  $\mu\text{S}/\text{cm}$ , for which the elevated EC was explained in a previous section. Samples BR15, BR16 and BR21, all with EC values above 15 700  $\mu\text{S}/\text{cm}$ , are not included due to their sample location relative to the Spektakel copper mine and its leaching ponds. The leaching ponds, which contains sulphuric acid in various molar percentages, are situated approximately between 40 and 200m up gradient of the boreholes from which the outlier EC values were obtained. Apart from the metals that are incorporated into the soils and groundwater due to the atmospheric exposure of the mine dumps, ions bound to soil particles along the groundwater flow path are dissolved and mobilised by the acidic groundwater (Smith, 1973; Edmunds & Smedley, 1996; Richards et al., 2000; Mulligan et al., 2001) which results in an increase in the groundwater EC values.

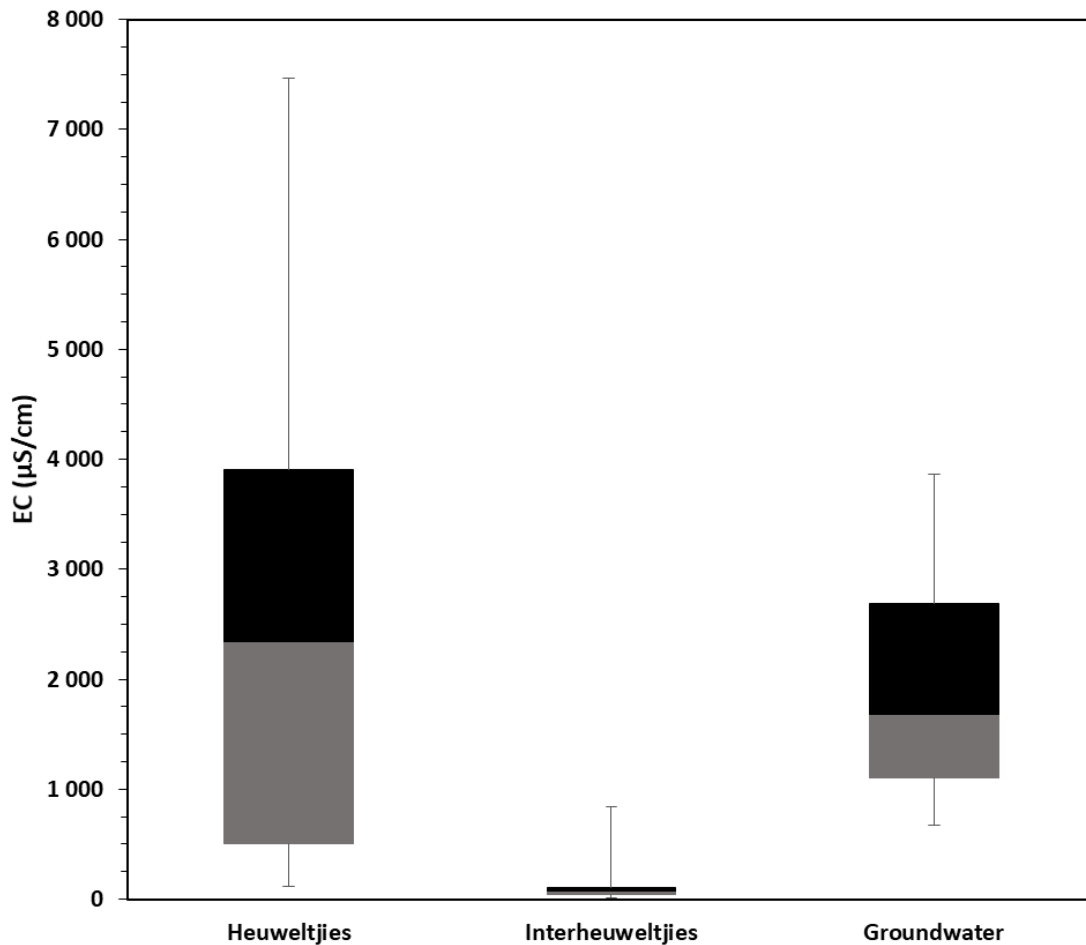


*Figure 5.2: Comparison between heuweltjie EC values, interheuweltjie EC values and groundwater EC values. Note that outliers are excluded from the groundwater dataset for this particular comparison.*

The distribution of heuweltjies in the Buffels River Valley is significant in that the majority of the heuweltjies are clustered towards the northern and southern ends of the valley. Sediments in these areas should therefore contain more salts than sediments in areas where heuweltjies are not present. The groundwater EC values of 2016 and 2017 were averaged and has been plotted with the maximum sediment EC values of the heuweltjies in Figure 5.3 to indicate that the EC values of groundwater does increase downstream of the heuweltjies. When comparing spatial distribution of heuweltjies to that of groundwater samples with elevated EC, it becomes clear that more saline groundwater is found in areas with high heuweltjie densities. Samples from boreholes that are situated against or on the escarpment generally have lower average EC values compared to that within or adjacent to the river bed,

with the exception of two samples, BR03 and BR11. Sample BR11 was taken from the southernmost borehole which is situated just south of the start of the valley, in an area where heuweltjies do not occur.

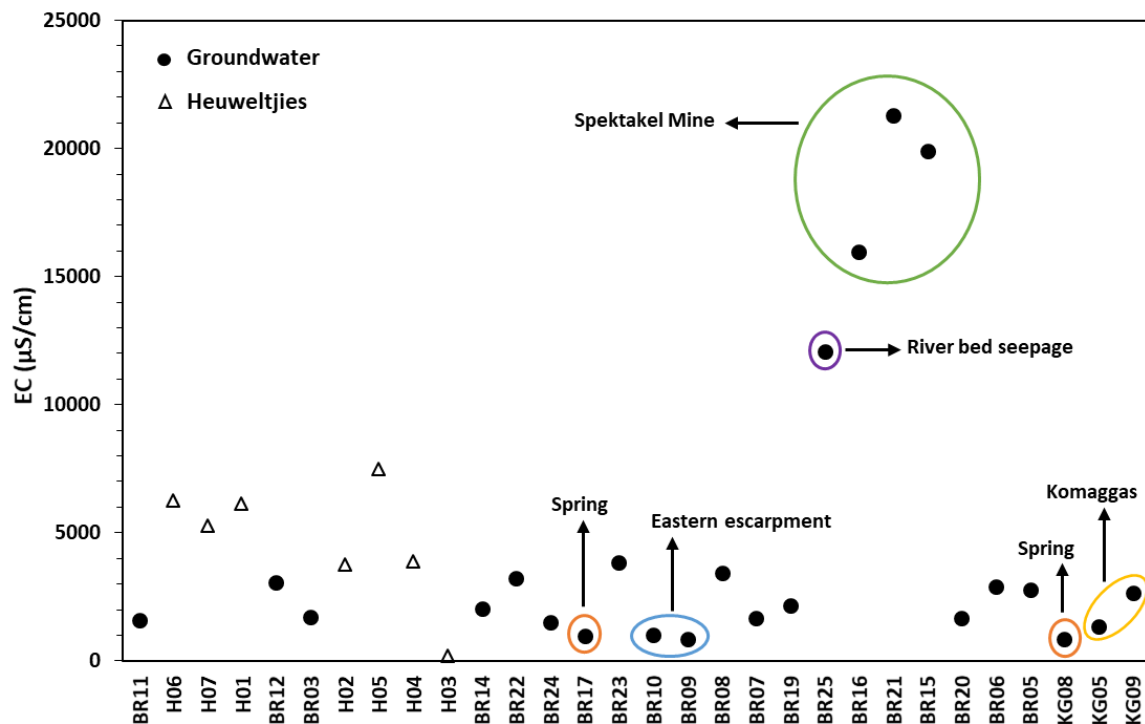


Figure 5.3: Comparison of the spatial distribution of heuweltjies and relative position of groundwater EC, plotted from south to north according to the direction of flow. Note that samples collected in Komaggas are not in the Buffels River Valley, and are plotted at the end.

Given the relationship between the spatial distribution of heuweltjies and the variation in the groundwater EC in the Buffels River Valley, heuweltjie salts could be considered as a contributor to salts in the groundwater in the Buffels River Valley. The mechanism by which the salts are transported to the groundwater is not fully understood but researchers (Milton & Dean, 1990; Moore & Picker, 1991) have proven that heuweltjies consist of a network of tunnels and cavities. Water percolates into the sediments causing dissolution of the heuweltjie salts. The cavities and tunnels in the heuweltjies may serve as conduits transporting the salt rich water downwards into the groundwater system, particularly the shallow alluvial aquifer.



### 5.2.3. Groundwater mixing

The  $^{36}\text{Cl}/\text{Cl}$  dataset obtained from the Buffels River Valley is very complex as the  $^{36}\text{Cl}/\text{Cl}$  ratios are highly variable ranging between  $25.94 \times 10^{-15}$  and  $156.19 \times 10^{-15}$ . It appears as if the data could be divided into three groups based on the relationships between  $^{36}\text{Cl}/\text{Cl}$  and  $\text{Cl}^-$  and  $^{36}\text{Cl}/\text{Cl}$  and  $^{36}\text{Cl}$  concentrations (Figure 5.4 and Figure 5.5). However, samples within these groups does not seem to have related trends in any of the other parameters. Furthermore, there are no significant trends in the spatial distribution of the boreholes from which these samples were collected.

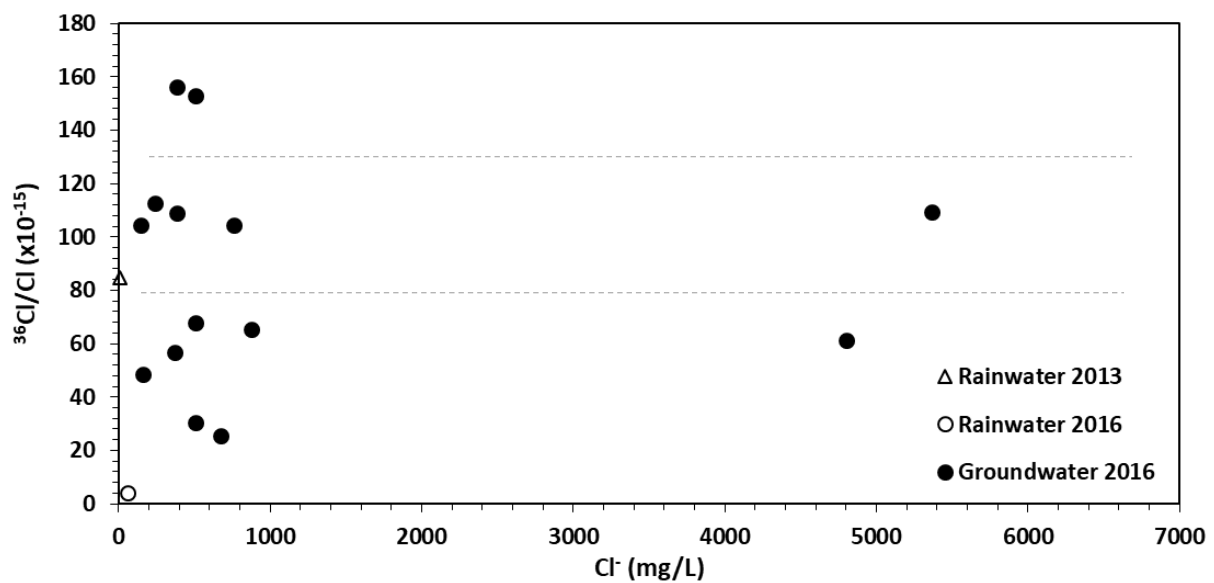


Figure 5.4: Relationship between  $^{36}\text{Cl}/\text{Cl}$  ratios and  $\text{Cl}^-$  concentration in the groundwater and rainwater samples.

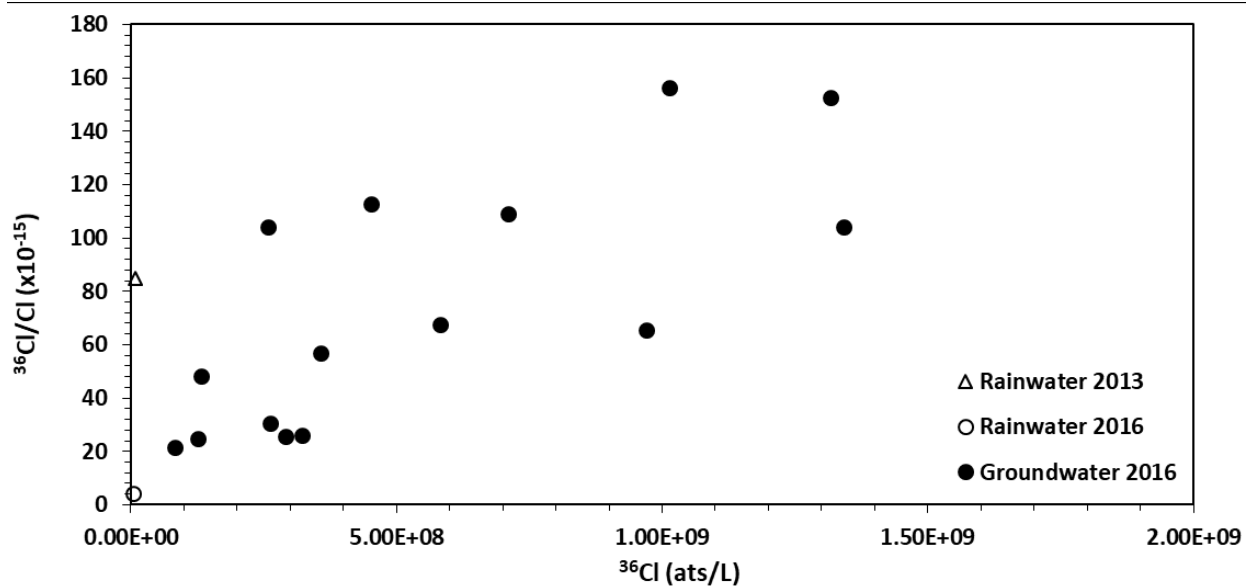


Figure 5.5: Relationship between  $^{36}\text{Cl}/\text{Cl}$  ratios and  $^{36}\text{Cl}$  content in groundwater and rainwater.

Although  $^{36}\text{Cl}/\text{Cl}$  ratios have served as a valuable tool in calculating residence times and groundwater ages in many studies (Andrews et al., 1986; Fröhlich et al., 1991; Cresswell et al., 1999; Moran & Rose, 2003; Davis et al., 2003; Guendouz & Michelot, 2006; Phillips, 2013; Howcroft et al., 2017),  $^{36}\text{Cl}/\text{Cl}$  ratios in the groundwater and rainwater from the Buffels River Valley are complicated and residence times could not be calculated. However, the  $^{36}\text{Cl}/\text{Cl}$  ratios obtained from the groundwater in the Buffels River Valley indicate that the samples were collected from groundwater resources that have been recharged in various locations. Groundwater with higher  $^{36}\text{Cl}/\text{Cl}$  ratios reflect recharge that occurred further inland, whereas the lower  $^{36}\text{Cl}/\text{Cl}$  ratios indicate recharge that occurred in coastal regions. The fact that the  $^{36}\text{Cl}/\text{Cl}$  ratios are spatially and quantitatively highly variable in a small area, but yet three groups exist in the dataset, provides some indication that the Buffels River Valley is a zone in which groundwater mixing occurs during which salts from one resource can contribute to the salinity of the other.

The dataset for noble gasses analyses was compromised by incomplete  $^3\text{He}$  production in the stainless-steel vessels. Incomplete  $^3\text{He}$  production in this case is an indication that very little  $^3\text{H}$  is present in the groundwater. This suggests that groundwater residence time is possibly more than 120 years. Furthermore, the relative abundance of  $^3\text{He}/^4\text{He}$  in the sample

compared to that in the source is expressed as  $R/R_a$  values (Aeschbach-Hertig et al., 1999; Beyerle et al., 1999; Klump et al., 2008; Kaudse et al., 2016). The  $R/R_a$  value for atmospheric helium is 1 and crustal or terrigenous helium is  $<0.1$ . The  $R/R_a$  values for groundwater samples from the Buffels River Valley indicate that five of the samples consist mostly of terrigenous helium. The remaining samples have  $R/R_a$  values of above 0.1 indicating that atmospheric helium and terrigenous helium is incorporated into the groundwater. Consequently, the samples consisting of both atmospheric and terrigenous helium provides evidence that groundwater mixing does occur.

#### **5.2.4. Water-rock interaction**

The geology of the Buffels River Valley is dominated by granite gneisses (Marais et al., 2001a, 2001b; Macey et al., 2017a), which typically have  $^{87}\text{Sr}/^{86}\text{Sr}$  ratios in excess of 0.71. Sr and Rb are abundant in granitic rocks as they easily substitute for calcium and potassium in minerals containing these elements, specifically feldspars and micas. Granites are rich in feldspars and micas therefore naturally contain Sr and Rb. However,  $^{87}\text{Sr}$  is also produced during radioactive beta-decay of  $^{87}\text{Rb}$  giving granitic rocks have distinctly radiogenic  $^{87}\text{Sr}/^{86}\text{Sr}$  ratios in comparison to other rock types (Goldstein & Jacobsen, 1988; Capo et al., 1998). Due to the long half-life of  $^{87}\text{Sr}$  ( $48.8 \times 10^9$  years), increased amounts of  $^{87}\text{Sr}$  implies that the system is old compared to the same rock type with low  $^{87}\text{Sr}$  concentrations. A greater  $^{87}\text{Sr}/^{86}\text{Sr}$  ratio indicate an older system (Shand et al., 2009). During weathering, strontium is released from the granites into the natural system and eventually incorporated in groundwater. In cases where groundwater residence times are long enough and the chemical composition is able to reach equilibrium, the groundwater takes on the strontium isotope ratio of the aquifer matrix (Négre, 1999; Vengosh et al., 1999, 2002; Pennisi et al., 2006; Santoni et al., 2016). Therefore, elevated  $^{87}\text{Sr}/^{86}\text{Sr}$  ratios in groundwater are typically associated with the water-rock interaction, and are often derived directly from the local granitic rocks.

$^{87}\text{Sr}/^{86}\text{Sr}$  ratios in groundwater in the Buffels River Valley was found to be elevated, ranging between 0.73030 and 0.78240. This can be related to the granitic environment which typically have elevated  $^{87}\text{Sr}/^{86}\text{Sr}$  ratios. The large variation in the  $^{87}\text{Sr}/^{86}\text{Sr}$  could indicate that groundwater samples collected in different areas have been in contact with different granitic

suites with variable ages. Groundwater with higher  $^{87}\text{Sr}/^{86}\text{Sr}$  ratios have been in contact with older granites while low  $^{87}\text{Sr}/^{86}\text{Sr}$  ratios indicates contact with younger rocks. Alternatively, the large variation in  $^{87}\text{Sr}/^{86}\text{Sr}$  ratios could imply that groundwater residence times are highly variable across the catchment. In this case, the contact time between groundwater and aquifer matrix have not been sufficient for complete equilibration in some of the groundwater samples. This implies that more than one aquifer system exists in the Buffels River Valley.

Interspersed spatial relationships exist between the groundwater  $^{87}\text{Sr}/^{86}\text{Sr}$  ratios from the Buffels River Valley, as seen on Figure 5.6. Sample BR20, which has the highest  $^{87}\text{Sr}/^{86}\text{Sr}$  ratio of 0.78240, is situated on a steep slope next to the Skaap River, one of the Buffels River's main tributaries. BR19 is which is also situated adjacent to the Skaap River, just before the confluence between the Skaap and Buffels rivers, have a  $^{87}\text{Sr}/^{86}\text{Sr}$  ratio of 0.74643, much lower than that of BR20. Significantly, sample BR14 which has an elevated  $^{87}\text{Sr}/^{86}\text{Sr}$  ratio of 0.77814 is situated in the river bed towards the centre of the Buffels River Valley. Samples which were taken in close proximity of BR14 have much lower  $^{87}\text{Sr}/^{86}\text{Sr}$  ratios, specifically sample BR03 ( $^{87}\text{Sr}/^{86}\text{Sr} = 0.74101$ ) which was taken 1.6 km upstream of sample BR14. Another interesting observation is that sample BR09 and BR10 were taken from boreholes which are 60m apart and yet there is a significant difference between their  $^{87}\text{Sr}/^{86}\text{Sr}$  ratios which are 0.76581 and 0.75358, respectively. This further strengthens the idea that more than one aquifer system exists in the Buffels River catchment.

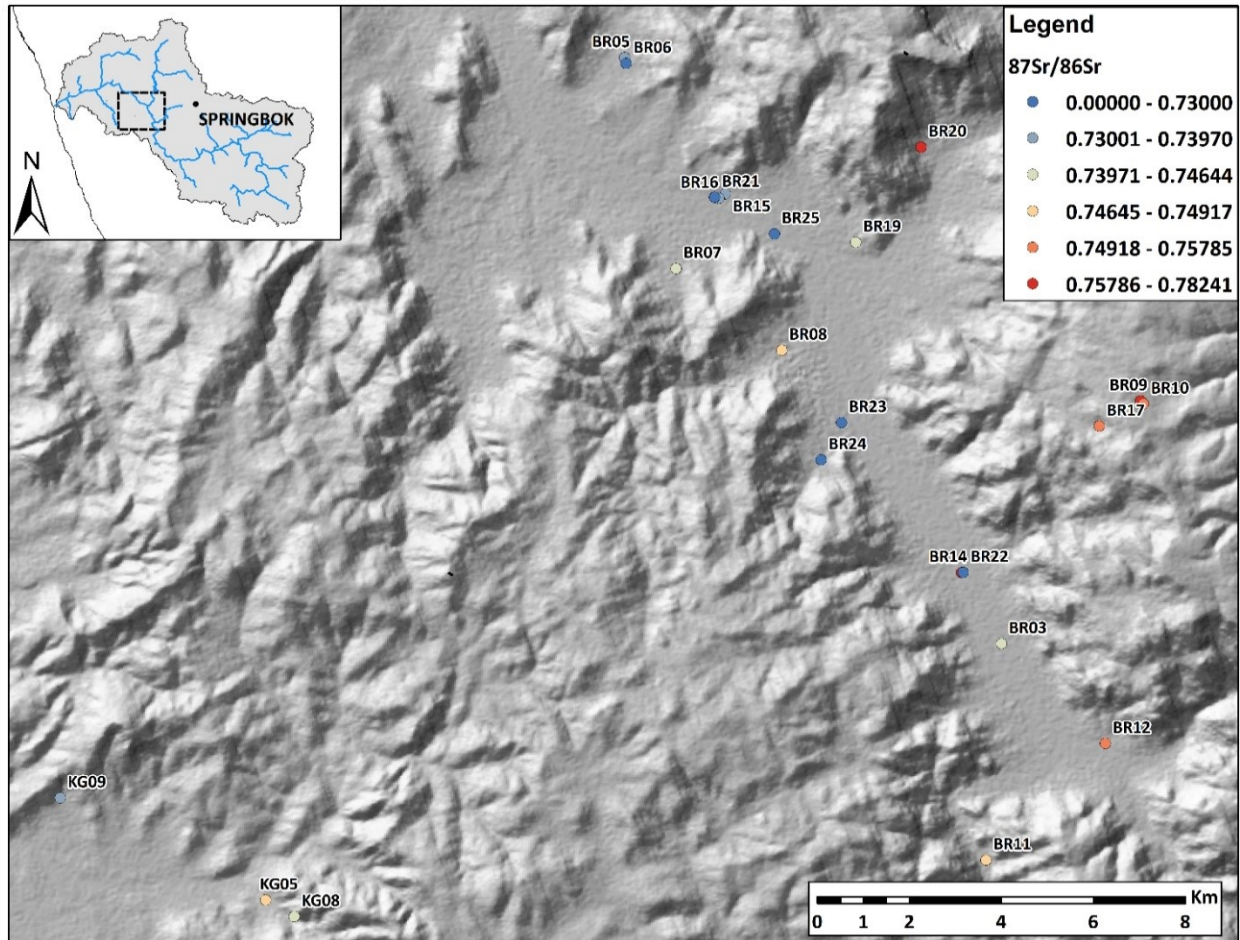


Figure 5.6: Spatial distribution of  $^{87}\text{Sr}/^{86}\text{Sr}$  ratios.

### 5.3. South African water quality standards and management practices

Water quality standards for domestic and agricultural use have been determined by the Department of Water and Sanitation (DWS) of South Africa. As groundwater is the only source of potable water for many communities in the Buffels River catchment, groundwater quality should fit the prescribed quality guidelines for the indented use. As EC is one of the proxies for the general salt content in water and therefore water quality, the groundwater EC will be used to determine whether the groundwater from the Buffels River Valley is of drinking water quality standards. Similarly, DWS has provided specifications for various agricultural practices which will be discussed below.

### **5.3.1. Domestic water quality standards**

The target quality EC range specified by DWS for domestic water is 0-700  $\mu\text{S}/\text{cm}$ . However, water is expected to have a salty taste at an EC of 450  $\mu\text{S}/\text{cm}$ . Domestic water with EC values ranging between 1500 and 3000  $\mu\text{S}/\text{cm}$  does not appear to have short term health effects but continuous consumption may be harmful as salt balances in the human body may be disturbed. Furthermore, groundwater of this quality has corrosive effects on household appliances and plumbing. Water with EC ranges between 3000 and 4500  $\mu\text{S}/\text{cm}$  may be tolerated on very short-term basis but salt imbalances in the human body is most likely to occur even with very short-term consumption. Consumption of water with EC values 4500  $\mu\text{S}/\text{cm}$  is not advisable. Serious health issues, such as kidney failure, may result from consuming water of this quality (DWS, 1996a).

Given that the groundwater quality in the Buffels River catchment is so variable, consumption of this water may result in some health issues among the community members. The borehole which provides potable water for the town of Buffels River had an EC value of 1674  $\mu\text{S}/\text{cm}$  in 2016 and 1728  $\mu\text{S}/\text{cm}$  in 2017. Although short term consumption may be tolerated, continuous consumption of water with these EC values may result in health issues. Groundwater used for domestic purposes in the town of Komaggas is slightly fresher with EC values of 1234 and 1470  $\mu\text{S}/\text{cm}$  in 2016 and 2017 respectively. Although these waters may have a salty taste, water with EC values below 1500  $\mu\text{S}/\text{cm}$  is still within the expected range and no health effects should arise from consumption of these waters.

### **5.3.2. Agricultural water quality standards and management**

Water use for agricultural purposes can be divided into irrigation use and livestock use, each with their own set of standards according to the tolerance of various crops and livestock. One of the main concerns of irrigating with saline water is disturbing the salt balance within soils, which is almost irreversible once it has occurred. DWS has indicated that the target quality range for irrigation water, in which salt sensitive crops can be grown without compromising yields, is EC values up to 400  $\mu\text{S}/\text{cm}$ . With increasing EC values, the yields of salt sensitive crops will decrease drastically and it is advised that salt tolerant crops should be cultivated.

Once the EC of irrigation water becomes  $>5400 \mu\text{S}/\text{cm}$ , the yields of salt tolerant crops may become limited. The DWS stipulates that soil remediation practises should be implemented in these conditions to ensure the sustainability of the soils (DWS, 1996b).

The water quality for livestock target EC range is  $0\text{-}1500 \mu\text{S}/\text{cm}$ . Sheep and cattle are generally the most salt tolerant, however, once EC values are above  $3000 \mu\text{S}/\text{cm}$ , they may initially be reluctant to drink but they should adapt within a week. This may cause a slight decline in their water intake during the adaption period. Sheep and cattle may only start showing complete reluctance when water EC levels become  $>9000 \mu\text{S}/\text{cm}$  and besides dehydration, no significant health effects have been reported. Both species are known to adapt to these conditions and care should be taken to ensure that dehydration does not occur. The long term tolerable limit for cattle is  $10\ 000 \mu\text{S}/\text{cm}$  while sheep are able to tolerate EC values  $>13\ 000 \mu\text{S}/\text{cm}$ . Pigs, poultry and dairy cows are the most sensitive to saline water and may start showing reluctance to drinking water with EC values of  $1500 \mu\text{S}/\text{cm}$ . Pigs and poultry can tolerate water with EC values up to  $4\ 600 \mu\text{S}/\text{cm}$ , whereas dairy cows can tolerate water with EC up to  $6\ 100 \mu\text{S}/\text{cm}$  without signs of health effects (DWS, 1996c).

Commercial and subsistence livestock farming is practised in the Buffels River catchment. The groundwater from most of the boreholes in the Buffels River Valley and the town of Komaggas seems fit for livestock consumption. However, cultivation of salt sensitive crops may become complex and costly. The Buffels River catchment is not ideal for crop farming but some of the most salt tolerant crops may be farmed successfully if the correct management practises are put in place. Water treatment would most probably involve desalination by reverse osmoses. This is very costly and not a realistic option in the Buffels River Catchment. Soil management practises should include artificial drainage systems and sporadic flooding.

## 6. CONCLUSION

The research completed during this study lead to the characterisation of groundwater and sediments in the Buffels River Valley for the purpose of evaluating mechanisms of salinisation in this region. A total of 29 groundwater samples have been collected and analysed for various geochemical parameters. Sediments from the river bed as well as heuweltjies and interheuweltjies have been sampled and analysed for sediment EC and pH.

Soil and groundwater EC and pH values were highly variable throughout the Buffels River Valley. However, heuweltjies had significantly higher EC values without major pH changes in comparison to inter-heuweltjie and rivers bed sediments. There was also evidence of a correlation between the density of heuweltjie distribution with increased salinity in groundwater samples. Although the hot, arid environment concentrates salts through evaporative processes, as seen by the stable isotope profiles, the heuweltjies have been created by paleo-bioactivity and represent a more complicated salt source. Even with the use of  $^{36}\text{Cl}$  isotopes, it is difficult to say whether the concentrated mounds of soil represent significant salt contributions to the groundwater resource.

The groundwater that is currently being accessed by the local population lies in and around the riverbed of the valley. The groundwater in this area is often outside of South African drinking water standards with elevated EC values that are too saline for domestic use. Throughout the duration of the study, no major changes in borehole chemistry were observed, besides a slight increase in average EC, showing the effect of salinisation in the field area. In order to better understand the variable distribution of EC in the Buffels River Valley, it is important to understand the flow regime of the groundwater. Sr isotope signals show generally elevated  $^{87}\text{Sr}/^{86}\text{Sr}$  ratios due to the granitic nature of weathered constituents that make up the alluvial aquifers. More inland, eastern samples show higher ratios in comparison to those in the river valley and especially to those down gradient toward the northernmost point of the valley. This indicates that groundwaters are being introduced from the high relief escarpment on the east of the valley as groundwater flows northwards.



Although salinity is increasing over time in a uniform manner, there are areas of the valley that have significantly high EC values but can be directly attributed to mining practices at the Spektakel Mine. Whether or not any natural and/or anthropogenic phenomena are driving spatially variable salinisation is still up for debate until further investigations have been undertaken. To assume that the concentrated mounds of salty soils are driving groundwater salinisation would be inconclusive with the current available data, but it is evident that conventional, semi-arid salinisation through evaporation is not the only driver in this regional system.

## 7. REFERENCES

- Adams, S., Titus, R. & Xu, Y. (2004). Groundwater recharge assessment of the basement aquifers of central Namaqualand. *WRC Report*. No. 1093/1 (4). p.p. 234.
- Aeschbach-Hertig, W., Peeters, F., Beyerle, U. & Kipfer, R. (1999). Interpretation of dissolved atmospheric noble gases in natural waters. *Water Resources Research*. [Online]. 35 (9). p.pp. 2779–2792. Available from: <http://dx.doi.org/10.1029/1999WR900130>.
- Andrews, J.N., Fontes, J.C., Michelot, J.L. & Elmore, D. (1986). In-situ neutron flux,  $^{36}\text{Cl}$  production and groundwater evolution in crystalline rocks at Stripa, Sweden. *Earth and Planetary Science Letters*. 77 (1). p.pp. 49–58.
- Aragüés, R., Medina, E.T., Martínez-Cob, A. & Faci, J. (2014). Effects of deficit irrigation strategies on soil salinization and sodification in a semiarid drip-irrigated peach orchard. *Agricultural Water Management*. [Online]. 142. p.pp. 1–9. Available from: <http://dx.doi.org/10.1016/j.agwat.2014.04.004>.
- Balderer, W., Synal, H.A. & Deak, J. (2004). Application of the chlorine-36 method for the delineation of groundwater infiltration of large river systems: Example of the Danube River in western Hungary (Szigetköz area). *Environmental Geology*. 46 (6–7). p.pp. 755–762.
- Beer, J., Muscheler, R., Wagner, G., Laj, C., Kissel, C., Kubik, P.W. & Synal, H.A. (2002). Cosmogenic nuclides during isotope stages 2 and 3. *Quaternary Science Reviews*. 21 (10). p.pp. 1129–1139.
- Benito, G., Rohde, R., Seely, M., Külls, C., Dahan, O., Enzel, Y., Todd, S., Botero, B., Morin, E., Grodek, T. & Roberts, C. (2010). Management of alluvial aquifers in two Southern African ephemeral rivers: Implications for IWRM. *Water Resources Management*. 24. p.pp. 641–667.
- Benito, G., Thorndycraft, V.R., Rico, M.T., Sánchez-Moya, Y., Sopeña, A., Botero, B.A.,

- Machado, M.J., Davis, M. & Pérez-González, A. (2011). Hydrological response of a dryland ephemeral river to southern African climatic variability during the last millennium. *Quaternary Research*. 75. p.pp. 471–482.
- Bennetts, D.A., Webb, J.A., Stone, D.J.M. & Hill, D.M. (2006). Understanding the salinisation process for groundwater in an area of south-eastern Australia, using hydrochemical and isotopic evidence. *Journal of Hydrology*. 323. p.pp. 178–192.
- Beyerle, U., Aeschbach-Hertig, W., Hofer, M., Imboden, D.M., Baur, H. & Kipfer, R. (1999). Infiltration of river water to a shallow aquifer investigated with  $3\text{H}/3\text{He}$ , noble gases and CFCs. *Journal of Hydrology*. 220 (3–4). p.pp. 169–185.
- Bial, J., Büttner, S.H. & Frei, D. (2015). Formation and emplacement of two contrasting late-Mesoproterozoic magma types in the central Namaqua Metamorphic Complex (South Africa, Namibia): Evidence from geochemistry and geochronology. *Lithos*. [Online]. 224–225. p.pp. 272–294. Available from: <http://dx.doi.org/10.1016/j.lithos.2015.02.021>.
- Bird, J.R., Davie, R.F., Chivas, A.R., Fifield, L.K. & Ophel, T.R. (1991). Chlorine-36 production and distribution in Australia. *Palaeogeography, Palaeoclimatology, Palaeoecology*. 84 (1–4). p.pp. 299–307.
- Blignault, H.J., van Aswegen, G., van der Merwe, S.W. & Colliston, W.P. (1983). Namaqualand Metamorphic Complex. *Special Publication, The Geological Society of South Africa*. 10. p.pp. 1–29.
- Bouchaou, L., Michelot, J.L., Vengosh, A., Hsissou, Y., Qurtobi, M., Gaye, C.B., Bullen, T.D. & Zuppi, G.M. (2008). Application of multiple isotopic and geochemical tracers for investigation of recharge, salinization, and residence time of water in the Souss-Massa aquifer, southwest of Morocco. *Journal of Hydrology*. 352 (3–4). p.pp. 267–287.
- Capo, R.C., Stewart, B.W. & Chadwick, O.A. (1998). Strontium isotopes as tracers of ecosystem processes: Theory and methods. *Geoderma*. 82 (1–3). p.pp. 197–225.
- Carlson, C.A., Phillips, F.M., Elmore, D. & Bentley, H.W. (1990). Chlorine-36 tracing of salinity

sources in the Dry Valleys of Victoria Land, Antarctica. *Geochimica et Cosmochimica Acta*. 54 (2). p.pp. 311–318.

Casey, R.E., Lev, S.M. & Snodgrass, J.W. (2013). Stormwater ponds as a source of long-term surface and ground water salinisation. *Urban Water Journal*. 10 (3). p.pp. 145–153.

Challan, M.B. (2016). Application of chlorine-36 technique in determining the age of modern groundwater in the Al-Zulfi province, Saudi Arabia. *Isotopes in Environmental and Health Studies*. [Online]. 52 (3). p.pp. 258–269. Available from: <http://www.tandfonline.com/doi/full/10.1080/10256016.2015.1061520>.

Chapman, G. (1948). Mima Mounds. *The Journal of Geology*. 56 (3). p.pp. 229–231.

Clifford, T.N., Barton, E.S., Stern, R.A. & Duchesne, J.C. (2004). U-Pb Zircon Calendar for Namaquan (Grenville) Crustal Events in the Granulite-facies Terrane of the O’okiep Copper District of South Africa. *Journal of Petrology*. [Online]. 45 (4). p.pp. 669–691. Available from: <https://academic.oup.com/petrology/article-lookup/doi/10.1093/petrology/egg097>.

Colliston, W.P. & Schoch, A.E. (1996). Proterozoic metavolcanic rocks and associated metasediments along the Orange River in the Pofadder terrane, Namaqua Mobile Belt. *South African Journal of Geology*. 99 (3). p.pp. 309–325.

Cook, P.G., Walker, G.R. & Jolly, I.D. (1989). Spatial variability of groundwater recharge in a semiarid region. *Journal of Hydrology*. 111. p.pp. 195–212.

Coplen, T.B., Böhlke, J.K., De Bièvre, P., Ding, T., Holden, N.E., Hopple, J.A., Krouse, H.R., Lamberty, A., Peiser, H.S., Revesz, K., Rieder, S.E., Rosman, K.J.R., Roth, E., Taylor, P.D.P., Vocke, R.D. & Xiao, Y.K. (2002). Isotope-abundance variations of selected elements (IUPAC Technical Report). *Pure and Applied Chemistry*. [Online]. 74 (10). p.pp. 1987–2017. Available from: <https://www.degruyter.com/view/j/pac.2002.74.issue-10/pac200274101987/pac200274101987.xml>.

Cornell, D.H., Thomas, R.J., Moen, H.F.G., Reid, D.L., Moore, J.M. & Gibson, R.L. (2006). The

Namaqua-Natal Sector. In: M. R. Johnson, C. R. Anhaeusser, & R. J. Thomas (eds.). *The Geology of South Africa*. Geological Society of South Africa, Johannesburg/Council for Geoscience, Pretoria, pp. 325–381.

Cramer, M.D., von Holdt, J.R.C., Uys, V.M. & Midgley, J.J. (2017). The present and likely past climatic distribution of the termite *Microhodotermes viator* in relation to the distribution of heuweltjies. *Journal of Arid Environments*. [Online]. 146. p.pp. 35–43. Available from: <http://dx.doi.org/10.1016/j.jaridenv.2017.07.010>.

Cramer, M.D., Innes, S.N. & Midgley, J.J. (2012). Hard evidence that heuweltjie earth mounds are relictual features produced by differential erosion. *Palaeogeography, Palaeoclimatology, Palaeoecology*. [Online]. 350. p.pp. 189–197. Available from: <http://dx.doi.org/10.1016/j.palaeo.2012.06.030>.

Cramer, M.D. & Midgley, J.J. (2015). The distribution and spatial patterning of mima-like mounds in South Africa suggests genesis through vegetation induced aeolian sediment deposition. *Journal of Arid Environments*. [Online]. 119. p.pp. 16–26. Available from: <http://dx.doi.org/10.1016/j.jaridenv.2015.03.011>.

Cresswell, R., Wischusen, J., Jacobson, G. & Fifield, K. (1999). Assessment of recharge to groundwater systems in the arid southwestern part of Northern Territory, Australia, using chlorine-36. *Hydrogeology Journal*. 7 (4). p.pp. 393–404.

Davis, S.N., Moysey, S., Cecil, D.L. & Zreda, M. (2003). Chlorine-36 in groundwater of the United States: empirical data. *Hydrogeology Journal*. 11 (2). p.pp. 217–227.

DWS (1996a). *South African Water Quality Guidelines (second edition). Volume 1: Domestic Use*.

DWS (1996b). *South African Water Quality Guidelines (second edition). Volume 4: Agricultural Use: Irrigation*.

DWS (1996c). *South African Water Quality Guidelines (second edition). Volume 5: Agricultural Use: Livestock Watering*.

- Edmunds, W.M. & Smedley, P.L. (1996). Groundwater geochemistry and health an overview. *Geological Society, London, Special Publications*. 113 (1). p.pp. 91–105.
- Eglinton, B.M. (2006). Evolution of the Namaqua-Natal Belt, southern Africa - A geochronological and isotope geochemical review. *Journal of African Earth Sciences*. 46 (1–2). p.pp. 93–111.
- Erens, H., Mujinya, B.B., Mees, F., Baert, G., Boeckx, P., Malaisse, F. & Van Ranst, E. (2015). The origin and implications of variations in soil-related properties within *Macrotermes falciger* mounds. *Geoderma*. [Online]. 249–250. p.pp. 40–50. Available from: <http://dx.doi.org/10.1016/j.geoderma.2015.03.003>.
- Evans, J.M., Stone, J.O.H., Fifield, L.K. & Cresswell, R.G. (1997). Cosmogenic chlorine-36 production in K-feldspar. *Nuclear Instruments and Methods in Physics Research, Section B: Beam Interactions with Materials and Atoms*. 123 (1–4). p.pp. 334–340.
- Farber, E., Vengosh, A., Gavrieli, I., Marie, A., Bullen, T.D., Mayer, B., Holtzman, R., Segal, M. & Shavit, U. (2004). The origin and mechanisms of salinization of the Lower Jordan River. *Geochimica et Cosmochimica Acta*. 68 (9). p.pp. 1989–2006.
- Fifield, L.K. (2017). Chlorine-36 in Hydrology - Principles and Practice. In: *GWD Conference*. 2017, Stellenbosch.
- Francis, M.L., Ellis, F., Lambrechts, J.J.N. & Poch, R.M. (2013). A micromorphological view through a Namaqualand termitaria (Heuweltjie, a Mima-like mound). *Catena*. 100 (February 2017). p.pp. 57–73.
- Fröhlich, K., Ivanovich, M., Hendry, M.J., Andrews, J.N., Davis, S.N., Drimmie, R.J., Fabryka-Martin, J., Florkowski, T., Fritz, P., Lehmann, B., Loosli, H.H. & Nolte, E. (1991). Application of isotopic methods to dating of very old groundwaters: Milk River aquifer, Alberta, Canada. *Applied Geochemistry*. 6 (4). p.pp. 465–472.
- Funch, R.R. (2015). Termite mounds as dominant land forms in semiarid northeastern Brazil. *Journal of Arid Environments*. 122. p.pp. 27–29.

- Gat, J.R. (1996). Oxygen and Hydrogen Isotopes in the Hydrologic Cycle. *Annual Review of Earth and Planetary Sciences*. 24 (1). p.pp. 225–262.
- Gibson, J.J. & Edwards, T.W.D. (2002). Regional water balance trends and evaporation-transpiration partitioning from a stable isotope survey of lakes in northern Canada. *Global Biogeochemical Cycles*. [Online]. 16 (2). p.pp. 10-1-10–14. Available from: <http://doi.wiley.com/10.1029/2001GB001839>.
- Goldstein, S.J. & Jacobsen, S.B. (1988). Nd and Sr isotopic systematics of river water suspended material: implications for crustal evolution. *Earth and Planetary Science Letters*. [Online]. 87 (3). p.pp. 249–265. Available from: [http://www.sciencedirect.com/science/article/pii/0012821X88900131%5Cnhttp://file//localhost\(null\)%5Cnpapers3://publication/uuid/4CC86267-EEC2-4E52-9AED-502A15F15155](http://www.sciencedirect.com/science/article/pii/0012821X88900131%5Cnhttp://file//localhost(null)%5Cnpapers3://publication/uuid/4CC86267-EEC2-4E52-9AED-502A15F15155).
- Guendouz, A. & Michelot, J.L. (2006). Chlorine-36 dating of deep groundwater from northern Sahara. *Journal of Hydrology*. 328 (3–4). p.pp. 572–580.
- Hartnady, C., Joubert, P. & Stowe, C. (1985). Proterozoic Crustal Evolution in Southwestern Africa. *Episodes*. 8 (4). p.pp. 236–244.
- Hogan, J.F., Phillips, F.M., Mills, S.K., Hendrickx, J.M.H., Ruiz, J., Chesley, J.T. & Asmerom, Y. (2007). Geologic origins of salinization in a semi-arid river: The role of sedimentary basin brines. *Geology*. 35 (12). p.pp. 1063–1066.
- Howcroft, W., Cartwright, I., Fifield, L.K. & Cendón, D.I. (2017). Differences in groundwater and chloride residence times in saline groundwater: The Barwon River Catchment of Southeast Australia. *Chemical Geology*. 451. p.pp. 154–168.
- Jacobs, J., Pisarevsky, S., Thomas, R.J. & Becker, T. (2008). The Kalahari Craton during the assembly and dispersal of Rodinia. *Precambrian Research*. 160 (1–2). p.pp. 142–158.
- Johnston, V.E. & McDermott, F. (2008). The distribution of meteoric Cl-36 in precipitation across Europe in spring 2007. *Earth and Planetary Science Letters*. 275 (1–2). p.pp. 154–

164.

Jolly, I.D., Walker, G.R. & Thorburn, P.J. (1993). Salt accumulation in semi-arid floodplain soils with implications for forest health. *Journal of Hydrology*. 150 (2–4). p.pp. 589–614.

Kaudse, T., Bani-Khalaf, R., Tuffaha, R., Freundt, F. & Aeschbach-Hertig, W. (2016). Noble gases reveal the complex groundwater mixing pattern and origin of salinization in the Azraq Oasis, Jordan. *Applied Geochemistry*. [Online]. 66. p.pp. 114–128. Available from: <http://dx.doi.org/10.1016/j.apgeochem.2015.12.003>.

Keywood, M.D., Fifield, L.K., Chivas, A.R. & Cresswell, R.G. (1998). Fallout of chlorine 36 to the Earth's surface in the southern hemisphere. *Journal of Geophysical Research: Atmospheres*. 103 (D7). p.pp. 8281–8286.

Klump, S., Grundl, T., Purtschert, R. & Kipfer, R. (2008). Groundwater and climate dynamics derived from noble gas,  $^{14}\text{C}$ , and stable isotope data. *Geology*. 36 (5). p.pp. 395–398.

Lapworth, D.J., Nkhuwa, D.C.W., Okotto-Okotto, J., Pedley, S., Stuart, M.E., Tijani, M.N. & Wright, J. (2017). Urban groundwater quality in sub-Saharan Africa: current status and implications for water security and public health. *Hydrogeology Journal*. [Online]. 25 (4). p.pp. 1093–1116. Available from: <http://link.springer.com/10.1007/s10040-016-1516-6>.

Leavy, B.D., Phillips, F.M., Elmore, D., Kubik, P.W. & Gladney, E. (1987). Measurement of cosmogenic  $^{36}\text{Cl}/\text{Cl}$  in young volcanic rocks: an application of accelerator mass spectrometry in geochronology. *Nuclear Instruments and Methods in Physics Research*. 29. p.pp. 246–250.

Macey, P.H., Bailie, R.H., Miller, J.A., Thomas, R.J., de Beer, C., Frei, D. & le Roux, P.J. (2017a). Implications of the distribution, age and origins of the granites of the Mesoproterozoic Spektakel Suite for the timing of the Namaqua Orogeny in the Bushmanland Subprovince of the Namaqua- Natal Metamorphic Province, South Africa. *in Review*. p.pp. 1–35.

Macey, P.H., Minnaar, H., Miller, J.A., Lambert, C., Kisters, A.F.M., Diener, J., Thomas, R.J., Groenewald, C., Indongo, J., Angombe, M., Smith, H., Shifatoka, G., Le Roux, P. & D., F.



(2015). *The Precambrian geology of the Warmbad Region, southern Namibia. An interim explanation to 1:50 000 Geological Map Sheets of the 1:250 000 2818 Warmbad sheet.*

Macey, P.H., Thomas, R.J., Minnaar, H.M., Gresse, P.G., Lambert, C.W., Groenewald, C.A., Miller, J.A., Indongo, J., Angombe, M., Shifotoka, G., Frei, D., Diener, J.F.A., Kisters, A.F.M., Dhansay, T., Smith, H., Doggart, S., Le Roux, P., Hartnady, M.I. & Tinguely, C. (2017b). Origin and evolution of the ~1.9 Ga Richtersveld Magmatic Arc, SW Africa. *Precambrian Research*. [Online]. 292. p.pp. 417–451. Available from: <http://dx.doi.org/10.1016/j.precamres.2017.01.013>.

Marais, J.A.H., Agenbacht, A.L.D., Prinsloo, M. & Basson, W.A. (2001a). *Explanation: Sheet 2916, The Geology of the Springbok Area*. Pretoria.

Marais, J.A.H., Agenbacht, A.L.D., Prinsloo, M. & Basson, W.A. (2001b). *The Geology of the Springbok Area*.

Masarik, J. & Beer, J. (1999). Simulation of particle fluxes and cosmogenic nuclide production in the Earth's atmosphere. *Journal of Geophysical Research*. 104 (D10). p.pp. 12099–12111.

McAuliffe, J.R., Timm Hoffman, M., Mcfadden, L.D. & King, M.P. (2014). Role of aeolian sediment accretion in the formation of heuweltjie earth mounds, western South Africa. *Earth Surface Processes and Landforms*. 39 (14). p.pp. 1900–1912.

Mehta, S., Fryar, A.E. & Banner, J.L. (2000). Controls on the regional-scale salinization of the Ogallala aquifer, Southern High Plains, Texas, USA. *Applied Geochemistry*. 15 (6). p.pp. 849–864.

Midgley, J.J., Harris, C., Harington, A. & Potts, A.J. (2012). Geochemical perspective on origins and consequences of heuweltjie formation in the southwestern Cape, South. *South African Journal of Geology*. 115 (4). p.pp. 577–588.

Midgley, J.J., Harris, C., Hesse, H. & Swift, A. (2002). Heuweltjie age and vegetation change based on  $^{13}\text{C}$  and  $^{14}\text{C}$  analyses. *South African Journal of Science*. 98. p.pp. 202–204.

- Milton, S.J. & Dean, W.R.J. (1990). Mima-like mounds in the southern and western Cape: are the origins so mysterious?. *South African Journal of Science*. 86 (4). p.pp. 207–208.
- Moen, H.F.G. & Toogood, D.J. (2007). *Explanation: Sheet 2818, The Geology of the Onseepkans Area*. Pretoria.
- Moore, J.M. & Picker, M.D. (1991). Heuweltjies (earth mounds) in the Clanwilliam district, Cape Province, South Africa: 4000-year-old termite nests. *Oecologia*. 86 (3). p.pp. 424–432.
- Moran, J.E. & Rose, T.P. (2003). A chlorine-36 study of regional groundwater flow and vertical transport in southern Nevada. *Environmental Geology*. 43. p.pp. 592–605.
- Mucina, L. & Rutherford, M.C. (2006). *The vegetation of South Africa, Lesotho and Swaziland*. L. Mucina & M. C. Rutherford (eds.). [Online]. Pretoria: South African National Biodiversity Institute. Available from: <http://ebooks.cambridge.org/ref/id/CBO9781107415324A009>.
- Mulligan, C., Yong, R.N. & Gibbs, B.F. (2001). Remediation Technologies for Metal-Contaminated Soils and Groundwater : An Evaluation. *Engineering Geology*. 60. p.pp. 193–207.
- Munns, R. & Tester, M. (2008). Mechanisms of Salinity Tolerance. *Annual Review of Plant Biology*. [Online]. 59 (1). p.pp. 651–681. Available from: <http://www.annualreviews.org/doi/10.1146/annurev.arplant.59.032607.092911>.
- Nakwafila, A.N. (2015). *Salinisation source(s) and mechanism(s) in shallow alluvial aquifers along the Buffels River, Northern Cape Province, South Africa*. Faculty of Science, Stellenbosch University.
- Négre, P. (1999). Geochemical study of a granitic area - the Margeride mountains, France: Chemical element behavior and  $^{87}\text{Sr}/^{86}\text{Sr}$  constraints. *Aquatic Geochemistry*. 5 (2). p.pp. 125–165.

- Nolte, E., Krauthan, P., Korschinek, G., Maloszewski, P., Fritz, P. & Wolf, M. (1991). Measurements and interpretations of  $^{36}\text{Cl}$  in groundwater, Milk River aquifer, Alberta, Canada. *Applied Geochemistry*. 6 (4). p.pp. 435–445.
- Palcsu, L., Major, Z., Köllő, Z. & Papp, L. (2010). Using an ultrapure  $^4\text{He}$  spike in tritium measurements of environmental water samples by the  $^3\text{He}$ -ingrowth method. *Rapid communications in mass spectrometry : RCM*. 24 (5). p.pp. 698–704.
- Pannell, D.J. (2001). Dryland salinity: economic, scientific, social and policy dimensions. *The Australian Journal of Agricultural and Resource Economics*. 45 (4). p.pp. 517–546.
- Peck, A.J. & Hatton, T. (2003). Salinity and the discharge of salts from catchments in Australia. *Journal of Hydrology*. 272 (1–4). p.pp. 191–202.
- Pennisi, M., Bianchini, G., Muti, A., Kloppmann, W. & Gonfiantini, R. (2006). Behaviour of boron and strontium isotopes in groundwater-aquifer interactions in the Cornia Plain (Tuscany, Italy). *Applied Geochemistry*. 21 (7). p.pp. 1169–1183.
- Pettersson, A., Cornell, D.H., Yuhara, M. & Hirahara, Y. (2009). Sm-Nd data for granitoids across the Namaqua sector of the Namaqua-Natal Province, South Africa. *Geological Society, London, Special Publications*. 323 (1). p.pp. 219–230.
- Phillips, F.M. (2013). Chlorine-36 dating of old groundwater. In: *Isotope methods for dating old groundwater*. Vienna: International Atomic Energy Agency, pp. 125–152.
- Phillips, F.M., Leavy, B.D., Jannik, N.O., Elmore, D. & Kubik, P.W. (1986). The Accumulation of Cosmogenic Chlorine-36 in Rocks : a Method for Surface Exposure Dating. *Science*. [Online]. 231 (4733). p.pp. 41–43. Available from: <http://www.jstor.org/stable/1696380>.
- Picker, M.D., Hoffman, M.T. & Leverton, B. (2007). Density of Microhodotermes viator (Hodotermitidae) mounds in southern Africa in relation to rainfall and vegetative productivity gradients. *Journal of Zoology*. 271 (1). p.pp. 37–44.
- Pietersen, K., Titus, R. & Cobbing, J. (2009). *Effective Groundwater Management in*

*Namaqualand Sustaining Supplies.*

Podmore, C. (2009). *Urban salinity – causes and impacts.*

Purdy, C.B., Mignerey, A.C., Helz, G.R., Drummond, D.D., Kubik, P.W., Elmore, D. & Hemmick, T. (1987). 36Cl: A tracer in groundwater in the aquia formation of Southern Maryland. *Nuclear Inst. and Methods in Physics Research, B.* 29 (1–2). p.pp. 372–375.

Reider, R.G., Huss, J.M. & Miller, T.W. (1996). A groundwater vortex hypothesis for mima-like mounds, Laramie Basin, Wyoming. *Geomorphology.* 16 (4). p.pp. 295–317.

Rengasamy, P. (2010). Soil processes affecting crop production in salt-affected soils. *Functional Plant Biology.* 37 (7). p.pp. 613–620.

Rengasamy, P. (2006). World salinization with emphasis on Australia. *Journal of Experimental Botany.* 57 (5). p.pp. 1017–1023.

Richards, B.K., Steenhuis, T.S., Peverly, J.H. & McBride, M.B. (2000). Effect of sludge-processing mode, soil texture and soil pH on metal mobility in undisturbed soil columns under accelerated loading. *Environmental Pollution.* 109. p.pp. 327–346.

Salama, R.B., Farrington, P., Bartle, G.A. & Watson, G.D. (1993). The chemical evolution of groundwater in a first-order catchment and the process of salt accumulation in the soil profile. *Journal of Hydrology.* 143. p.pp. 233–258.

Salama, R.B., Otto, C.J. & Fitzpatrick, R.W. (1999). Contributions of groundwater conditions to soil and water salinization. *Hydrogeology Journal.* 7 (1). p.pp. 46–64.

Santoni, S., Huneau, F., Garel, E., Aquilina, L., Vergnaud-Ayraud, V., Labasque, T. & Celle-  
Jeanton, H. (2016). Strontium isotopes as tracers of water-rocks interactions, mixing processes and residence time indicator of groundwater within the granite-carbonate coastal aquifer of Bonifacio (Corsica, France). *Science of the Total Environment.* [Online]. 573. p.pp. 233–246. Available from: <http://dx.doi.org/10.1016/j.scitotenv.2016.08.087>.

- Scanlon, B.R., Keese, K.E., Flint, A.L., Flint, L.E., Gaye, C.B., Edmunds, W.M. & Simmers, I. (2006). Global synthesis of groundwater recharge in semiarid and arid regions. *Hydrological Processes*. 20. p.pp. 3335–3370.
- Scanlon, B.R., Reedy, R.C., Stonestrom, D.A., Prudic, D.E. & Dennehy, K.F. (2005). Impact of land use and land cover change on groundwater recharge and quality in the southwestern US. *Global Change Biology*. 11 (10). p.pp. 1577–1593.
- Schimmelpfennig, I., Benedetti, L., Garreta, V., Pik, R., Blard, P.H., Burnard, P., Boursès, D., Finkel, R., Ammon, K. & Dunai, T. (2011). Calibration of cosmogenic  $^{36}\text{Cl}$  production rates from Ca and K spallation in lava flows from Mt. Etna (38°N, Italy) and Payun Matru (36°S, Argentina). *Geochimica et Cosmochimica Acta*. 75 (10). p.pp. 2611–2632.
- Schoups, G., Hopmans, J.W., Young, C.A., Vrugt, J.A., Wallender, W.W., Tanji, K.K. & Panday, S. (2005). Sustainability of irrigated agriculture in the San Joaquin Valley, California. *Proceedings of the National Academy of Sciences*. [Online]. 102 (43). p.pp. 15352–15356. Available from: <http://www.pnas.org/cgi/doi/10.1073/pnas.0507723102>.
- Shand, P., Darbyshire, D.P.F., Love, A.J. & Edmunds, W.M. (2009). Applied Geochemistry Sr isotopes in natural waters : Applications to source characterisation and water – rock interaction in contrasting landscapes. *Applied Geochemistry*. 24. p.pp. 574–586.
- Sharp, Z.D. (2017). *Principles of stable isotope geochemistry*. 2nd Ed.
- Sheffield, J., Wood, E.F., Chaney, N., Guan, K., Sadri, S., Yuan, X., Olang, L., Amani, A., Ali, A., Demuth, S. & Ogallo, L. (2014). A drought monitoring and forecasting system for sub-sahara african water resources and food security. *Bulletin of the American Meteorological Society*. 95 (6). p.pp. 861–882.
- Smith, A.E. (1973). A study of the variation with pH of the solubility and stability of some metal ions at low concentrations in aqueous solution. Part I. *Analyst*. 98 (1162). p.pp. 68–68.
- Spennemann, D.H.R. (2001). The creeping disaster: dryland and urban salinity and its impact on heritage. *Cultural Resource Management*. 24 (8). p.pp. 22–25.

- Stone, J.O., Evans, J.M., Fifield, L.K., Allan, G.L. & Cresswell, R.G. (1998). Cosmogenic Chlorine-36 Production in Calcite by Muons. *Geochimica et Cosmochimica Acta*. 62 (3). p.pp. 433–454.
- Stone, J.O., Allan, G.L., Fifield, L.K. & Cresswell, R.G. (1996). Cosmogenic chlorine-36 from calcium spallation. *Geochimica et Cosmochimica Acta*. 60 (4). p.pp. 679–692.
- Sturchio, N.C., Caffee, M., Beloso, A.D., Heraty, L.J., B?hlke, J.K., Hatzinger, P.B., Jackson, W.A., Gu, B., Heikoop, J.M. & Dale, M. (2009). Chlorine-36 as a tracer of perchlorate origin. *Environmental Science and Technology*. 43 (18). p.pp. 6934–6938.
- Thomas, R.J., Agenbacht, A.L.D., Cornell, D.H. & Moore, J.M. (1994a). The Kibaran of southern Africa: Tectonic evolution and metallogeny. *Ore Geology Reviews*. 9 (2). p.pp. 131–160.
- Thomas, R.J., Cornell, D.H., Moore, J.M. & Jacobs, J. (1994b). Crustal evolution of the Namaqua-Natal metamorphic province, southern Africa. *South African Journal of Geology*. 97 (1). p.pp. 8–14.
- Thomas, R.J., Macey, P.H., Spencer, C., Dhansay, T., Diener, J.F.A., Lambert, C.W., Frei, D. & Nguno, A. (2016). The Sperrgebiet Domain, Aurus Mountains, SW Namibia: A ~2020–850 Ma window within the Pan-African Gariiep Orogen. *Precambrian Research*. [Online]. 286 (September 2016). p.pp. 35–58. Available from: <http://dx.doi.org/10.1016/j.precamres.2016.09.023>.
- Titus, R., Beekman, H., Adams, S. & Strachan, L. (2009). *The Basement Aquifers of Southern Africa*. South Africa.
- Tosaki, Y., Tase, N., Sasa, K., Takahashi, T. & Nagashima, Y. (2012). Measurement of the <sup>36</sup>Cl deposition flux in central Japan: Natural background levels and seasonal variability. *Journal of Environmental Radioactivity*. [Online]. 106. p.pp. 73–80. Available from: <http://dx.doi.org/10.1016/j.jenvrad.2011.11.010>.
- UN-WWAP (2015). *The United Nations World Water Development Report 2015: Water for a Sustainable World*. [Online]. Paris: United Nations World Water Assessment Programme.

Available from: <http://unesdoc.unesco.org/images/0023/002318/231823E.pdf>.

UN Department of Economic and Social Affairs (2015). *World population prospects*. [Online]. New York. Available from: <http://www.ncbi.nlm.nih.gov/pubmed/21798940>.

Vengosh, A., Gill, J., Davisson, M.L. & Hudson, G.B. (2002). A Multi-Isotope (B, Sr, O, H, C) and Age Dating ( $^3\text{H}$ - $^3\text{He}$ ,  $^{14}\text{C}$ ) Study of Ground Water from Salinas Valley California: Hydrochemistry, Dynamics, and Contamination Processes. *Water Resources Research*. 38 (1). p.p. 9 1-17.

Vengosh, A., Spivack, A.J., Artzi, Y. & Ayalon, A. (1999). Geochemical and boron, strontium, and oxygen isotopic constraints on the origin of the salinity in groundwater from the Mediterranean coast of Israel. *Water Resources Research*. 35 (6). p.pp. 1877–1894.

Washburn, A. (1988). *Mima mounds*.

Weaver, J.M.C., Cavé, L. & Talma, A.S. (2007). *Groundwater Sampling: A Comprehensive guide for sampling Methods*. [Online]. Available from: <http://www.wrc.org.za/Knowledge Hub Documents/Research Reports/TT303-07.pdf>.

van Weert, F., Van Der Gun, J. & Reckman, J. (2009). *Global Overview of Saline Groundwater Occurrence and Genesis*. Utrecht.

Williams, W.D. (2001). Anthropogenic salinisation of inland waters. *Hydrobiologia*. 466. p.pp. 329–337.

Wright, E.P. (1992). The hydrogeology of crystalline basement aquifers in Africa. *Geological Society, London, Special Publications*. [Online]. 66 (1). p.pp. 1–27. Available from: <http://sp.lyellcollection.org/lookup/doi/10.1144/GSL.SP.1992.066.01.01>.

Wu, J., Li, P., Qian, H. & Fang, Y. (2014). Assessment of soil salinization based on a low-cost method and its influencing factors in a semi-arid agricultural area, northwest China. *Environmental Earth Sciences*. 71. p.pp. 3465–3475.





## 8. APPENDIX

Table 8.1: Heuweltjie EC and pH data.

Sample	pH	EC µS/cm
H01 North 25 cm	8.66	3548.39
H01 Middle surface	8.98	888.41
H01 Middle 50 cm	8.63	4010.75
H01 Middle 1 m	8.18	6123.99
H01 South surface	8.51	2001.08
IH01 North Surface	9.16	99.26
IH01 North 50cm	9.03	303.68
IH01 East Surface	8.99	94.90
IH01 East 10cm	8.33	156.70
IH01 South Surface	9.03	84.03
IH01 South 10cm	8.63	99.14
IH01 West Surface	9.09	76.35
IH01 West 45cm	9.24	153.09
H02 North surface	9.16	297.02
H02 North 50 cm	9.29	2533.69
H02 Middle surface	8.43	3754.67
H02 Middle 50 cm	8.59	3750.68
H02 South surface	9.07	144.43
H02 South 50 cm	8.66	2495.91
IH02 North Surface	8.97	101.53
IH02 North 15cm	9.16	123.21
IH02 East Surface	8.59	17.70
IH02 East 50cm	8.74	17.24
IH02 South Surface	8.20	14.99
IH02 South 25cm	8.04	16.84
IH02 West Surface	7.99	16.51
IH02 West 35cm	8.51	86.84
H03 North Surface	9.02	118.53
H03 Middle Surface	9.10	171.88
H03 South Surface	9.18	144.13
IH03 North Surface	8.64	15.07
IH03 North 20cm	8.54	286.36
IH03 East Surface	9.14	109.32
IH03 East 50cm	9.12	838.53
IH03 South Surface	8.90	65.27
IH03 South 50cm	9.07	63.75
IH03 West Surface	8.72	73.09
IH03 West 50cm	8.69	14.61
H04 North surface	9.39	568.36
H04 North 30 cm	8.86	939.33
H04 Middle surface	8.61	1713.17
H04 Middle 50 cm	8.48	3097.49
H04 South surface	8.76	738.72
H04 South 30 cm	8.20	3876.75
IH04 North 40cm	8.33	134.63
IH04 East Surface	8.86	13.62
IH04 East 15cm	8.98	64.76
IH04 South Surface	9.02	73.28
IH04 South 20cm	9.31	105.84
IH04 West Surface	9.07	18.54
IH04 West 50cm	9.11	72.56
H05 North Surface	9.35	235.29
H05 Middle Surface	8.17	7463.69
H05 Middle 10 cm	8.43	4595.51
H05 South Surface	8.16	4134.45
IH05 North Surface	8.06	16.02
IH05 North 20cm	8.67	106.82
IH05 East Surface	9.40	64.86
IH05 East 15cm	9.15	16.96
IH05 South Surface	8.86	72.20
IH05 South 10cm	8.12	66.33
IH05 West Surface	9.02	61.01
IH05 West 30cm	9.14	15.65
H06 East Surface	8.32	3742.30
H06 East 50 cm	8.32	4334.26
H06 Middle Surface	8.41	1717.65
H06 Middle 50cm	8.52	6242.25
H06 Middle 1 m	8.08	5723.94
H06 West Surface	8.84	126.57
H06 West 50 cm	8.95	156.55
IH06 North Surface	8.96	74.00
IH06 North 50cm	9.47	125.01
IH06 East Surface	9.48	17.15
IH06 East 15cm	8.39	69.08
IH06 South Surface	9.23	94.15
IH06 South 50cm	9.03	83.02
IH06 West Surface	9.02	63.80
IH06 West 50cm	9.83	129.25
H07 North surface	9.37	225.84
H07 North 50 cm	8.43	2183.24
H07 Middle Surface	8.81	2826.82
H07 Middle 50 cm	8.27	5259.05
H07 South Surface	8.67	768.80
IH07 North Surface	9.57	76.66
IH07 North 15cm	9.17	194.76
IH07 East Surface	8.76	17.82
IH07 East 30cm	8.90	97.65
IH07 South Surface	7.92	546.37
IH07 West Surface	9.01	70.92
IH07 West 15cm	9.14	109.80

*Table 8.2: River sediment EC and pH data*

Sample	pH	EC $\mu\text{S/cm}$
RS01	7.7	13.71
RS02	7.75	11.54
RS03	7.57	13.56
RS04	8.15	18.18
RS05	7.99	15.05
RS06	8.03	12.42
RS07	8.27	15.56
RS08	8.06	13.50
RS09	8.42	13.72
RS10	8.68	15.55
RS11	9.02	289.13
RS12	8.19	2156.33
RS13	8.24	14.56
RS14	7.71	12.50
RS15	7.38	11.29
RS16	8.25	76.13
RS17	7.46	9.66
RS18	7.68	9.78
RS19	7.43	7.99
RS20	7.58	8.78
RS21	8.13	62.73
RS22	7.9	13.43
RS23	7.56	9.20
RS24	7.53	9.91
RS25	7.47	6.94
RS26	7.82	11.49
RS27	7.63	8.99
RS28	7.63	8.46
RS29	7.34	6.67
RS30	7.13	17.87
RS31	7.6	11.20
RS32	8.83	76.56
RS33	8.37	11.83
RS34	7.74	92.57
RS35	8.28	69.27

Table 8.3: EC, pH and depth data for sediment samples taken in the grid

Sample	Sample Depth	pH	EC μS/cm
GR01	50	8.26	2277.62
GR02	50	8.78	247.73
GR03	20	9.03	93.11
GR04	15	8.86	78.64
GR05	25	9.83	207.71
GR06	30	8.39	230.51
GR07	25	8.14	345.30
GR08	20	8.19	524.65
GR09	15	8.36	174.73
GR10	20	8.15	460.85
GR11	15	9.23	142.41
GR12	40	8.49	18.05
GR13	20	8.35	814.53
GR14	20	8.79	187.49
GR15	20	8.59	117.88
GR16	25	8.11	72.58
GR17	10	8.25	502.25
GR18	10	9.15	225.13
GR19	10	8.78	145.69
GR20	25	9.01	191.64
GR21	25	8.07	224.18
GR22	50	8.74	135.62
GR23	50	8.34	1801.68
GR24	50	8.35	1818.99
GR25	40	8.71	249.44
GR26	30	7.98	193.95
GR27	25	8.23	73.63
GR28	30	8.55	19.20
GR29	20	8.71	162.68
GR30	10	8.6	159.44
GR31	30	8	151.75
GR32	50	8.17	132.09
GR33	50	8.3	2659.15
GR34	50	8.4	3335.21
GR35	50	8.12	2531.07
GR36	10	8.7	164.06
GR37	35	8.44	81.68
GR38	35	7.81	383.05
GR39	40	8.31	246.33
GR40	10	8.16	238.42
GR41	25	8.22	189.15
GR42	40	8.29	107.12
GR43	50	8.72	1584.27
GR44	50	8.18	4090.40
GR45	45	8.2	2551.72
GR46	20	8.63	174.62
GR47	10	8.72	419.32
GR48	20	8.29	1562.50
GR49	50	8.54	1877.62
GR50	5	8.03	1169.41
Sample	Sample Depth	pH	EC μS/cm
GR51	20	8.83	119.32
GR52	20	8.76	106.48
GR53	45	9.59	142.51
GR54	50	8.91	663.98
GR55	35	9.11	185.60
GR56	15	8.59	369.05
GR57	5	8.56	438.86
GR58	50	8.5	2885.06
GR59	50	8.34	3461.32
GR60	5	8.2	4385.27
GR61	15	8.84	81.58
GR62	25	9.25	133.90
GR63	40	9.21	313.14
GR64	15	8.99	385.23
GR65	5	9.04	148.56
GR66	5	8.79	332.95
GR67	5	9.21	96.66
GR68	5	8.3	454.24
GR69	25	8.32	2745.76
GR70	15	9.31	663.28
GR71	10	8.29	178.81
GR72	20	9.01	197.42
GR73	20	8.91	971.91
GR74	50	8.42	4790.96
GR75	5	8.3	2850.70
GR76	15	8.61	166.50
GR77	15	8.14	17.54
GR78	30	8.95	143.05
GR79	35	9	129.10
GR80	50	8.44	785.31
GR81	15	7.39	293.79
GR82	25	9.27	146.59
GR83	20	8.29	193.92
GR84	35	9.68	2647.89
GR85	10	8.69	312.11
GR86	10	9.23	139.72
GR87	5	8.26	221.52
GR88	10	8.41	104.38
GR89	20	8.42	209.92
GR90	15	8.49	925.84
GR91	10	8.56	17.69
GR92	10	8.06	378.59
GR93	35	8.76	258.76
GR94	25	9.08	85.08
GR95	25	9.1	117.86
GR96	5	8.43	19.47
GR97	5	8.67	94.12
GR98	10	7.87	293.26
GR99	20	8.74	180.34
GR100	15	8.28	333.52

Table 8.4: Stable isotope data for both groundwater and rainwater samples. Groundwater data is presented on the right while that of rainwater on the left.

Sample	d <sup>2</sup> H ‰	d <sup>18</sup> O ‰	d-excess
<b>2016</b>			
BR03	-18.5	-4.28	15.7
BR05	-16.3	-4.00	15.7
BR07	-12.3	-3.23	13.5
BR08	-10.4	-2.65	10.8
BR09	-15.4	-3.71	14.3
BR10	-13.7	-3.41	13.5
BR11	-25.2	-4.71	12.5
BR12	-17.8	-3.79	12.5
BR14	-19.1	-3.95	12.5
BR15	-4.5	-0.71	1.1
BR16	-18.2	-3.71	11.5
BR17	-17.2	-4.23	16.6
BR19	-14.5	-3.23	11.4
BR20	-14.1	-3.62	14.8
KG05	-15.8	-4.04	16.5
KG08	-15.7	-4.19	17.8
KG09	-14.1	-3.47	13.7
<b>2017</b>			
BR03	-19.3	-3.85	11.5
BR05	-15.3	-3.15	9.9
BR06	-15.7	-3.5	12.3
BR07	-10.9	-2.48	8.9
BR09	-15.6	-3.67	13.8
BR10	-13.3	-3.38	13.7
BR11	-23	-4.5	13.0
BR12	-17.1	-3.68	12.3
BR14	-17.6	-3.83	13.0
BR15	-3.7	-0.42	-0.3
BR16	-14.6	-2.56	5.9
BR17	-16.8	-4.18	16.6
BR19	-13.6	-3.02	10.6
BR21	-17.1	-3.37	9.9
BR22	2.2	-1.95	17.8
BR23	-12.7	-2.57	7.9
BR24	-12.4	-2.74	9.5
BR25	-14.7	-3.12	10.3
KG08	-14.8	-3.79	15.5
KG05	-15.2	-3.79	15.1

Sample	d <sup>2</sup> H ‰	d <sup>18</sup> O ‰	d-excess
BRRW23/04	-1.51	-2.04	14.9
BRRW13/05	-19.75	-4.92	19.6
BRRW20/06	0.53	-2.08	17.2
BRRW01/07	34.17	2.64	13.1
BRRW24/08	29.34	6.08	-19.3
BRRW16/09	9.93	1.45	-1.7
BRRW27/09	9.28	-0.02	9.5
KGRW29/04	-5.77	-2.22	12.0
KGRW13/05	-18.19	-3.67	11.2
KGRW17/06	8.73	0.69	3.2
KGRW04/07	23.71	1.75	9.7
KGRW27/07	-22.59	-4.63	14.5
KGRW28/07	-15.11	-3.31	11.4
KGRW03/08	-24.31	-4.89	14.8
KGRW17/09	-21.67	-4.43	13.8
NARW23/04	-7.53	-2.79	14.8
NARW30/04	-9.59	-2.60	11.2
NARW30/04	-10.32	-2.62	10.6
NARW1-13/05	-22.22	-5.19	19.3
NARW2-13/05	-29.46	-5.73	16.4
NARW24/05	-2.34	-2.60	18.5
NARW10/06	2.38	-1.53	14.6
NARW15/06	-2.80	-1.46	8.9
NARW16/06	-1.86	-1.72	11.9
NARW20/06	-13.36	-4.27	20.8
NARW01/07	-0.18	-2.95	23.5
NARW06/07	8.26	-2.25	26.3
NARW22/07	-6.71	-2.57	13.9
NARW1-27/07	-32.23	-6.70	21.4
NARW2-27/07	-21.32	-4.95	18.2
NARW3-27/07	-28.48	-5.75	17.6
NARW1-28/07	-25.39	-5.11	15.5
NARW2-28/07	-33.37	-5.72	12.4
NARW1-31/07	-10.55	-2.35	8.2
NARW2-31/07	-18.14	-3.68	11.3
NARW3-31/07	-19.29	-3.79	11.0
NARW01/08	-24.67	-5.24	17.2
NARW13/08	3.54	-1.12	12.5
NARW21/08	-9.98	-2.94	13.5
NARW05/09	1.90	-1.11	10.8
NARW1-16/09	-8.72	-3.66	20.6
NARW2-16/09	-37.32	-6.75	16.7
NARW3-16/09	-35.57	-6.82	19.0
NARW17/09	-33.77	-6.38	17.3
NARW26/09	-1.43	-1.34	9.3
NARW27/09	-2.37	-2.03	13.8
NARW01/11	1.09	1.57	-11.5
NARW23/11	-0.40	-1.89	14.7